Multiple Satellite Imaging System

A Major Qualifying Project

Submitted to the faculty of

Worcester Polytechnic Institute

in partial fulfillment of the requirements for the

Degree of Bachelor of Science

Submitted By:

Roland Cormier

Katie Elliott

Jason Frey

Isaiah Janzen

Submitted To:

Project Advisor: Islam Hussein

Date: February 29, 2008

Abstract

This Major Qualifying Project explores the theory of multiple satellite imaging with consideration given to aperture movement, field of view of each aperture, number of apertures, aperture spacing, frequency of interest, and time; simulates the concept through a Matlab simulation in both one and two dimensions; provides the groundwork for a physical experiment to demonstrate the concept through three different wave types: infrared, radio, and acoustic.

Executive Summary

Prior to civilization, nomads roamed the Earth learning every cave and crest; after all land was conquered in Europe, royals hired ships and sailors to scour the seas for new territories; in 1902 the Wright Brothers successfully launched *The Flyer* thus inspiring a technological boom allowing mass transit by air; and in 1957 as Sputnik completed its first orbit around Earth inspiring a generation to reach for the stars. Discovery and exploration has fueled man's imagination since the dawn of time. Humanity seeks to know its place in the universe.

Successful implementation of a multiple satellite imaging system would allow for more in depth exploration of the regions of space and time. An advanced imaging system would produce photographical evidence of what exists beyond the Milky Way Galaxy by exploring existing objects in space with higher resolution and thus providing better clarity. With improved imaging technology we may capture enhanced images of these celestial bodies and, from these images, obtain invaluable amounts of information about celestial life cycles, planet properties, and much more.

The project goals include, but are not limited to, the following: to a) understand the operation and mathematical concepts of single and multiple satellite imaging systems, b) prepare a literature survey on single and multiple aperture imaging, current ground-based and space-based imaging systems, and any future multiple satellite imaging system (MSIS) technologies, c) to construct a Matlab-based simulation toolbox to demonstrate the capabilities of multiple satellite imaging systems, and d) study the technical and financial feasibility of a table top experimental setup to demonstrate capabilities of MSIS.

Project Deliverables

The deliverables of this project are based on our initial research and understanding of the operation of a multiple satellite imaging system. With this we will produce both one and two dimensional Matlab simulations that demonstrate the main concepts of multiple satellite imaging. These concepts include aperture movement, field of view functions, number of apertures, aperture spacing, frequency of interest, and time. Each of these Matlab codes will demonstrate greater improvement in imaging of a multiple satellite system over that of an individual satellite.

In addition to the Matlab codes we will research the feasibility for an experiment to physically demonstrate these concepts. This experiment will be a simplified, scaled model of a multiple satellite imaging system.

Table of Contents

Table of Figures

Table of Tables

1.0   Introduction

Prior to civilization, nomads roamed the Earth learning every cave and crest; after all land was conquered in Europe, royals hired ships and sailors to scour the seas for new territories; in 1902 the Wright Brothers successfully launched *The Flyer* thus inspiring a technological boom allowing mass transit by air; and in 1957 as Sputnik completed its first orbit around Earth inspiring a generation to reach for the stars. Discovery and exploration has fueled man's imagination since the dawn of time. Humanity seeks to know its place in the universe.

Advances in exploration demand advances in technology. Even as a minimum, improving upon existing technology, the ability to explore further into the unknown grows. At the current stage in space exploration an improved imaging system is required, one with the ability of achieving an enhanced view of detecting deep space objects and phenomena. A multiple satellite imaging system is the most feasible and promising technological advancement for achieving these goals. A multiple satellite imaging system is the "telescope" to launch civilization into a new phase of exploration.

Successful implementation of a multiple satellite imaging system would allow for more in depth exploration of the regions of space and time. An advanced imaging system would produce photographical evidence of what exists beyond the Milky Way Galaxy by exploring existing objects in space with higher resolution and thus providing better clarity. With improved imaging technology we may capture enhanced images of these celestial bodies and, from these images, obtain invaluable amounts of information about celestial life cycles, planet properties, and much more.

If energy measured by the imaging system were to consist of visible electromagnetic waves, or visible light, its higher resolution images would represent more accurate estimates of the visible light emanating from the source. By analyzing the rest of the spectrum more information can be determined. For example, infrared energy can signal volcanic activity and radio waves may signal intelligent life.

Another parameter of interest is the age of the light collected. An image is generated by capturing light emitted from the target source. Considering that this light must travel the distance between the source and the imaging system, the image shows the source when the light was emitted not the current view of the source. There is a time delay between when light is emitted by the target source and when the light is captured. This amount of time is directly proportional to the distance between the source and the imaging system. The history of the universe becomes unveiled as the depths of space are explored. By exploring farther and farther into space we are also investigating the history of the universe, allowing for discoveries not only in space exploration, but into the origins of the universe. The average person does not believe what they are told nearly as much as what they can see.

These are just a few applications of the multiple satellite imaging system that will stimulate the interest of the general public and return their attention to the importance of space exploration. People are interested in what lies beyond their view, curious about the unknown. This yearning to know what is beyond reach fuels desire for interstellar discovery, and will ultimately determine when a multiple satellite imaging system becomes a reality.

Technology has advanced and evolved in stride with man's ambition for exploration. Beginning when Galileo pointed a telescope towards the sky and saw the moons of Jupiter, to massive ground observatories and the first Earth orbiting telescope, a multiple satellite imaging system is the next innovation in a long line of advances in space exploration. By examining previous and current technology and improving on their flaws while utilizing their strengths a more efficient invention can economically be produced.

2.0   Background Theory

2.1 Basics of Optics

Light may be considered as waves of varying lengths which are divided into specific sections, Gamma rays, X-ray, Ultraviolet, Visible, Infrared, and Radio waves. Humans can only perceive wavelengths between 380 and 780 nanometers; this group of wavelengths is defined as "visible light". Humans view these wavelengths as colors while the rest of the spectrum is undetected by the naked eye.
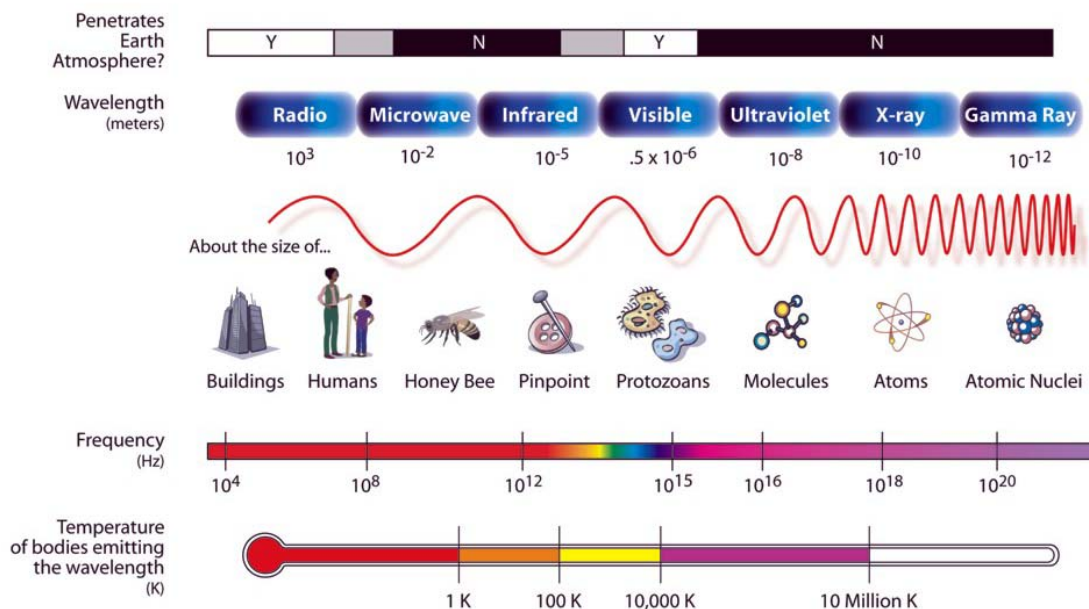
Figure 1: The Electromagnetic Spectrum[3]

The human eye is the simplest, yet most crucial piece of optical equipment. It consists of one convergent lens, the iris, and the retina. The lens deflects rays of light that pass through it, focusing these rays on the retina. This causes almost parallel rays of light entering the lens to converge on the receptors found on the retina. The two types of receptors on the retina are rods, for black and white, and cones, for color, which convert

light into electrical impulses sent to the brain. The iris controls the amount of light entering the eye by contracting and expanding over the lens, changing the size of the pupil.

Cameras function similar to a human eye, but it replaces the iris with an aperture stop and the retina with film. Cameras use a single convergent lens to create a picture on the film. There are several ways to control the picture formed on the film. The two most common are adjusting the aperture stop and the shutter speed. Both adjustments affect the amount of light entering the lens. To take a picture of a moving object, a short shutter speed is needed to prevent blurring while the aperture needs to be large enough to allow a sufficient amount of light to create the picture on the film. Less common methods are different blends of chemicals on the film or more or less responsive photon sensors so that the image is lighter or darker. The picture can also be illuminated with a flash or a filter can be used over the lens to control the light that eventually reaches the receptor. However, these controlled variables such as a flash are not possible for stellar imaging.

Since analog cameras are not feasible because of the data transfer to Earth, a popular choice of receptors for digital cameras and similar devices are charge coupled devices (CCDs). This method consists of an array of detectors or pixels. This array forms a shift register through a high density of potential-well capacitors. Each capacitor consists of a thin layer of silicon dioxide grown on silicon substrate. Covering the silicon dioxide is a transparent electrode that acts as a gate. When a positive electrical potential applied to the electrode, an electrical potential well is formed in the silicon substrate. Incident light from the aperture focused through the lens creates electron-hole pairs which are filled by free electrons created by the incident photons. By measuring the quantity of electrons in

the potential well, the intensity of the incident light can be measured. This charge

package is then transferred to edges of the array through the propagation of potential

wells until they are detected by external circuits. These circuits then take the information

to a central processing unit to be converted into an image.

Due to the size of the rods and cones in the human eye, the human eye cannot detect

differences in light if the rays form an angle less than 0.15 rad between them, which

occurs when an image is far away. During the early 1600s the telescope was invented to

aid the human eye. A telescope consists of two lenses: the first is called the objective

lens. This lens focuses the incoming light into an inverted picture. The second lens is the

eyepiece lens. This lens has the same focal point as the objective lens and converts the

light, which has become divergent after passing through the focal point of the objective

lens, into parallel rays which the eye converts into an image. Below is a schematic of this

process for a basic telescope.
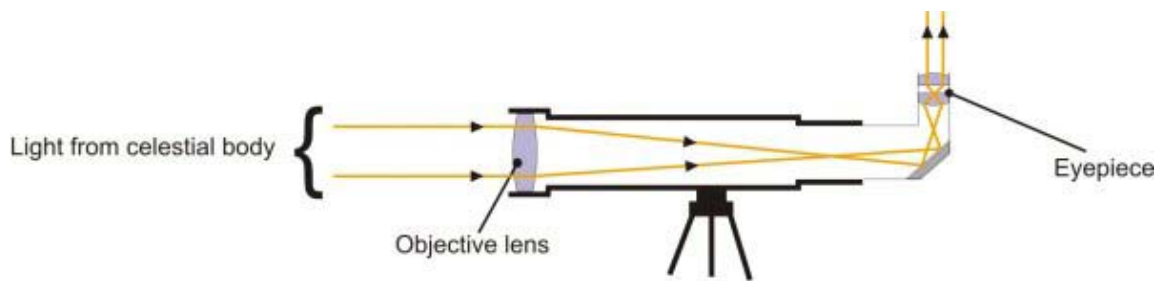
Figure 2: Schematic of a Basic Telescope [5]

2.2 Single Aperture Optics

A single aperture system consists of a number of components that are also applicable to the multiple satellite imaging systems. The first of which is a concentrator, whose function is to take the incoming signal from a large area and concentrate it to a much smaller size. This may be a glass lens in a simple telescope, a large concave mirror, or a parabolic satellite dish. Its purpose is to capture a large amount of the desired incoming signal and concentrate that onto a smaller surface. The signals may be concentrated by refracting the light through a lens or, in very long distance imaging, a reflection from the surface of a mirror, known as the primary mirror, or a parabolic dish is used. Reflecting telescopes are more common due to their relative ease of manufacturing compared to glass lenses as well as their relatively compact length and durability. The signal in reflecting telescopes, the systems of most interest to us, is concentrated onto an image processing device. This could be done directly or with another, secondary mirror, or even multiple reflections after the initial collection. The number and angle of reflections depends on the desired location of the image collector which is an important factor in any space-borne telescope due to moment of inertia, guidance issues, and payload faring restrictions. The image processing device can be any device which converts the incoming signal to a storable media. Most commonly this is done with a CCD. It can also be done with standard analog film, photodiodes, or any other sensor capable of converting the chosen signal to a useful medium.

Next, it is important to further understand the operation of a camera. The first characteristic of a camera is the aperture size. The aperture size determines the amount of light allowed to pass through. On typical high level camera models this is an easily

adjustable feature. However, in long distance space imaging, a variable aperture is not necessary because the shutter times are generally so long that the maximum aperture size is always desirable. So while it is important to be able to change aperture size depending on light conditions, in space the light conditions are nearly always the same. The next factor is shutter time. An average camera shutter speed is $1/1000^{th}$ of a second; however, Hubble Space Telescope has a minimum shutter time of $1/10^{th}$ of a second.[17] Generally, longer shutter times are desirable because they allow more light to be captured and produce a more definitive image. The entire idea of multiple satellite imaging is collecting a larger amount of the desired signal than is possible with a single aperture.

2.3 Fourier Transforms – One and Two Dimensional Cases

In imaging, we are attempting to measure the intensity of light reflected off of an object in order of creating an estimate of its source. The reception of only a small portion of the reflected light from a source is done automatically due to the nature of single aperture optics. Mathematically, we can represent the process of creating an estimate image using the Fourier Transform.

Every process has inputs and outputs. For imaging, the input is the light reflected or produced from an object. This wave may be represented in the form of a periodic function and is called the truth function. Periodic functions are typically used since they operate at a given frequency just like a beam of light. If the properties of the signal were already known, it would make the analysis much simpler. Any periodic signal may be broken down into sine and cosine functions that, when added together, create the input signal. This decomposition into trigonometric functions, known as the Fourier series,

makes it simpler to analyze the system. For example a simple approximation of a square

wave is illustrated using the following equation:

$$y = \sum_{i=1}^{n} \frac{\sin(2nt - t)}{2n - 1}$$

This approximation if carried out with infinite terms would result in a perfect square

wave. The first order terms are thus basic low frequency terms that result in a general

approximation and as more terms are added, higher frequencies are added and the

resulting estimation becomes closer to the truth function. The image below is a graph of

the function above computed in Matlab for various values of n.
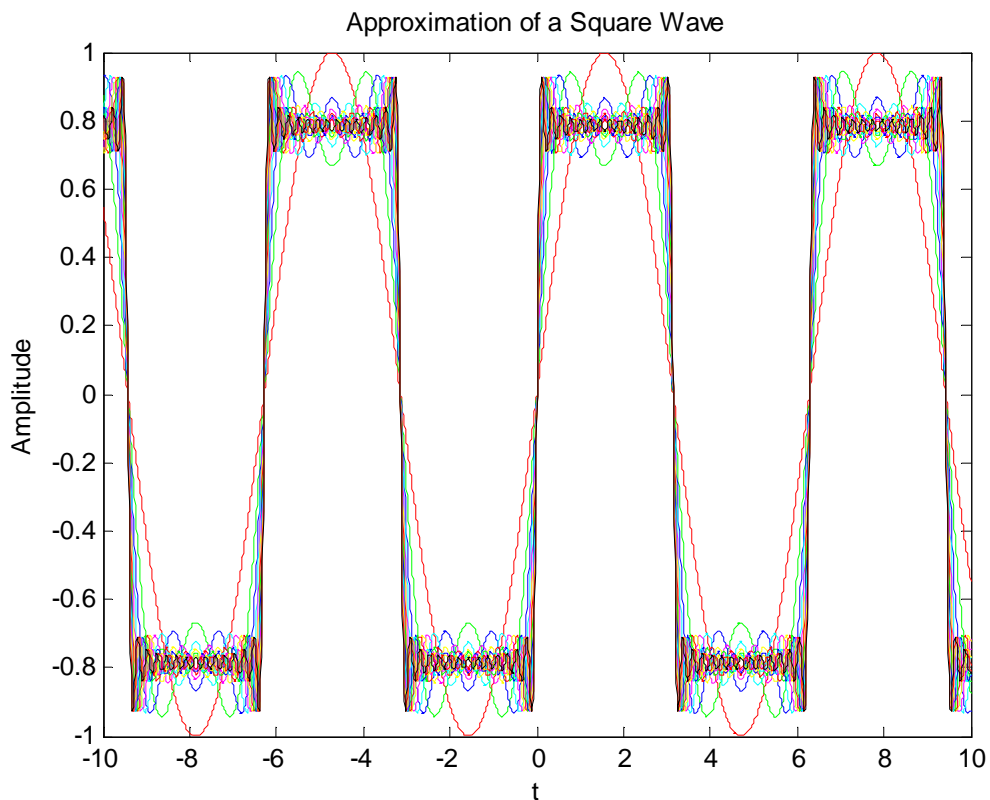
Figure 3: Approximation of a Square Wave Using Matlab

If we were to use an approximation with more higher order terms, it will result in a better

approximation of the square wave.

This is where the Fourier transform is introduced. The Fourier series is defined as:

$$f(x) = \frac{a_0}{2} + \sum_{n=1}^{\infty} \left[a_n \cos(nx) + b_n \sin(nx) \right]$$

with the Fourier coefficients defined as:

$$a_n = \frac{1}{\pi} \int_{-\pi}^{\pi} f(x) \cos(nx) dx$$

$$b_n = \frac{1}{\pi} \int_{-\pi}^{\pi} f(x) \sin(nx) dx$$

The Fourier transform allows for the computation of the coefficients, a_n and b_n, for the Fourier series. "[The Fourier Series plays] an important role in modern physical optics, not only in the determination of diffraction patterns and the description of interference phenomena, but also in the description of imaging systems and in spectral analysis" (Reynolds 8). With these computations, the signal may be decomposed into its equivalent trigonometric functions and then studied in terms of its wavelengths. The Fourier domain, also known as, the frequency domain is an alternate method for analyzing a signal. A signal in the frequency domain is referred to as a spectrum.

The Fourier transform is symmetrical about the origin; if a signal operates at a given spatial wavelength, it also operates at the negative of that wavelength. The image below shows functions on the left with their corresponding Fourier transform on the right.
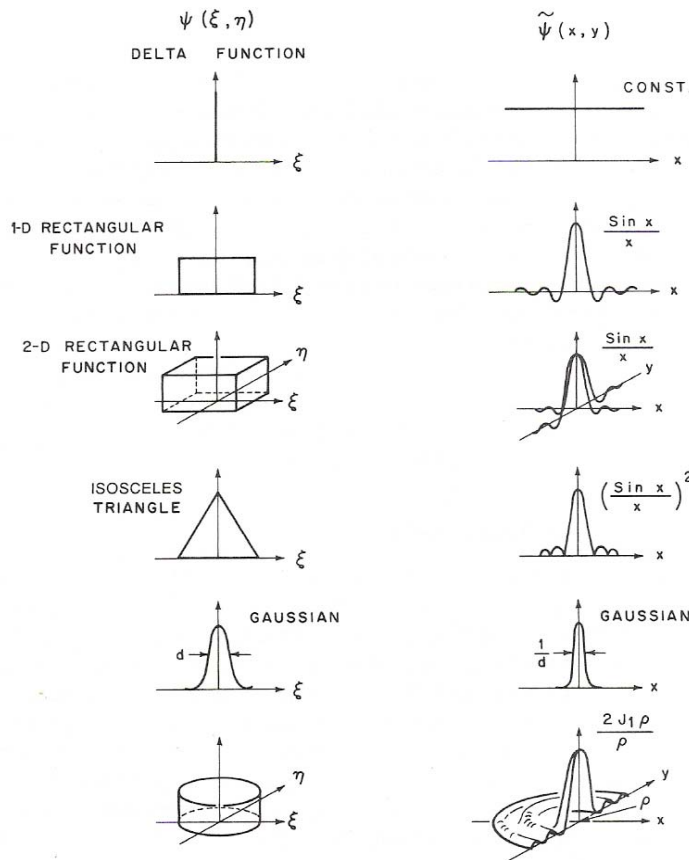
Figure 4: Functions and their Corresponding Fourier Transforms[24]
(Copyright © 1989 The Society of Photo-Optical Instrumentation Engineers)

A Fourier transform is the representation of a signal in terms of the frequencies that occur within the signal. The following equation is the one dimensional Fourier transform of the signal g(x). The signal is a collection of magnitudes. Those magnitudes are multiplied by the exponent term which describes the frequencies (f_X) and converts to the frequency domain using the imaginary unit vector (j). That quantity is then integrated along from negative infinity to positive infinity along the variable (x) as shown below.

$$F\{g\} = \int_{-\infty}^{\infty} g(x)\exp[-j2\pi(f_X x)]dx$$

The two dimensional Fourier transform case is the same as the one dimensional

case with the exception that the integration occurs in two directions corresponding to the

signal having two dimensions. For a digital picture with magnitude varying with x and y,

the Fourier transform is simply the frequencies in both the x and y directions becoming

computed instead of just one direction as shown below.

$$F\{g\} = \int_{-\infty}^{\infty} \int g(x,y) \exp[-j2\pi(f_X x + f_Y y)] dx dy$$

The inverse Fourier transform does exactly the opposite of the Fourier transform.

It takes a collection of magnitudes of frequencies $G(f_X)$ and multiplies them by the same

factor that was used in the original Fourier transform to convert between frequency

domain and the signal domain. It is then integrated from negative infinity to positive

infinity along the frequencies (f_X). The result is the inverse Fourier transform of the

frequencies $G(f_X)$ as shown below.

$$F^{-1}\{G\} = \int_{-\infty}^{\infty} G(f_X) \exp[-j2\pi(f_X x)] df_X$$

Similarly, for the two dimensional inverse Fourier transform the frequencies are

integrated in two dimensions. This allows complete reconstruction of all frequencies as

shown below.

$$F^{-1}\{G\} = \int_{-\infty}^{\infty} \int G(f_X, f_Y) \exp[-j2\pi(f_X x + f_Y y)] df_X df_Y$$

For the infinite Fourier transform and inverse transform the reconstruction is

exactly the original truth image as shown below

$$g(x,y) = F^{-1}[F(g(x,y))]$$

Matlab uses a Fast Fourier transform which is an integration that is between two

discrete numbers. This approximation allows the computation to take much less

computing power and thus save a large amount of time. However, it is also inaccurate because of the error introduced by the finite summation.

2.4 Optical and Modulation Transfer Function

2.4.1 The Optical Transfer Function

The optical transfer function (OTF) is a graphical distribution of the varying light intensity emitted by a source. In the case of optics, the source is the object that is being imaged and the OTF is one of the processes the data will go through to produce an estimate image.

The OTF can be displayed in its complex form as:

$$OTF(\Phi) = \mathrm{T}(\omega)\varepsilon^{i\Phi(\omega)}$$

Where T represents the real the modulation transfer function (MTF) and Φ is the phase. For simplification purposes, we ignore phase dynamics and only consider the role of the MTF. We are only interested in the magnitude of the signal and not its phase.

2.4.2 Field of View Function & Picture Frame Function

The picture frame function is the "geometrical projection of the exit pupil into the image plane" (Goodman 152). Typically this is represented by a rectangular or circular function. A rectangular shape is used to represent the exit pupil since it is the same shape as a typical digital picture while a circular shape may be used to more closely represent a camera aperture. A typical picture frame function is shown in Figure 5:
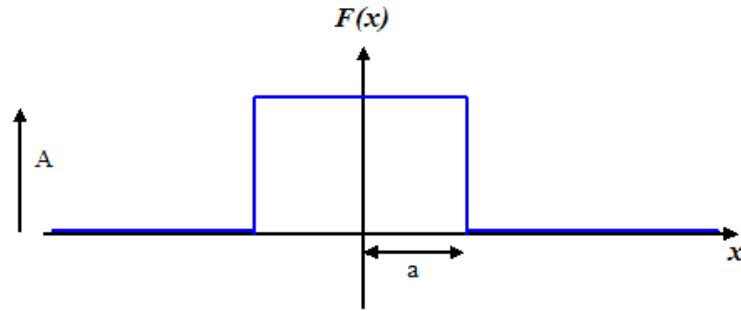
Figure 5: Graphical Representation of a Rectangular Function[25]

Here, the one-dimensional picture frame function is represented as a rectangular

function, centered about the origin, with a width of *2a* and a height of *A=1*. For all

values with an absolute value greater than *a*, the function has a value of zero, thus

representing the area of the image plane we cannot capture in our image. Also, the

picture frame function is centered about the origin in order of simplifying the analysis

once we introduce the Fourier Transform. This is only a one dimensional picture frame

function; its equivalent for a two dimensional case would appear as a hat-shaped function.

Now that we have defined the shape of our image, it is important to understand

what role it plays in the imaging process. If we take the Fourier transform of the picture

frame function, the result is known as the point spread function seen in Figure 6.
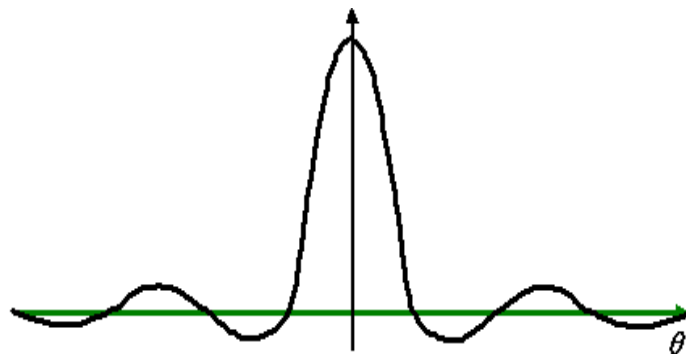
Figure 6: The Fourier Transform of a Rectangular Function[25]

In mathematics, this is also commonly referred to as the sinc function (which is the Fourier transfer of the square function). In optics, the point spread function represents the degradation of the image. The output of a camera is only an estimate of the object we are trying to capture. The camera records the intensity of the light emitted by an object and then creates an estimate. Since a perfect optical system, one capable of collecting all the light reflected off of an object, does not exist, the error of an approximation must be taken into account. This is where the point spread function is useful.

The low spots of the point spread function that extend below the θ axis are known as blind spots. These areas represent the wavelengths at which the system has a low efficiency for reading the intensity of light. In contrast, the peaks represent wavelengths that are efficiently measured. Typically, the strongest peak for a point spread function is located at the origin. This shows that lower frequencies are easier to capture than higher frequencies. Lower frequencies represent basic heavily contrasted components and higher frequencies represent finer details. For example, if we take a picture of a typical house with a tree in the front yard, any camera will be able to tell that there is a house with a tree in the yard. However, a camera with higher resolution, i.e. better coverage of higher frequencies and fewer blind spots, will be able to discern the shingles on the roof or the veins of the leaves on the tree. This is because the PSF of the high resolution camera captures more frequencies, thus more detail.

2.5 Multiple Aperture

A multiple aperture system is not necessarily a single satellite composed of multiple apertures, but could also be an array of several single aperture satellites as we consider here. Each of the satellites in the array would communicate the data it receives

to a collector. This collector would then take each signal and combine them to produce one signal. The major concept of a multiple satellite array is that the quality of the final signal improves as the number of satellites in the array increases. There are many advantages from a multiple aperture system. One of which is that the array will still work even if a satellite malfunctions. This malfunction will result in a decrease in quality of the estimate, but the decrease will still allow for an estimate. In contrast, if a single aperture system were to malfunction, no estimate could be created. Multiple satellite arrays also have an amount of versatility not previously afforded by giant telescopes of the past. Given a large array of imaging satellites and two short range targets, instead of producing two high quality images of both the array may be told to devote half of its satellites to image each target. Both targets will be imaged in the amount of time it would have taken to image one. The resulting images will be of less quality than if all satellites were utilized in imaging both satellites, however a high resolution estimate may still be obtained in less time. The array has the ability to be used in its entirety or may be divided so that each satellite has a given task.

The design of the array can be created to fulfill certain mission requirements. To image Earth, a satellite with multiple imagers attached by a boom may be selected. This configuration improves the capabilities of the imager and by keeping the imagers close together, ensures that the area being imaged does not change before the next imager is in position. For a deep space imaging mission, multiple satellites could be launched over a series of missions and individually placed into an orbit of choice. Depending on wavelengths in interests, the spacing of the satellites could be changed or motion could

be introduced. This flexibility can allow, in certain cases, the changing of the mission objective without changing the equipment.

2.6 Current Systems

To even attempt to answer this question we must first find where we are now. Light from far reaching bodies of the universe continuously collides with the Earth. The age of this light depends directly upon the distance it has traveled from its source. Analyzing light from distant bodies is a way to look into the past and observe the origins of the universe or the life and depth of much younger objects such as planets and stars.

2.6.1 Satellite Systems versus Ground Systems

Since the beginning of man's infatuation with the cosmos we have tried to devise methods of seeing farther into the night's sky. Until the concept of a space-based telescope was proposed in the middle of the 20th century all data was collected from ground stations. While the ground based telescope method is relatively simple and accessible, there are several problems inherent in ground based telescopes.

There are two major issues with using a ground based telescope, and both result from the Earth's atmosphere. The atmosphere acts as both a lens and a filter, causing distortion and inaccuracy in images. It partially blocks some of the light that is directed towards the Earth. Instead of receiving the full spectrum of light, including ultraviolet, gamma, and x-rays, a reduced spectrum is collected. The angle of received light is also changed due to refraction in the atmosphere. By altering the location of the system so that it orbits the Earth and is outside of its atmosphere these issues are negated.

2.6.2 Current Operating Systems of the Origins Program

The Origins program was established by the National Aeronautics and Space Administration (NASA) for the purpose of analyzing distant bodies so as to look into the past and observe the origins of the universe. The program has created many structures, fixed and mobile, that utilize different technologies to advance our understanding of the universe.

Hubble Space Telescope (HST)

One of the major milestones of the Origins program was the creation of the Hubble Space Telescope (HST) in 1990. The idea of launching a telescope into Earth orbit with the ability to send its collected data back to Earth greatly increased the capabilities of space exploration.

The HST has made indescribable observations since its inception. It has redefined the age of the universe to be approximately 13 to 14 billion years, where previous estimates ranged from 10 to 20 billion years. In addition, the Hubble Space Telescope was significant in the discovery of dark energy and has allowed the scientific community to view galaxies of all ages. Another unique feature of HST is that anyone may submit a proposal for satellite time to observe objects or points of interest. There is a review board in place to decide whether a proposal warrants the use of the HST or not and all the data collected by the HST is archived for the general public.

Powered completely using solar power, the Hubble Space telescope contains a primary mirror measuring 2.4 meters in diameter and can complete a full trip around the earth in 97 minutes, equating approximately to a velocity of 8 kilometer per second. The HST is a Cassegrain reflector telescope; light hits the telescope's main mirror then

bounces off towards a secondary mirror. This second mirror focuses the light through a hole in the center of the primary mirror leading to various scientific instruments. This process is illustrated in Figure 2:
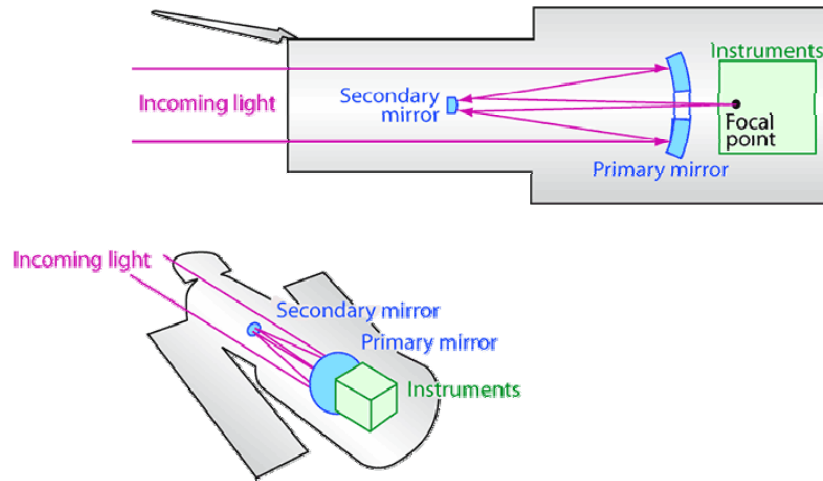
Figure 7: Schematic of Hubble Space Telescope Mirrors[30]

The Hubble Space Telescope houses a system of instruments which aid studies of the universe. These instruments include, but are not limited to: 1) The Advanced Camera for Surveys (ACS) which detects visible light and is instrumental in mapping the distribution of dark matter and the detection of distant objects, 2) The Near Infrared Camera and Multi-Object Spectrometer (NICMOS) – a heat sensor that allows for observation of objects hidden by interstellar dust, 3) a Space Telescope Imaging Spectrograph (STIS) acting as a prism to provide wavelength mapping of an object that is being observed in hopes of determining characteristics such as temperature, chemical composition, density, and motion, and 4) a Wide Field and Planetary Camera 2 (WFPC2) that is responsible for many of the Hubble Space Telescope's most famous images.

Spitzer Space Telescope

First launched on August 25, 2003, the Spitzer Space Telescope is a cryogenically cooled infrared observatory capable of looking into the distant reaches of the universe. The telescope is cooled so as to eliminate any heat produced as a byproduct of its operation. This heat acts as noise or a disturbance when attempting to detect weak infrared signals from distant astronomical objects.
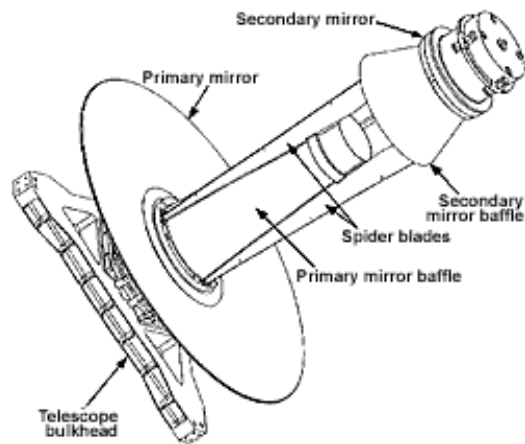
Figure 8: Diagram of Spitzer's Mirrors[26]

This observatory is comprised of an 85 centimeter diameter telescope with three cryogenically cooled instruments. It is capable of studying light at infrared wavelengths between 3 and 180 microns. In addition to cryogenics for heat reduction, engineers designed Spitzer's orbit not around Earth, but the Sun. Spitzer orbits behind the Earth as it orbits the Sun and drifts away from the Earth at approximately 1/10th of an astronomical unit per year.

Spitzer uses three main technologies: 1) an infrared array camera that allows for imaging at near to mid-infrared wavelengths, 2) an infrared spectrograph which decomposes light into its equivalent wavelengths in order of studying emission and

absorption lines, and 3) a multiband imaging photometer which uses a scan mirror to map large areas of the sky at infrared wavelengths.

Keck Interferometer

The only other currently operational space satellite that is part of the Origins program is the Far Ultraviolet Spectroscopic Explorer (FUSE). The Origins program combines the capabilities of these space observatories with its ground based multiple aperture system known as the Keck Interferometer.

The Keck Interferometer is a ground based multiple aperture system located at the summit of the dormant Mauna Kea volcano in Hawaii. Consisting of two twin telescopes with a separation of 85 meters, this is the largest telescope for optical and near-infrared astronomy. Due to the separation distance, this interferometer has an equivalent resolution to that of an 85 meter diameter ground-based telescope.

The subsystems include: 1) an Adaptive Optics System which removes the distortion caused by Earth's atmosphere using a many-element deformable mirror, 2) the Dual Star Module that uses one star as a reference while studying a more distant star, 3) the Coude Train Beam Transport that combines the beams of light, 4) a Delay Lines and Metrology system which, under the assumption that light from a given star will reach the two telescopes at separate times due to the varying distances of the two to the star, uses these varying distances to determine the distance of the star, 5) a Fringe Tracker that measures interference and syncs the twin telescopes, 6) the Angle Tracker that corrects for small tilts in light beams so that all beams overlap once they are combined, and finally 7) a Nulling Combiner which cancels out light from a star so that the dust surrounding the star may be studied.

With this technology, the primary goal of the Keck Interferometer is to measure the amount of dust surrounding nearby stars. This will provide information about planet formation around other stars.

Terrestrial Planet Finder

These observatories all lead up to the Terrestrial Planet Finder program. The Terrestrial Planet Finder consists of two separate but complimentary observatories. Its purpose, as declared by NASA, is to "conduct advanced telescope searches for Earth like planets and habitable environments around other stars".[10] These two observatories, a visible light coronagraph and an infrared interferometer flying in formation, will measure and study the formation, size, temperature, placement, and composition of planets outside of our solar system.

These observatories and the Terrestrial Planet Finder will all help to uncover knowledge about how planets form by studying the dust around distant stars. In addition, NASA hopes to be successful in using these technologies to understand some of the most plaguing philosophical questions of our time: How the Universe was created and is there life outside of Earth?

3.0   Methodology

We began this MQP by outlining the goals for the project. We then began to study the theories behind multiple satellite imaging. This began with a literature search of the library as well as a number of papers that Professor Hussein recommended. Multiple satellite imaging is a very complex process and to understand it thoroughly it is necessary to study a number of different aspects that we were not familiar with through

the standard aerospace curriculum. Many of these concepts related to optical properties.

Since optical properties are what make multiple satellite imaging possible, it was

necessary for us to become comfortable with concepts such as the frequency domain and

Fourier transforms.

During the latter stages of our literature search, we began to create a Matlab

simulation of an optical system. The simulation began as a one dimensional single

aperture estimation. We created a generalized code so that we could input a standard

signal, such as a sine wave or a square wave, isolate a small portion of the signal, Fourier

transform it, and estimate the original truth signal. Due to a limited amount of initial

experience using Matlab a large amount of time was spent learning the software features

and basic commands. There is also some amount of difference between real optical

operations and the mathematical operations that represent those functions. The Fourier

transform operations in particular took us some time to understand, as well as the

difference between the field of view and the aperture size. Field of view and aperture

size are inversely proportional with larger apertures able to capture a smaller field of

view. The entire issue of precision stellar imaging is the ability to concentrate a large

amount of incoming light from a source onto a receiver. This is different than standard

imaging on earth.

With standard imaging, we can use a larger lens that allows us to capture more

light. Due to the incredible distance between the source and the imager, apertures need to

be larger than s standard lens allows. Instead, the light is reflected off of several mirrors

to focus it on a much smaller area. In the Hubble Space Telescope, the light collected

passes through a tube with light absorbing panels on the sides so that the light that

eventually hits the sensors is from directly in front of the satellite and not from the surrounding area.

The field of view is dependant on physical characteristics of the optical instrument which can be altered but only slightly. Instead, multiple satellite imaging proposes to greatly enlarge the aperture size and thus achieve very high resolution while maintaining a similar field of view to current stellar imaging systems. One of the difficulties we encountered in Matlab, was that as our program only allowed us to change the field of view, instead of the aperture size, which is essential to truly approximate our proposed system. This demonstrates the need for physical testing of multiple satellite imaging concepts.

We then wrote Matlab code for a multiple aperture system in one dimension building on the previous code. This code demonstrates how two apertures would work together to provide greater coverage of the wave plane in the frequency domain. This increase in coverage creates an enhanced estimation of the truth function over the previous single aperture simulation.

The next step was to change the code to make it generic for n number of apertures and any motion chosen by the user. The code was changed so that there were multiple inputs that determined the looping of the code throughout the time it ran. Instead of each number of the point spread function being an integer each number corresponded to a frequency that we were imaging. Since low frequencies are near the middle of the point spread function and the Fourier transform of the estimated signal and higher frequencies are farther away from zero, it would be possible to see what frequencies are being imaged with the new code. The code was also modified so that the motion of n satellites could be

determined by the user and a symmetric motion was possible so that the individual point spread functions did not overlap and simulate two apertures in the same place imaging the same signal, which is physically impossible.

The Matlab code was then changed so that it would simulate imaging a two dimensional figure, and code was added so that any JPEG image could be modified for use. With any imaging system it is only possible to image some of the (temporal) frequencies that are emitted or reflected from the object. This is one of the reasons behind using black and white (i.e., monochromatic) and not color in the image reconstruction process. The JPEG image is selected and renamed. Then the two dimensions corresponding to color are deleted while the brightness of the JPEG is retained. Many of the changes that were made were simply changing the size of various matrices to be square rather than one row. The code was also deleted that removed the outsides of the shifted point spread function. This created a more concise modulation transfer function with a greater overall intensity than the sum of the shifted point spread functions.

4.0   MATLAB Simulation

In order to analysis the capabilities of a multiple satellite imaging system, we need to be able to simulate the system. For this project several Matlab codes were developed in hopes of modeling and understanding each step of the process. We began with a single aperture one dimensional simulation and progressed to a two dimensional simulation of a multiple aperture imaging system.

4.1 Stationary One Dimensional Single Aperture Simulation

The first code constructed was for a one dimensional stationary single aperture system with a periodic function as the input. This input signal, or truth function, is Fourier transformed, multiplied by the modulation transfer function, and then the product is inverse Fourier transformed to create an estimate of the truth function.

The first objective of the code is to define the input signal. The input signal is defined as a square wave for time defined between negative and positive 10. After we have defined the signal, we plot the signal as the truth function:
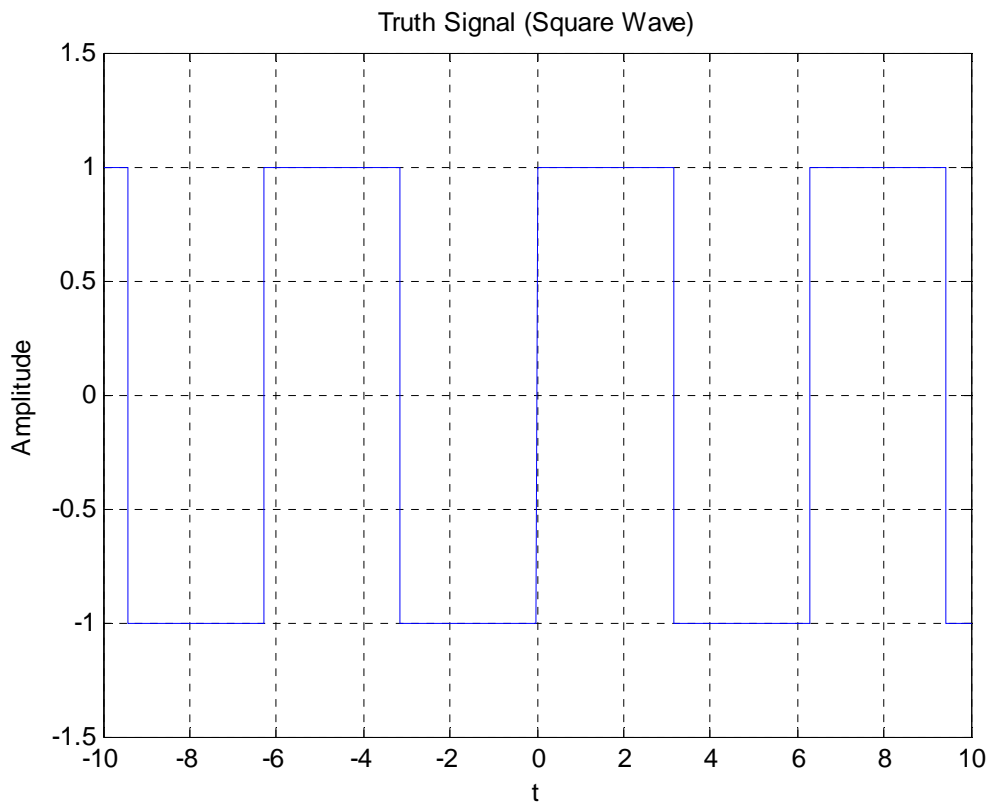
Figure 9: Square Wave Input Signal

Although the input signal here is defined as a square wave, this may be changed to any function of *t*.

Next we define the picture frame function. The picture frame function, as discussed earlier is the projection of the entry pupil onto the image plane. Here we define a rectangular picture frame function. This could be changed for a circular picture if desired. There are two distinct apertures defined within the code. The first is a larger picture frame function represented by all ones as shown in Figure 10:
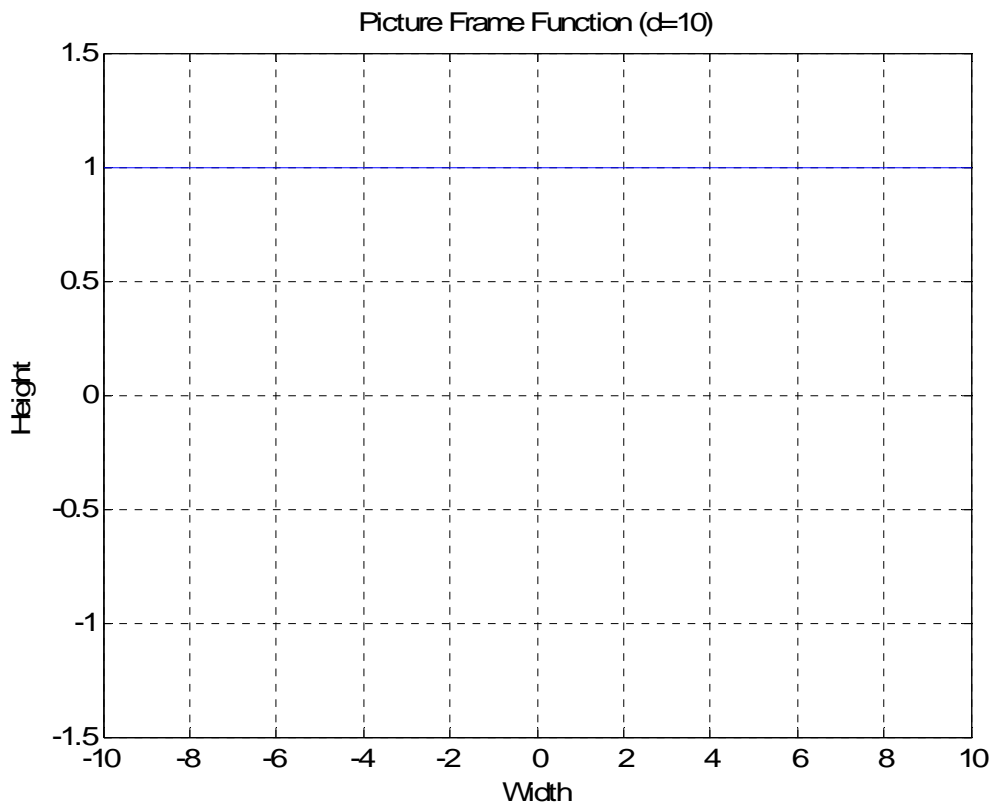
Figure 10: Picture Frame Function for *aperture1*

The second picture frame function is smaller with ones only from –*d* to *d*; where *d* represents one half the width of the picture frame function. The value of *d* may be changed to whatever value is desired. Here we selected *d=0.1* so as to show a much smaller picture frame:
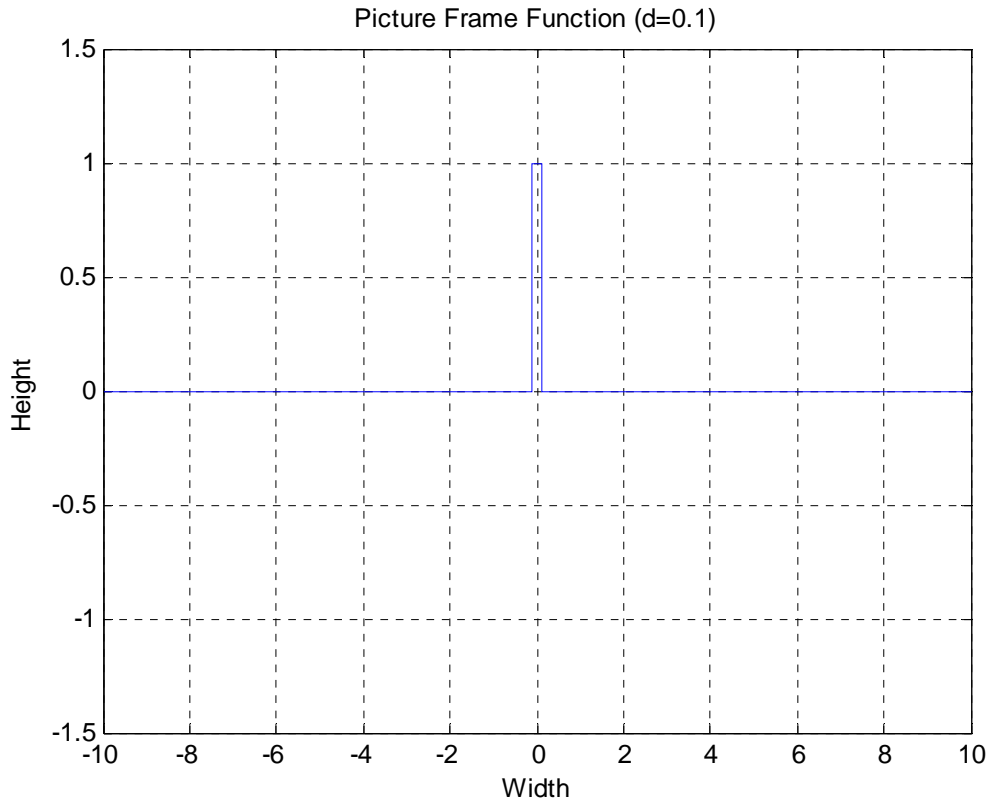
Figure 11: Picture Frame Function for *aperture2*

In imaging, the point spread function represents the efficiencies with which specific wavelengths may be represented. Mathematically, the point spread function is the Fourier transform of the picture frame function. For *aperture1*, the corresponding point spread function is shown in Figure 12:
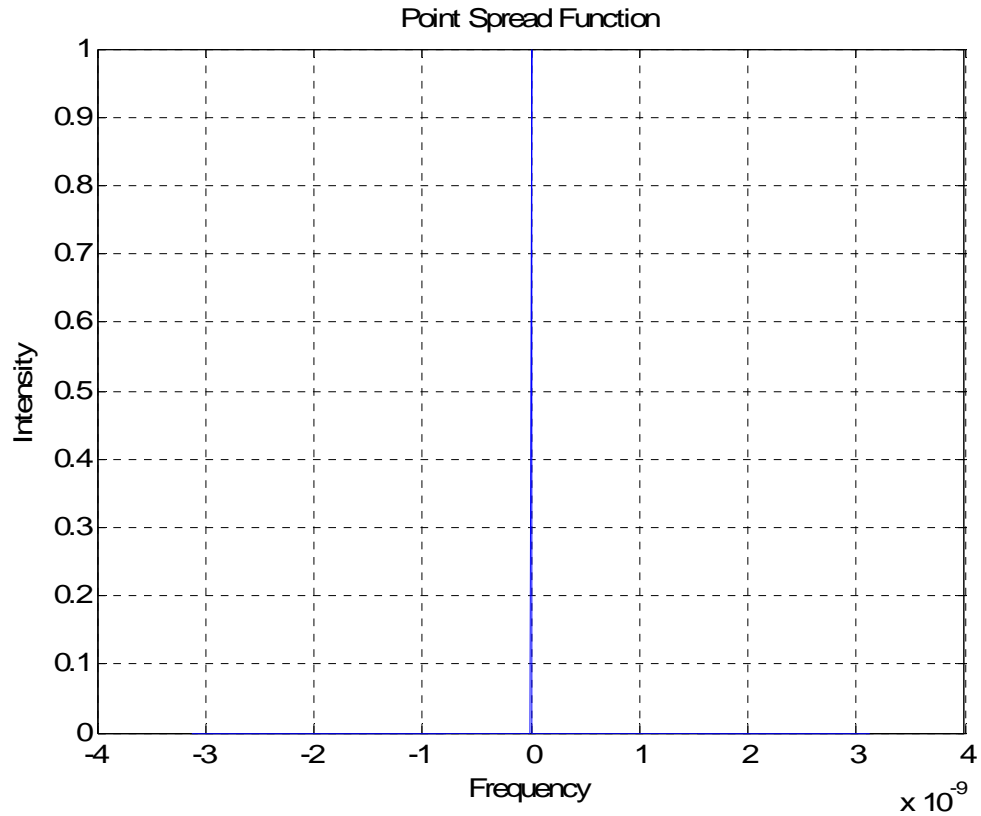
Figure 12: Point Spread Function for *aperture1*

Here we notice that there is a sharp spike located approximately at the horizontal origin with zeros for all other values. With *aperture1*, we will have very high efficiencies with lower frequencies and virtually no capability at detecting high frequencies. For *aperture2*, we defined the picture frame function to be as small as matrix compatibility would allow:
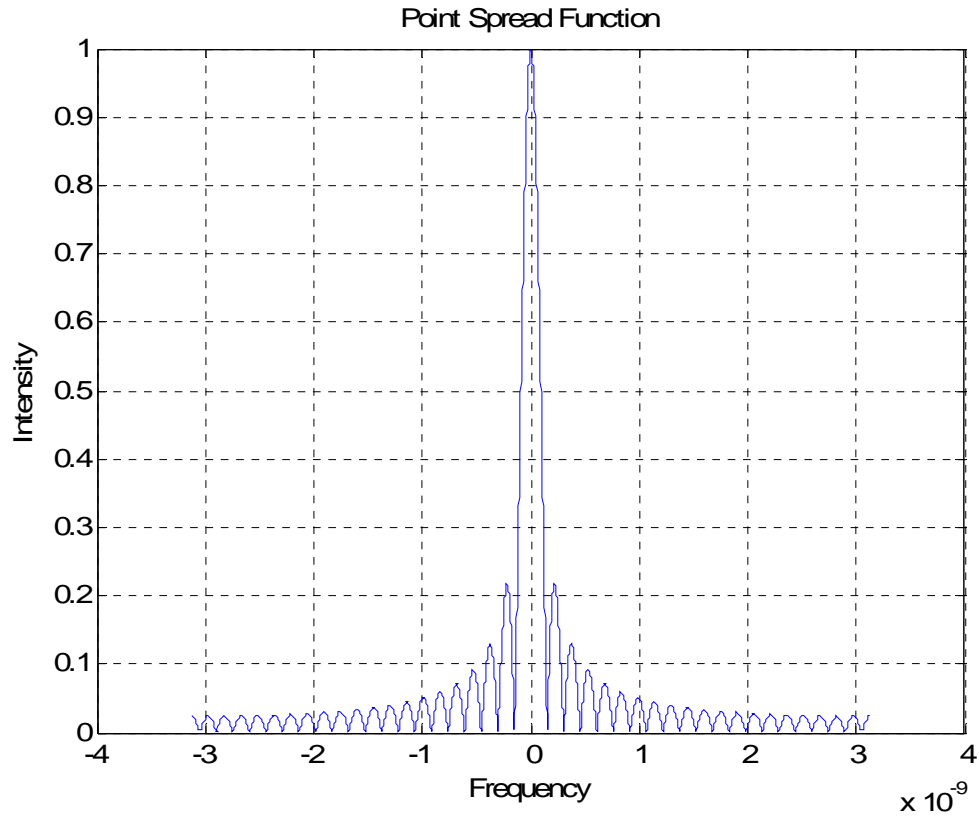
Figure 13: Point Spread Function for *aperture2*

With *aperture2*, we still see a central peak, but we now see a diminishing ripple as the frequency increases. There are some blind spots, but we have a better capability of determining higher frequencies than the point spread function for *aperture1* allowed.

Next, the truth signal is Fourier transformed and then multiplied by the point spread function provided by *aperture2* since it provides the best range for frequency efficiency. After these two are multiplied, the result is inverse Fourier transformed yielding what is known as the image estimate or the picture:
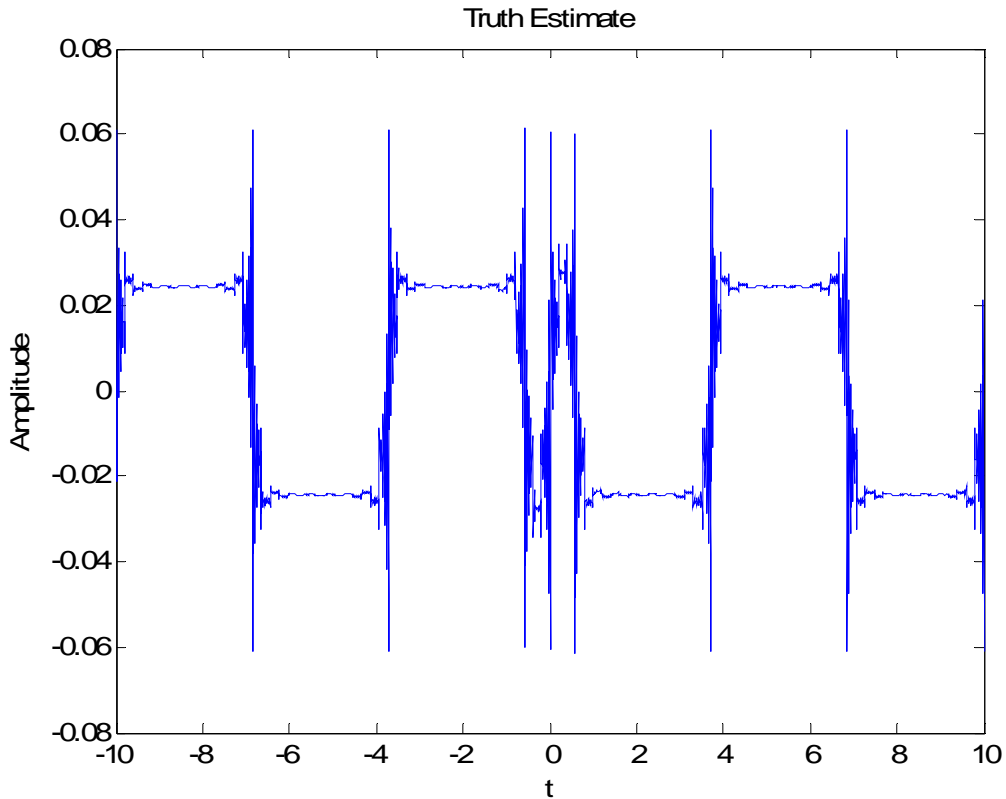
Figure 14: Resultant Estimate for *aperture2* with *d*=0.1

This is still not a clear square wave. While there is a square wave pattern, the wavelength is not constant and there are sharp spike outside of the range of the truth object. However, this is still a better estimate than if *aperture1* was used. This is because the variable *d* in the coding is not the size of the aperture as was originally thought, but the size of the picture frame function. We originally assumed that an "*aperture*" defined in the code defined the size of the camera or telescope with which we are imaging. Under this assumption, the larger the value *d*, the better the output estimate.

Deep space imaging focuses on objects with very large ranges, some light years away. Essentially, these objects are assumed to be point sources. If we have a smaller picture frame function or field of view that fits tighter around the object, it will yield a

better estimate than the larger picture frame function which only adds unnecessary data.

Below are some graphs to help illustrate how the estimate increases as the value of d

changes:

d	Point Spread Function	Estimate
1		
.05		
.01		

Table 1: Table Correlating d with Resultant PSF and Truth Estimate

4.2 One Dimensional Multiple Aperture Simulation

While there are many different possible configurations for a multiple aperture array only two models were chosen to be simulated. For these simulations, there are only two apertures used to simplify the number of possible orientations. The first model describes two satellites positioned at a given distance away from one another. The resulting modulation transfer function and truth estimate are shown below.
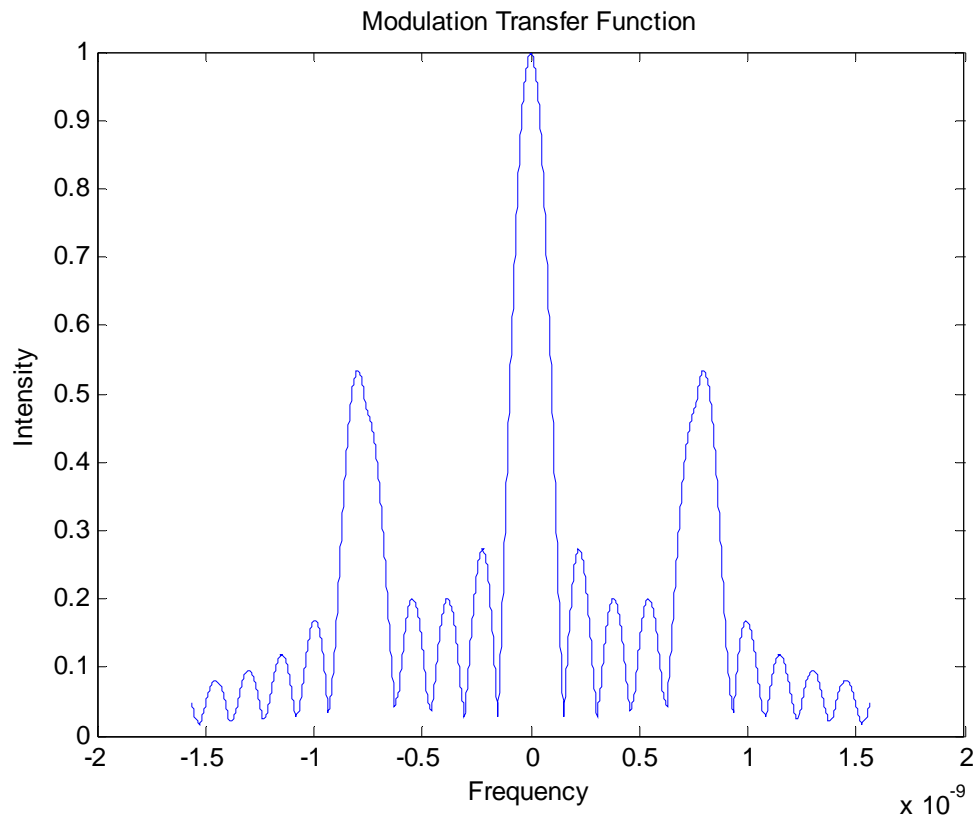
Figure 15: Point Spread Function for Stationary Multiple Aperture System
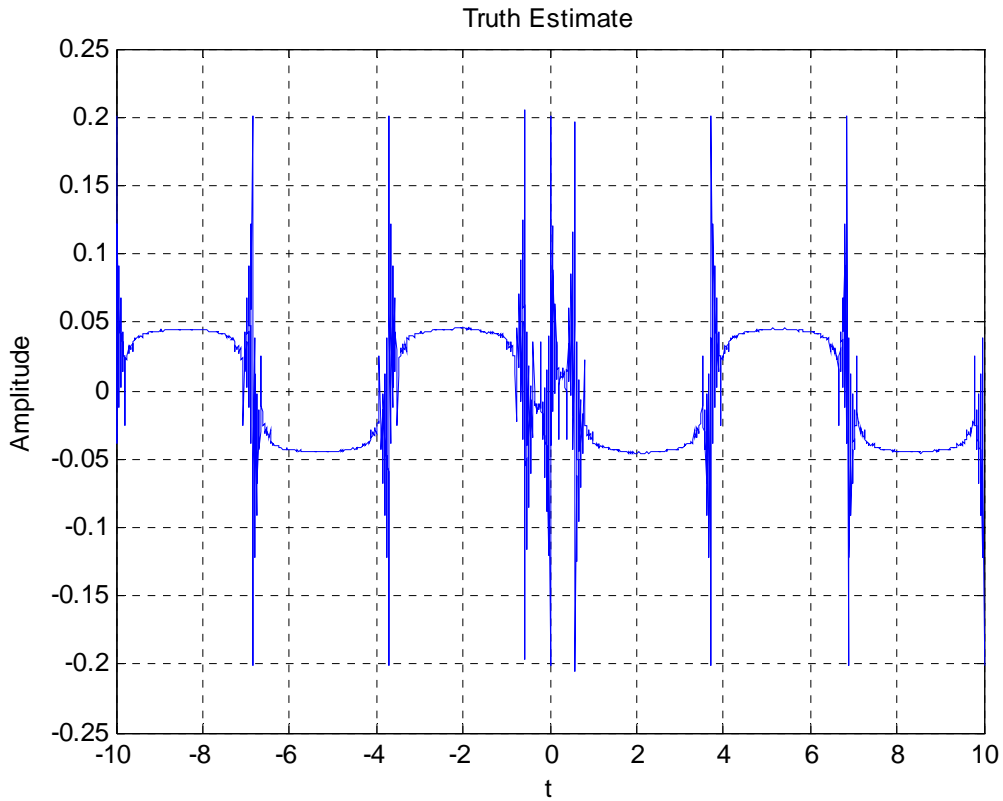
Figure 16: Resultant Estimate for Stationary Multiple Aperture System

The second model describes two apertures that begin at a common point and move away from each other at a constant velocity. As the two apertures move away from the origin, the *PSF* is shifted as if there were satellites located at those instantaneous positions. This motion results in an average increase of the intensity for the higher frequencies. In the above modulation transfer function for the stationary array (Figure 17), there are two significant peaks at approximately $\omega = \pm.8x10^{-9}$. In the modulation transfer function for the moving satellites, seen below, there is an almost even intensity value across the frequencies of interest. The modulation transfer function shown below is an increase from the original point spread function corresponding to a single stationary

aperture since it does not have any blind spots or points where the intensity is equal to
zero.
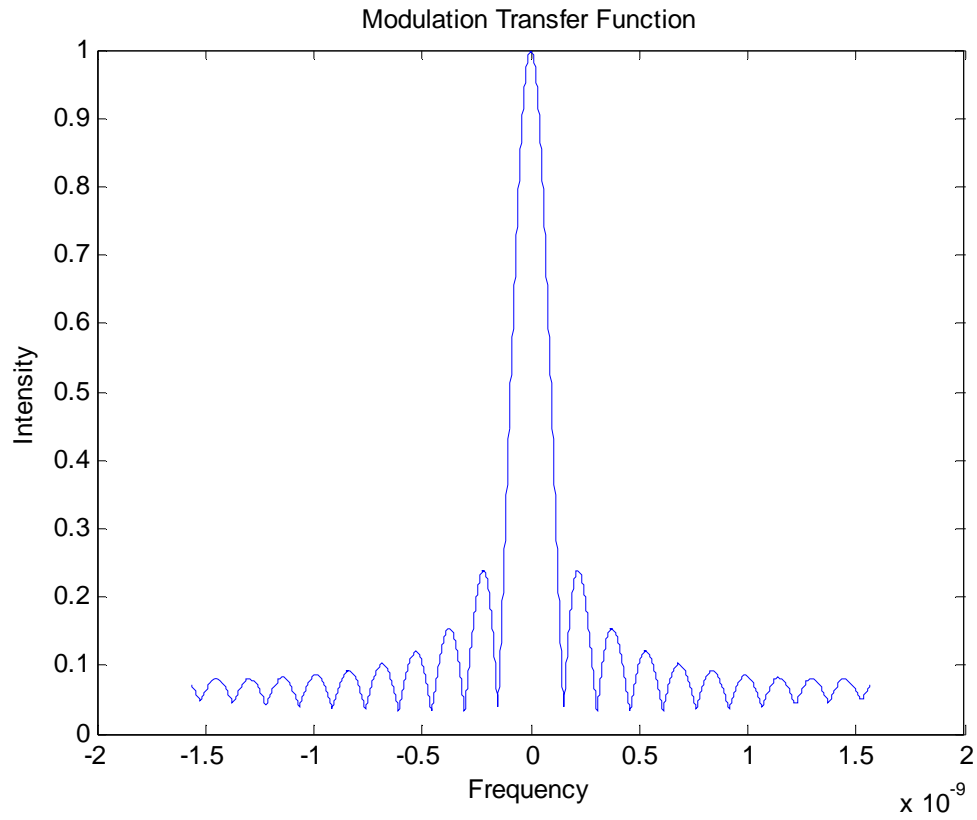
Figure 17: Point Spread Function for Moving Multiple Aperture System
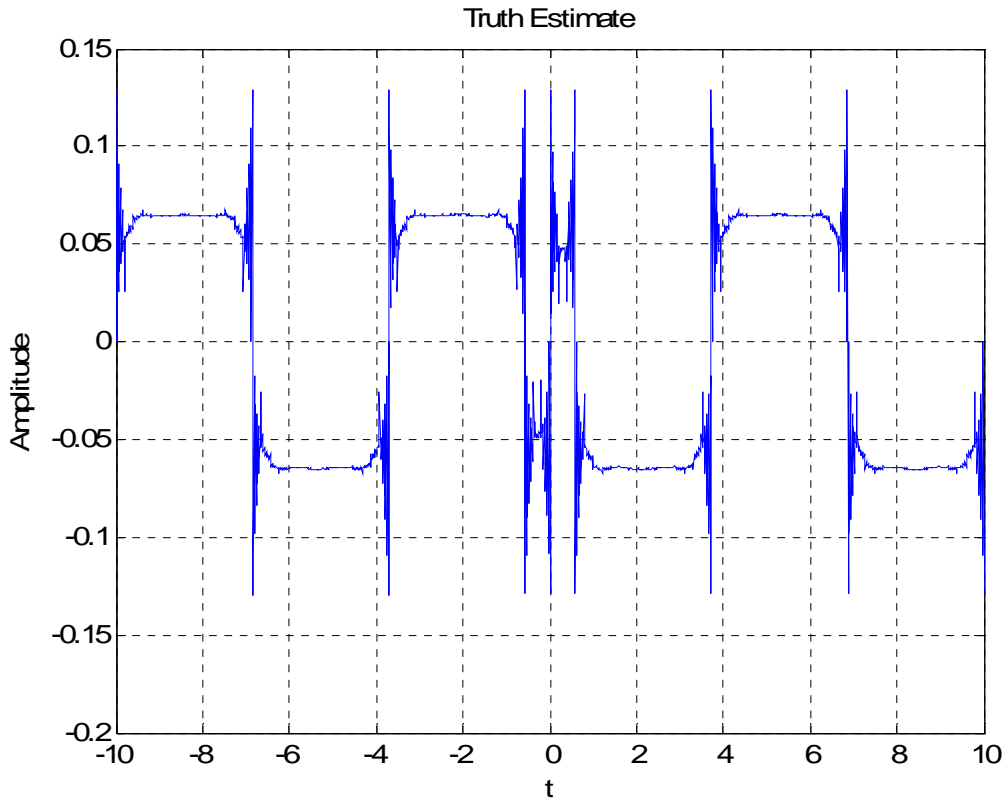
Figure 18: Resultant Estimate for a Moving Multiple Aperture System

The motion of the satellites results in a more uniform increase of intensity across all wavelengths where as the stationary array only results in an increase in intensity over a small range of frequencies.

4.3 One Dimensional Matlab Toolbox

Finally, we constructed a Matlab toolbox for processing one dimensional signals, given a linear array of *N* of satellites. The toolbox constructs the resultant Modulation Transfer Function and an estimate for the one dimensional truth signal. First, we must define the variables of interest to the simulation. In this toolbox, *range* is the estimated distance between the linear array of satellites and the source of the signal. For this

experiment we assume the range to be 10^{16} meters. *Lambda* is defined as the wavelength of interest, or the wavelength of the signal. In this simulation we assume that the input signal is occurring at a wavelength equivalent to that of infrared electromagnetic waves, *Lambda*=10^-6 meters. Next, we must define the composition of the linear array of satellites. We assume an origin about which the satellites are positioned and rotating around. However, the results output by the code are instantaneous. Two variables are necessary for the definition of the satellites' positions. The first of these variables is *D* the minimum distance between two satellites. The next variable is the matrix *X* which defines the positions from the origin.

Next, we define the truth signal. Similar to the previous one dimensional simulations, a square wave is used as the truth signal. The square wave is defined for an independent variable, *t*, with a step of *deltt*. For example, if *deltt=.1* and *t=[0:deltt:1]* then *t=[0 0.1 0.2 0.3 0.4 0.5 0.6 0.7 0.8 0.9 1.0]*. So then we define the square wave:
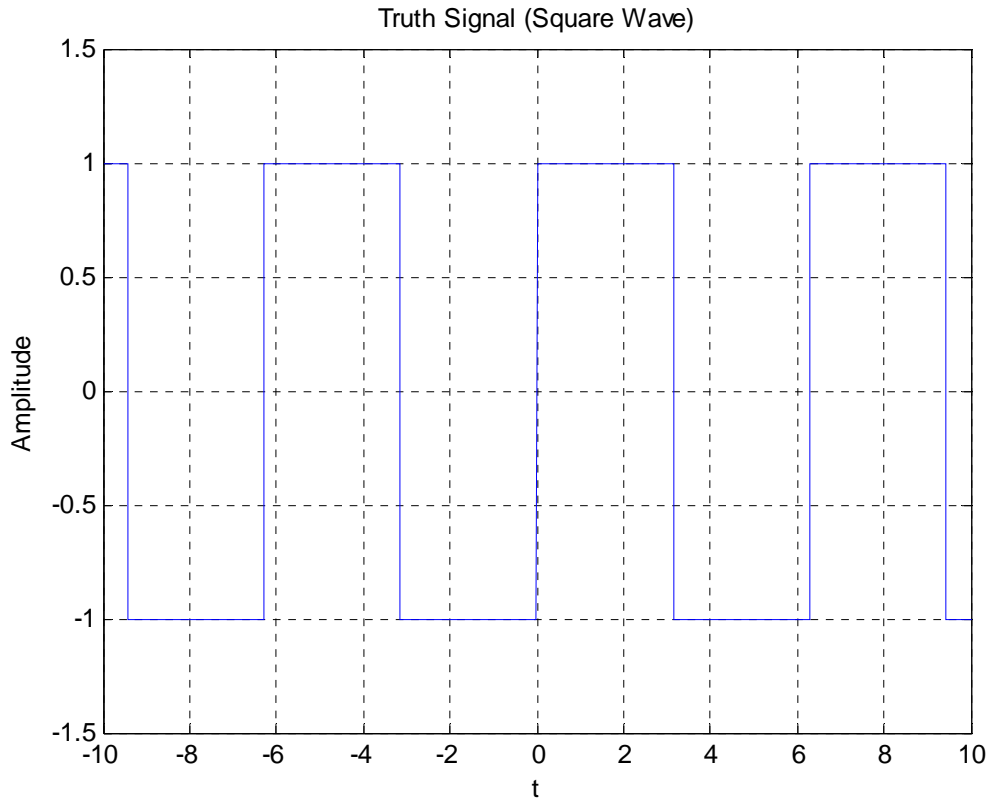
Figure 19: Square Wave Input Signal

Next we define the field of view function. As previously discussed *d* is one half of the width of the field of view function. The narrower, the field of view function, the wider the point spread function. The resultant point spread function for one satellite is found by taking the Fourier transform of the field of view function. The point spread function shows how well energy at a given frequency is imaged by a single aperture system with 1 being the best and 0 the worst. The field of view function and resultant point spread function for one satellite are seen below:
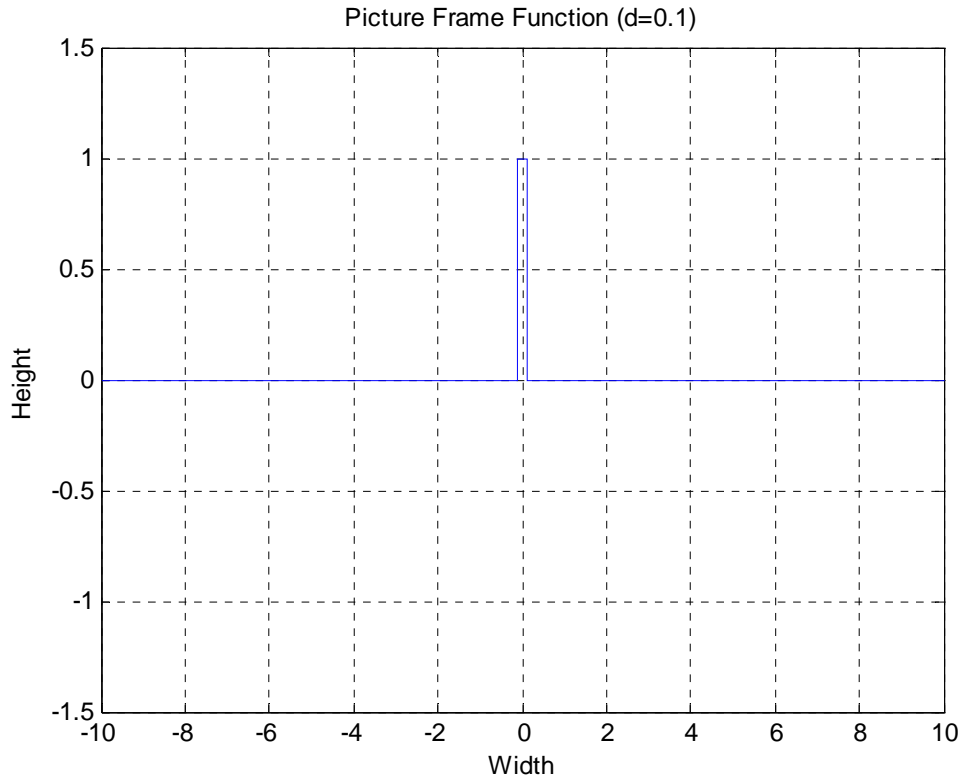
Figure 20: Field of View Function for a Single Aperture System
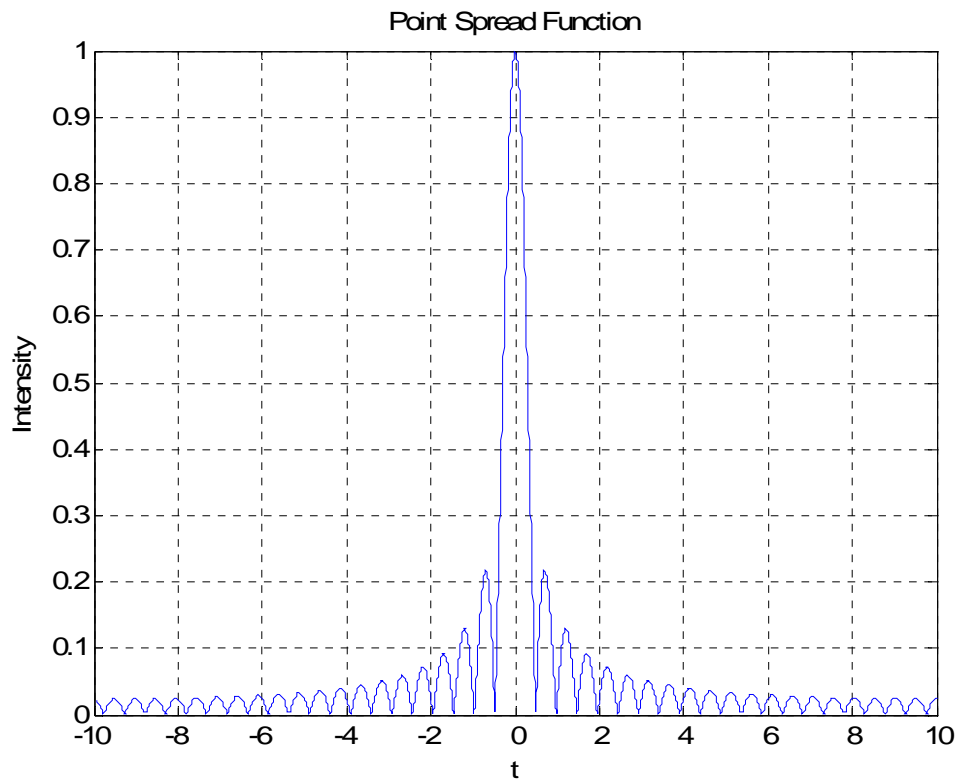
Figure 21: Point Spread Function for a Single Aperture System

However, we need to determine the proper range of frequencies against which we should plot the point spread function. Contrary to what is seen above, it should not be plotted against the independent variable t. In order of determining the proper domain of frequencies, we must first determine the sampling rate. The sampling rate, S, is defined as:

$$S = \frac{1}{Lambda * range}$$

From this, we may determine the appropriate domain of frequencies by using the following equation:

$$\omega = \frac{S(-10 : 10)}{deltt * 64}$$

When $Lambda = 10^{-6}$m and $range = 10^{16}$m, we find that the sampling frequency is 10^{-10} and that the frequencies of interest range from negative $4*10^{-9}$ to positive $4*10^{-9}$. Now we plot the point spread function against this range of frequencies resulting in the following:
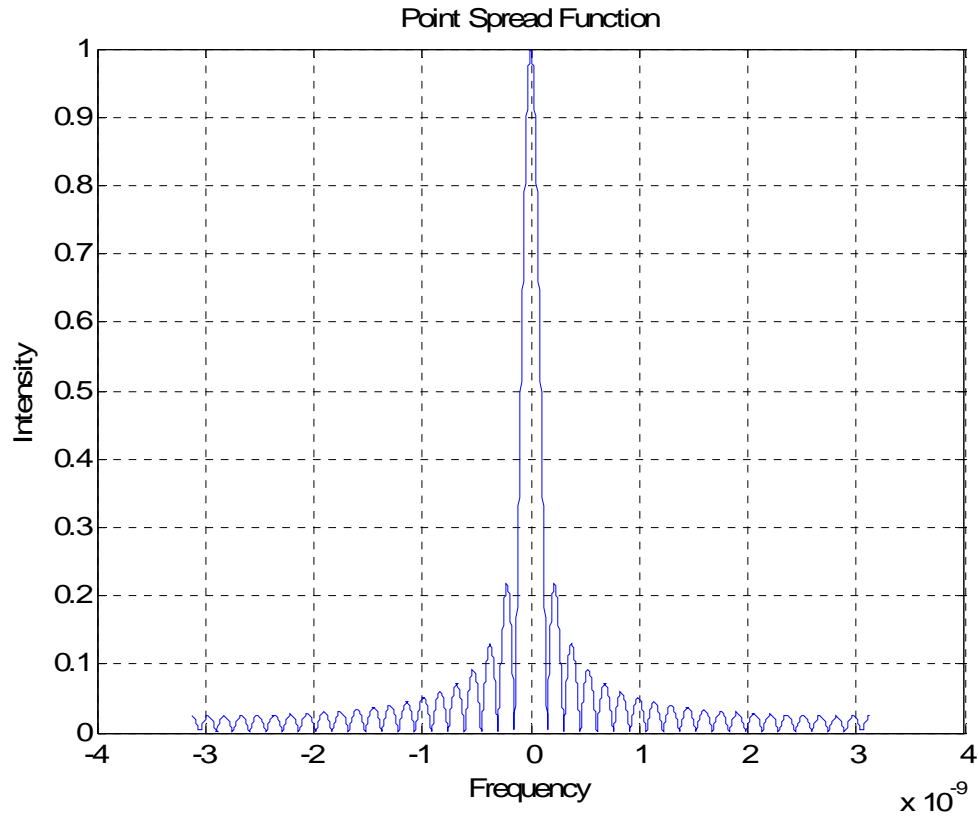
Figure 22: Point Spread Function vs. Frequency

As we can see from this point spread function, one satellite has high efficiencies with imaging low frequencies and little to no efficiency in imaging high frequencies. This means that we will be able to determine large contrasts such as the difference between black and white, but we will not be able to determine any finer details. In order of obtaining better efficiencies we add more satellites to the system and distance them apart. The compilation of the point spread functions from the individual satellites over time is known as the modulation transfer function. In order of calculating the modulation transfer function for a given system of satellites, we developed a series of loops in the Matlab code.

The first of these loops is the *i* loop. This loop in the code is purely for integration purposes. It defines a time interval over which we integrate the modulation transfer function. This is used to simulate the time over which light is taken in by a mirror of a satellite. The longer the period of time for which light is gathered, the better the estimate will be. This is due to the fact that we are collecting more data to process and can therefore be more assured of what the estimate shows us since we have more data upon which to base our estimate.

The next loop is the *j* loop. This loop defines one satellite to be held constant for the duration of the loop. Not only do we need to calculate the contributions from individual satellites, but we also need to consider the added effects between satellites. When we add more satellites to the system we are increasing the total resolution. For example, if two smaller satellites are placed ten meters apart, their equivalent resolution is of a satellite with a 10 meter diameter mirror. This is due to point spread functions resulting from the distance between the satellites. This is illustrated for a three satellite system below:
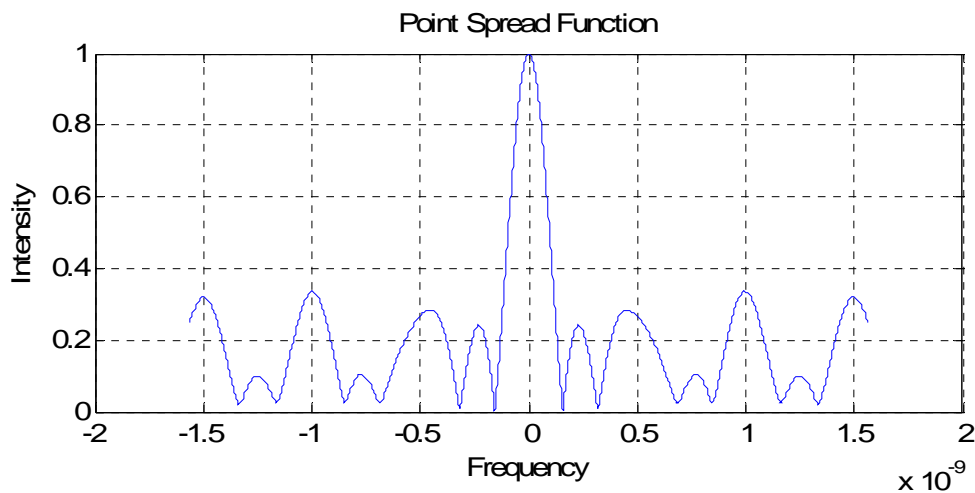
Figure 23: Modulation Transfer Function for Three Satellite System

The middle peak represents the point spread functions for the three individual satellites. This peak does not change because the maximum efficiency obtainable is one. However, we begin to see the added effects. There is a peak for each of the following:

a) The distance from satellite 1 to satellite 2

b) The distance from satellite 1 to satellite 3

c) The distance from satellite 2 to satellite 3

d) The distance from satellite 3 to satellite 2

e) The distance from satellite 3 to satellite 1

f) The distance from satellite 2 to satellite 1

The resulting modulation transfer function has seven independent major peaks including the central peaks. To determine these peaks, we need to hold one satellite constant and calculate the added effects of the distance between this satellite j and another satellite. For the j loop, we hold one satellite constant and define its position Q from the origin.

The next loop in the code is the k loop. In this loop we pick the second satellite for determining the point spread function. In the j loop we held a satellite still while now we calculate the added effects of the distance from j to k. We define q as the distance of satellite k from the origin. We then define a new variable *cuemn* as the distance between satellite j and satellite k:

$$cuemn = Q - q$$

Now that we have determined the distance between the two satellites, we need to calculate the resultant shift of a point spread function induced by this distance. In order to do this we introduce a new loop: the l loop. We define the range of l as being the

length of the frequencies of interest. The shift induced by distance between two satellites, *cuemn*, is given by:

$$\Delta\omega = \frac{cuemn}{Lambda * range}$$

After calculating $\Delta\omega$, we need to determine which component of the frequency matrix it is equivalent to. For a given component of the frequency matrix $\omega(l)$ we define a variable *dista* equal to the difference between $\Delta\omega$ and $\omega(l)$. We also define *dist1* equal to infinity. We compare the two and if *dista* is less than *dist1* then we redefine *dist1=dista*. This process is continued until *dist1* approximately equals *dista*. In this instance, we create and index variable *indexvalueA=l*. This variable defines the component of the frequency matrix, $\omega(l)$, that is equal to the necessary shift of the point spread function, $\Delta\omega$. We then define an equation for the appropriate shift and perform a *circshift* of the matrix *PSF* in Matlab. The compilation of the shifted *PSF*s, the modulation transfer function is denoted in the code as *KK*.

The next step is to integrate the effects over time. For a given time step the modulation transfer function may be approximated as:

$$M_i = M_{i-1} + \Delta t(KK)$$

We denote change in time by *dt* since it is denoted as the time step in the *i* loop. For each time interval we are adding to the original point spread function. As we add, we begin to see that the central peak has a maximum value larger than one, which is the highest possible value. To negate this, we divide by the central component which is also the maximum component, so that the central peak now has a maximum value of one.

The results are graphed for each time step so that growth of the modulation transfer function may be seen. Below we show the final modulation transfer functions and the resulting estimate of the truth signal for systems with varying numbers of satellites.

Number of Satellites	Modulation Transfer Function (MTF)
1	
2	

3	
4	
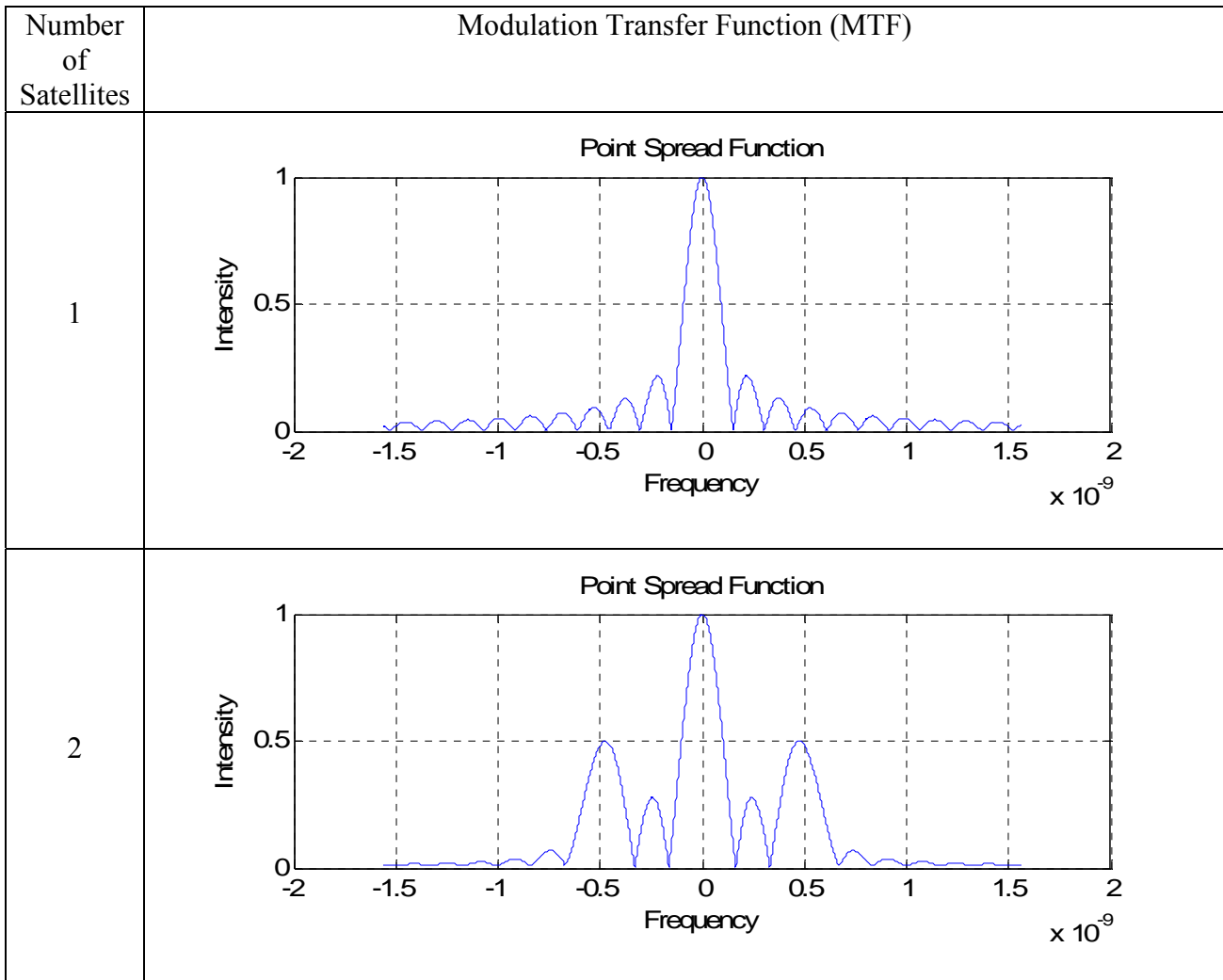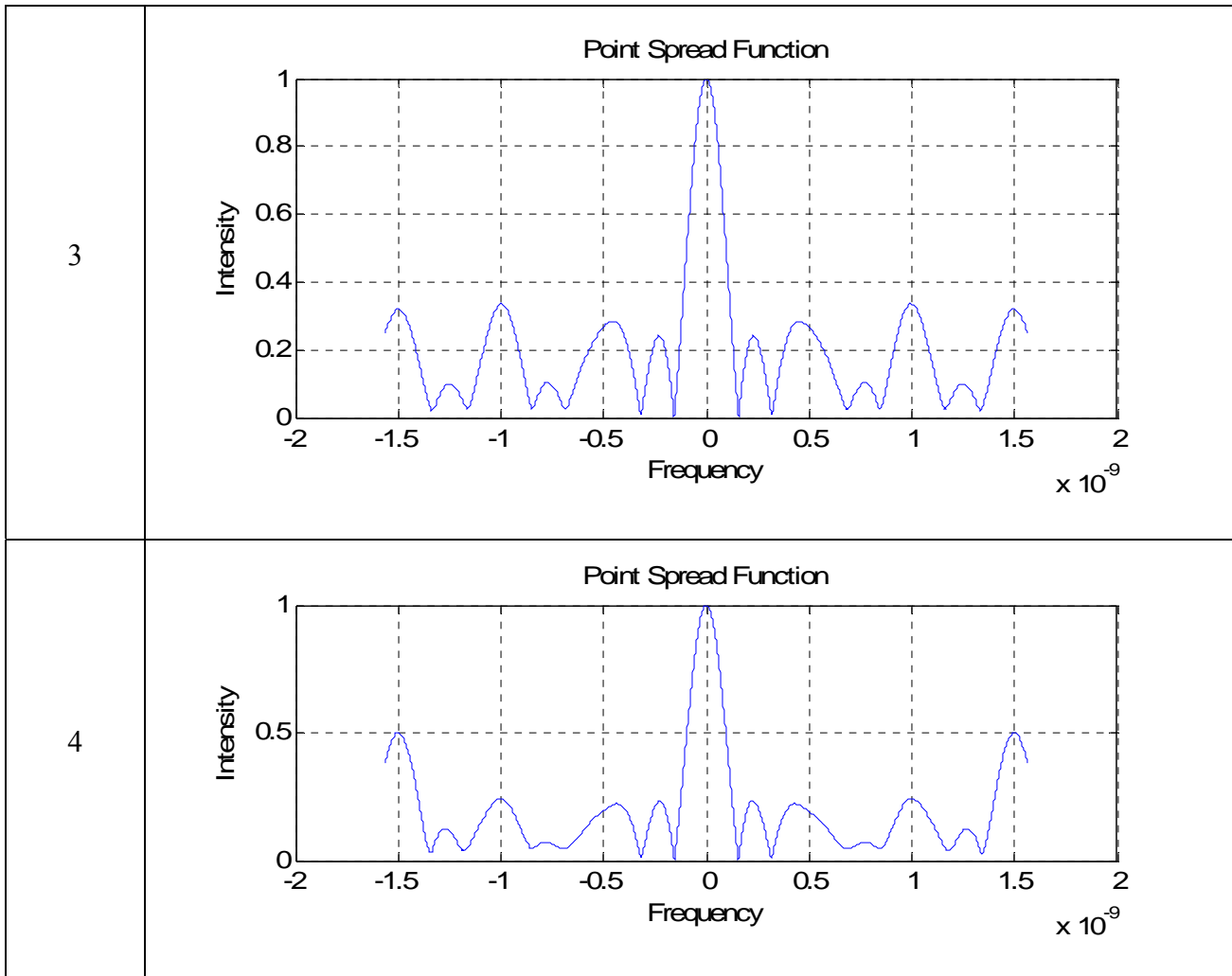
Table 2: Modulation Transfer Functions for Arrays of Varying Numbers of Satellites

Number of Satellites	Estimate of Truth Signal
1	 Truth Estimate
2	 Truth Estimate
3	 Truth Estimate
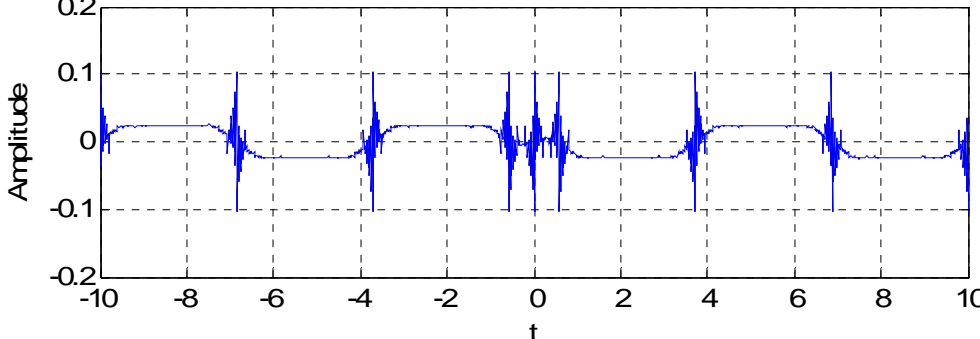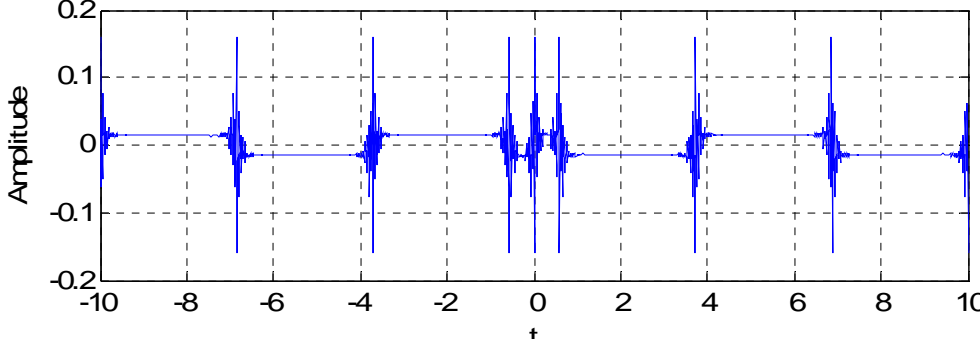
4	Truth Estimate
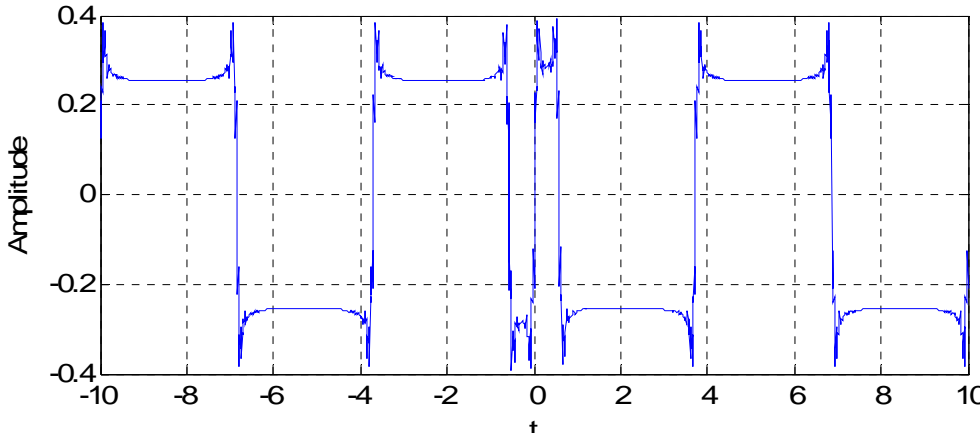
Table 3: Signal Estimates for Systems with Different Numbers of Satellites

In the first estimate, a system with one satellite, we see that the estimate is almost equivalent to zero which would represent no energy or no signal being read. As we add more satellites to the system, we see successive estimates evolving into a more clearly defined square wave. If we were able to have an efficiency of one for all wavelengths on the modulation transfer function, then the estimate would reflect a perfect truth signal. What we can see from Table 3 is that the error in the signal estimate decreases as we add satellites to the system.

Now we need to examine the effects of the individual parameters to the code. What happens if we hold all values to be constant except the range? The point spread functions are plotted for different values of *range* in Figures 24-26.
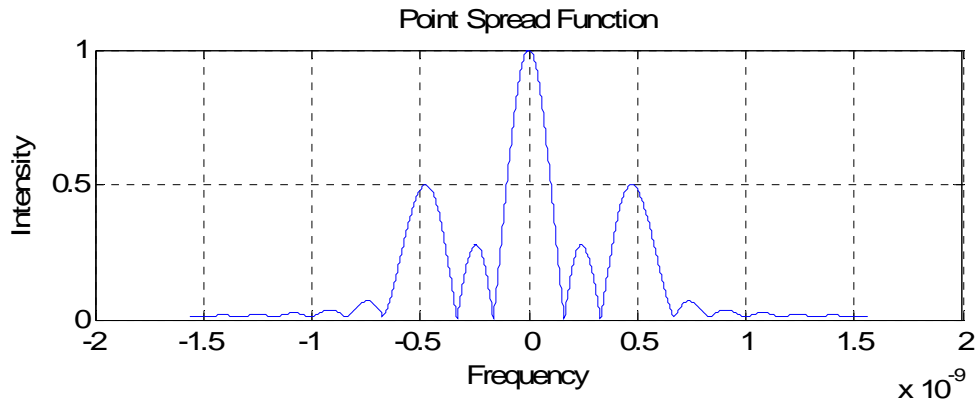
Figure 24: *PSF* **for** *range* $= 10^{16}$ **meters**
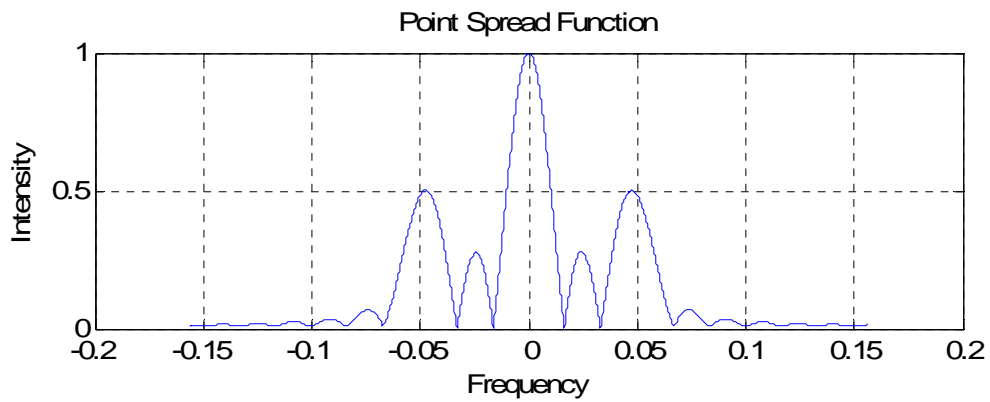
Figure 25: *PSF* **for** *range* $= 10^{8}$ **meters**
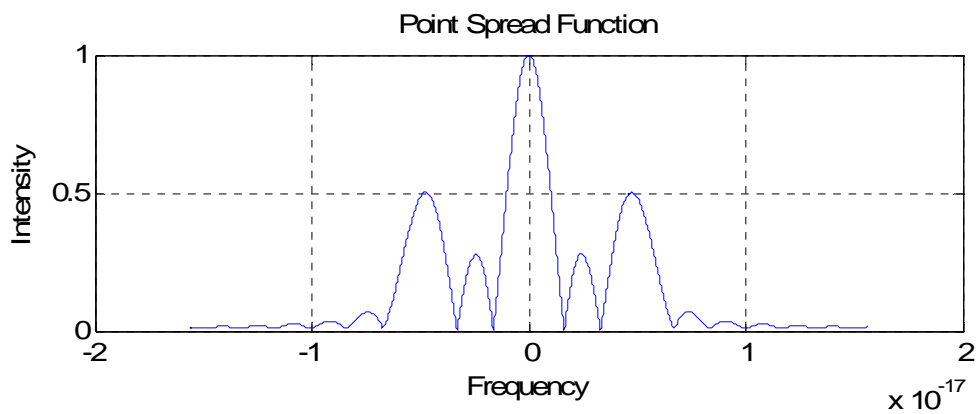
Figure 26: *PSF* **and Truth Estimate for** *range* $= 10^{24}$ **meters**

At first glance, the resulting point spread functions for the varying ranges are the same. Upon closer inspection we see that it is the same point spread function but that it applies to a different domain of frequencies. For *range* $= 10^{16}$ meters we see that the

appropriate frequency domain to which the point spread function is applied is on the order of magnitude of 10^{-9}. For *range* $= 10^8$ meters we see that the appropriate frequency domain to which the point spread function is applied is on the order of magnitude of 10^{-1}. For *range* $= 10^{24}$ meters we see that the appropriate frequency domain to which the point spread function is applied is on the order of magnitude of 10^{-17}. This shows that as the aperture is moved closer to the source that we gain efficiency at measuring the intensity at higher frequencies, and in contrast we lose efficiency at measuring the intensity at higher frequencies as the range is increased. This is confirmed by the fact that when you move closer to an object you are better able to discern its finer details.

Finally, we hold all parameters constant with the exception of D, the minimum distance between two satellites. The point spread functions and resulting truth estimates are plotted for varying values of D.
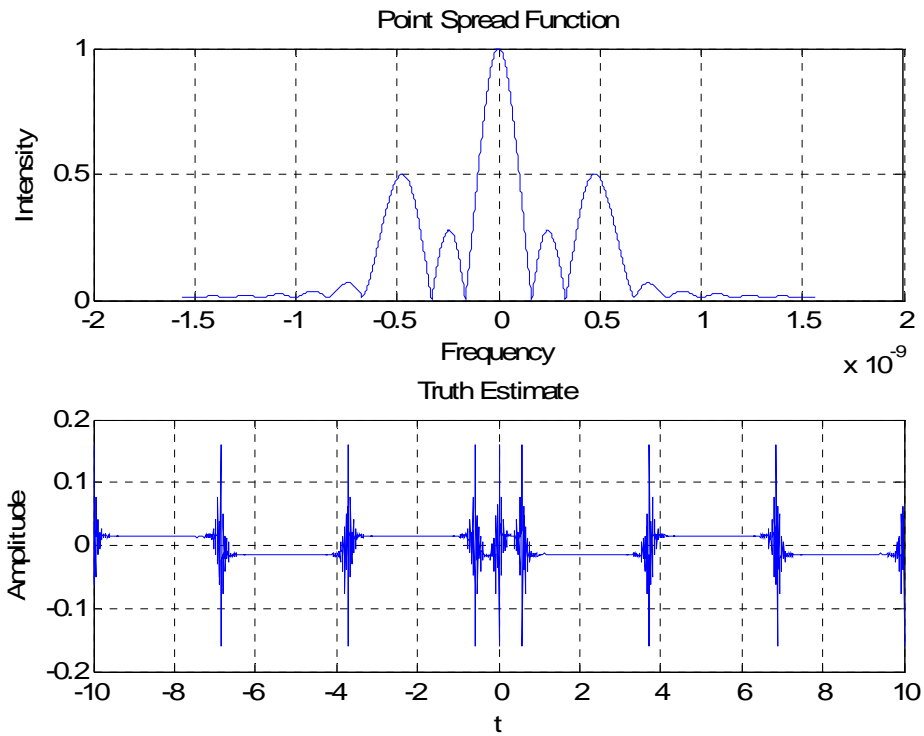
Figure 27: *PSF* **and Estimate for** *D* **= 5 meters**
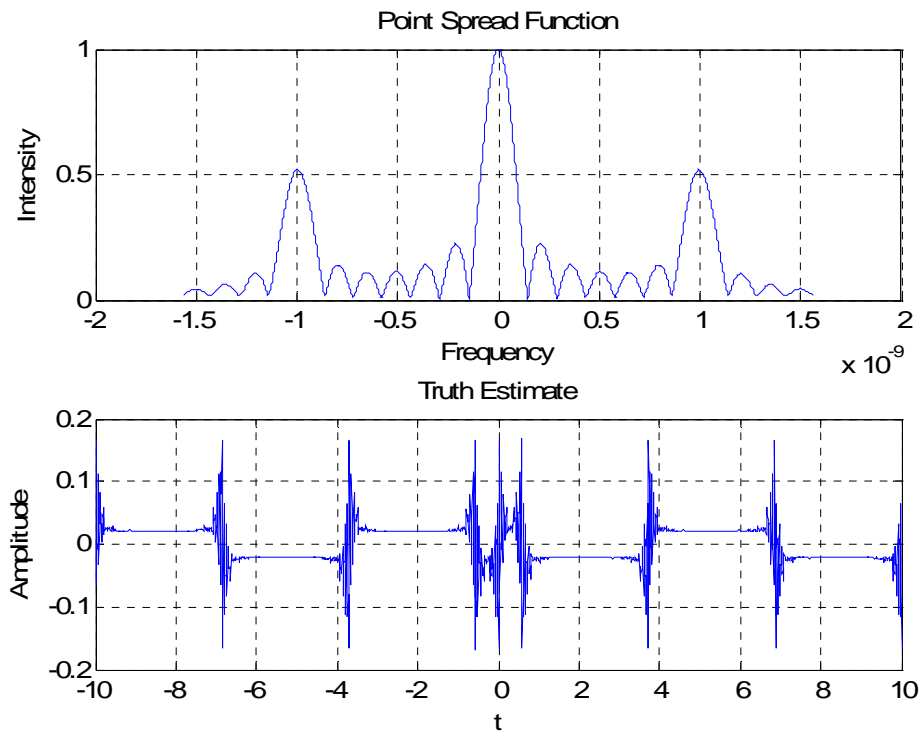
Figure 28: *PSF* **and Estimate for** *D* **= 10 meters**
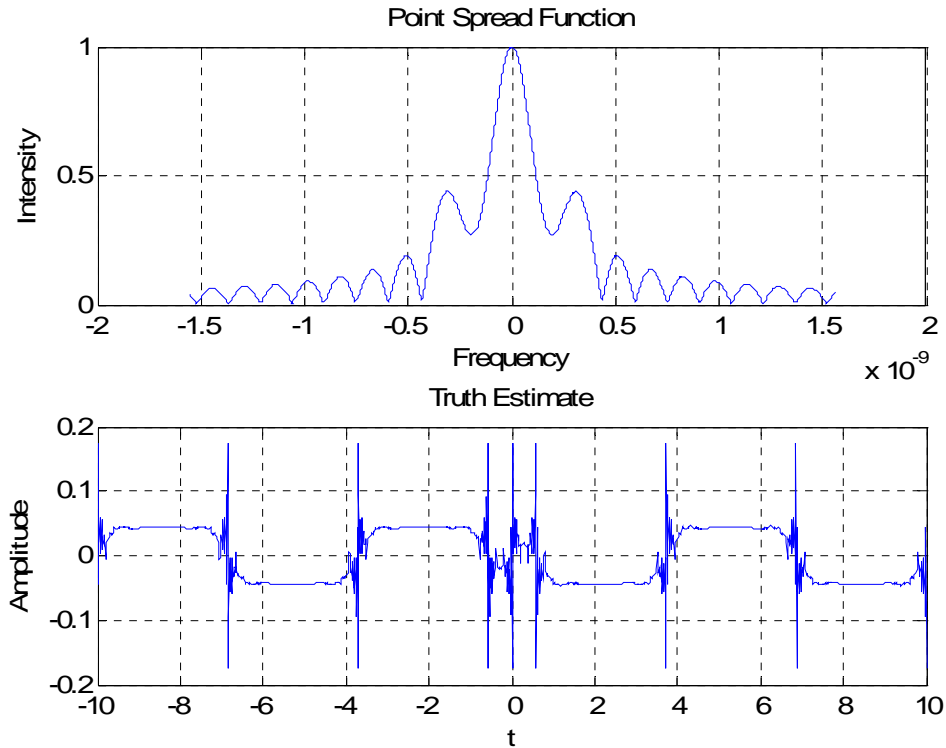
Figure 29: *PSF and estimate for D = 2.5 meters*

For D = 5m we have a considerable efficiency over the approximate frequency domain [-0.6*10^{-9},0.6*10^{-9}]. For D = 10 meters we have a considerable efficiency over the approximate frequency domain [-1.2*10^{-9},1.2*10^{-9}]. For D = 2.5 meters we have a considerable efficiency over the approximate frequency domain [-0.4*10^{-9},0.4*10^{-9}]. As we decrease the distance between the satellites, we see that the effects of the added resolution from the multiple apertures is not as noticeable as when we increase the distance between the apertures. This confirms the theory that if two satellites are located a given distance D apart that they have an equivalent resolution of an aperture with a diameter of D.

4.4 Single Aperture Two Dimensional Matlab Code

This code is relatively simple and is included in the two dimensional multiple aperture code, so that the difference between one aperture and multiple apertures with interferometric technology can be seen and analyzed.

It is important to first create a .mat file that includes the desired truth image with the name "*sat*". A .mat file saves all the current variables in the workspace on Matlab so that they can be accessed later when that file is opened. It is important that the truth image be a JPEG named "sat" because any other name or image type will not be processed correctly. For the purpose of these simulations, we used a JPEG file as the input or truth signal.

Figure 30: Truth JPEG

This code first creates a field of view whose width (*2d*) may be specified by the user. Here we show the field of view function with a width approximately equal to *1/10*th of the length of the input JPEG.
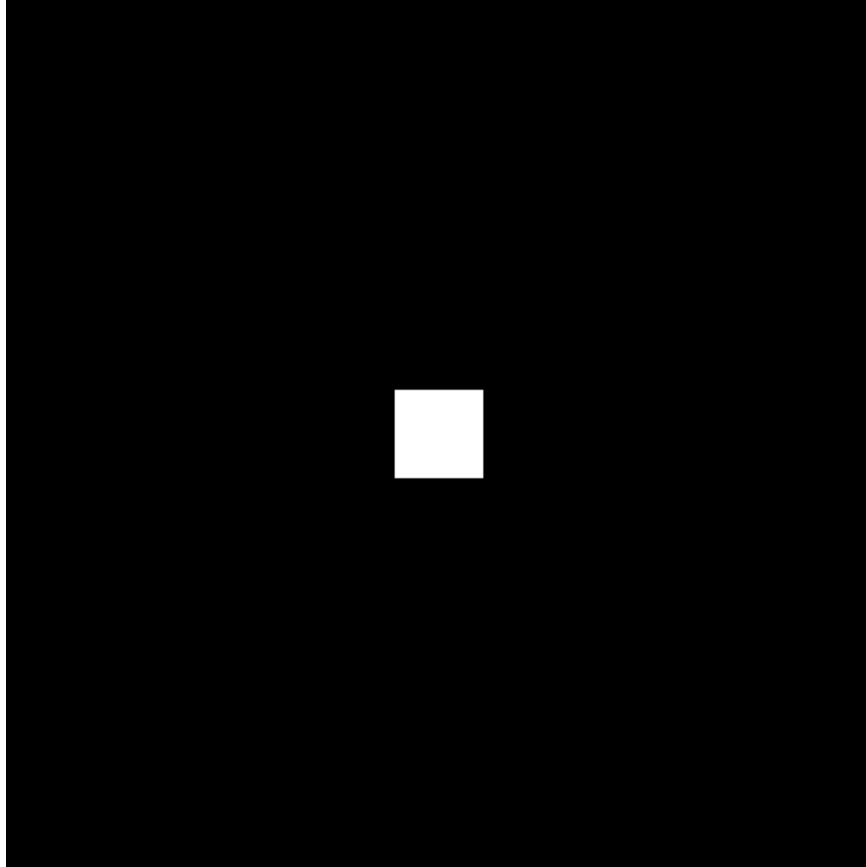
Figure 31: Field of View Function

This field of view (*fov*) which is a square due to physical limitations of imaging devices and ease of computation, is then two dimensionally fast Fourier transformed into the point spread function (*PSF*).
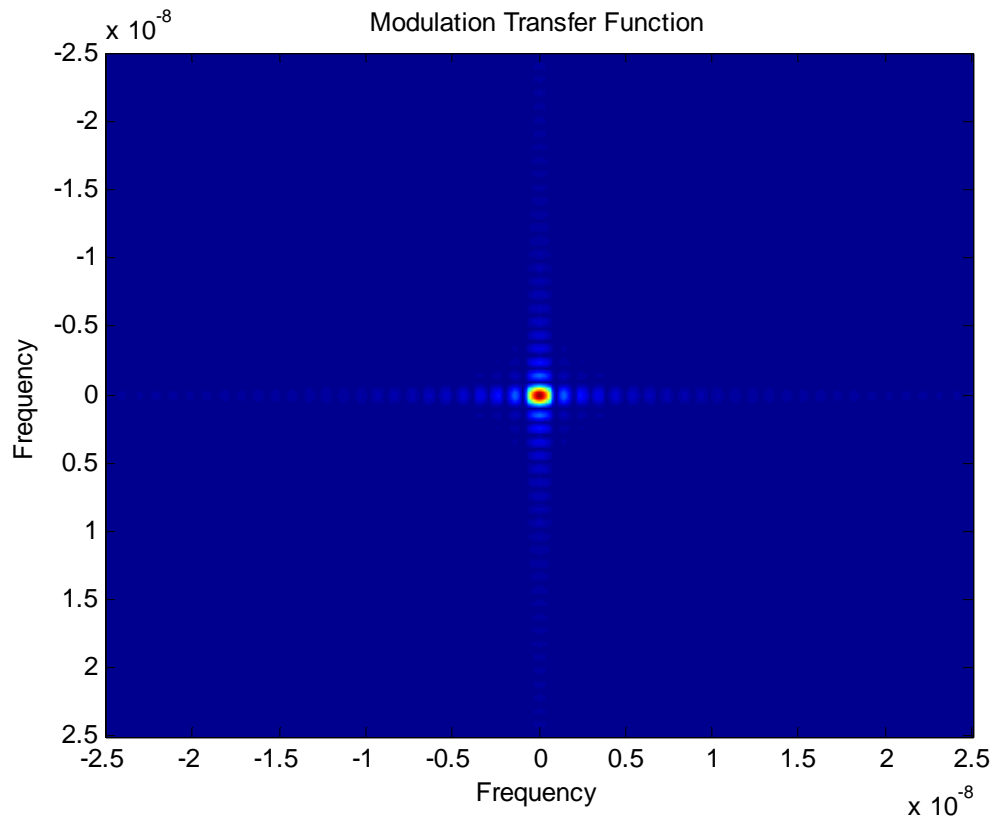
Figure 32: Two Dimensional Representation of the Point Spread Function
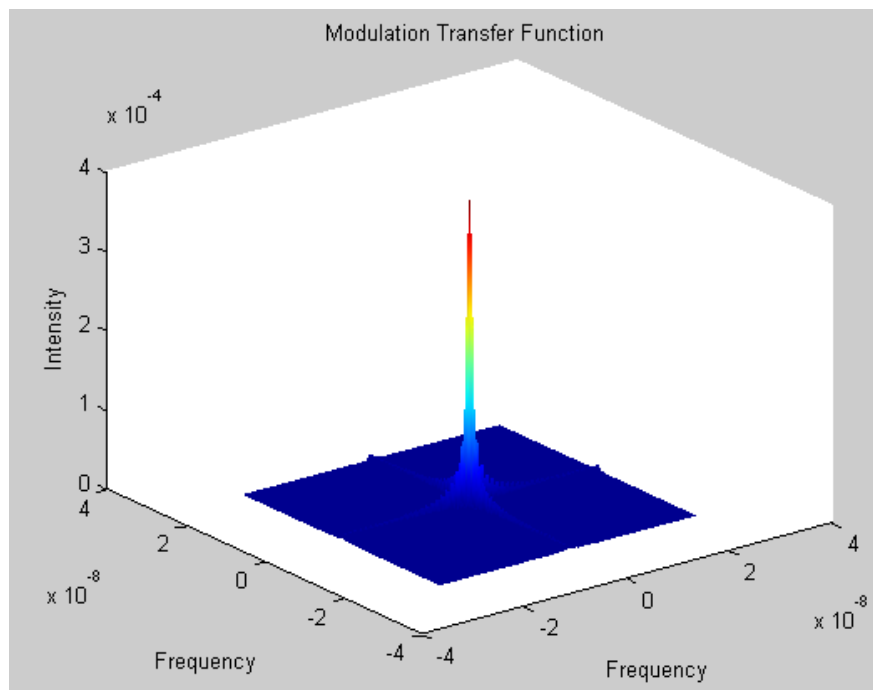
Figure 33: Three Dimensional Representation of the Point Spread Function

The variable *psf* is then scaled by a factor of one over the highest magnitude of psf

squared, due to propagation of waves from a sphere, so that the values are relatively low

and multiplied element wise by the two dimensional fast Fourier transform of the

adjusted input JPEG. The inverse Fourier transform is then taken and the absolute value

of that taken. This gives a single aperture approximation of the truth object.
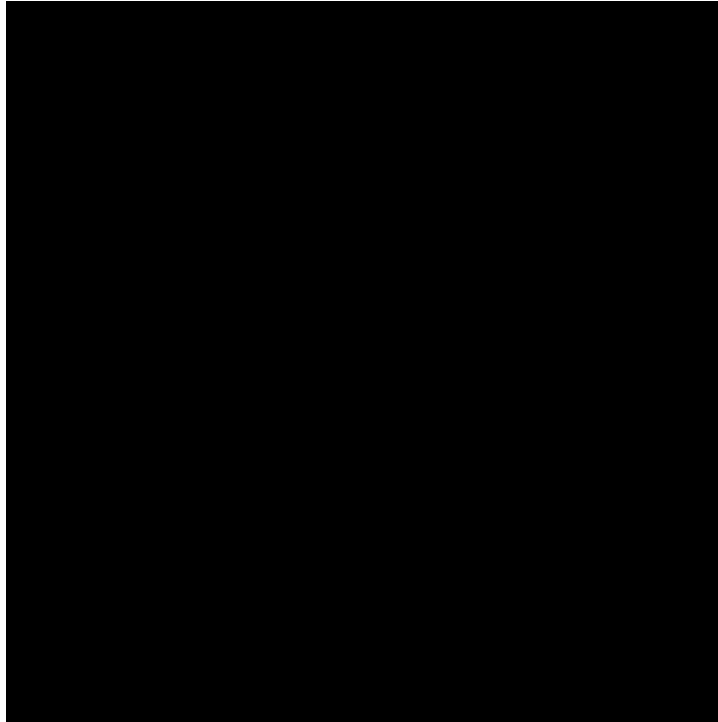
Figure 34: Resulting Estimate for a Single Aperture

As we can see from this estimate, one satellite is not enough to capture an image

in deep space imaging. We need to capture more signal in order to read any detail from

the energy originating light years away. We can obtain the increase in resolution by

adding more satellites to the imaging system.

4.5 Multiple Aperture Two Dimensional Matlab Code

The multiple aperture two dimensional simulation is more complicated than the single aperture simulation. It retains all of the code for the single aperture approximation and adds much of the code from the one dimensional multiple aperture simulation modified to be effective for two dimensions. There are a number of loops based on the interferometry and the compilation over time that would occur with a multiple satellite imaging system.

The truth image, the variable *sat*, is initially sized so that its dimensions are known and can be used for further processing. Then for the standard color JPEG the two degrees of the image matrix that correspond to color and divide the element that corresponds to brightness by the maximum brightness for a JPEG image, which is 255. This is also done if the JPEG is black and white. The result of both is an *m* by *n* matrix with values between zero and one.

The matrix is then changed to a standard size that will be used throughout the code so that element wise multiplication if possible. Then, we find the longest dimension of the matrix and declare it as variable I think its *nn*. Next we declare the long dimension of the matrix to be one pixel larger than the longest dimension so that there will be a central element about which the apertures rotate. This also applies for careful dimension JPEGs, which most pictures are even. Whether add black area around the matrix *sat* so that it becomes a square image. A square image is easier to manipulate than a general rectangle. The truth image is displayed so it will remain throughout the following reconstruction. This figure, denoted as "*Figure (1)*" in the code, is considered perfect and

any estimate that we create can be compared against it to evaluate the amount of error in the estimation.

Figure 35: Truth JPEG

Next, variables required to define motion and positions are declared. Lines 61-63 then declare the initial position of the satellites. The variable *tf* is declared to be the amount of time the simulation will run. The increment of the time step between each individual aperture location is *dt*. The variable *time* is a matrix with every time step. The code is also configured for any number of rotations described by the variable *rotations*.

The field-of-view is then defined as the *fov* variable. This represents the relative view angle that the aperture has and the amount of light that can be received. That means that a larger area of white in the *fov* variable means a wide angle lens and less resolution

at the plane of the truth object than a very small white square. A simple analogy is taking a photograph of a chess board from across a room. With a wide angle lens it is possible to see the entire checkerboard but the squares appear blurry. With a narrow, high magnification lens it is possible to see only one square of the chess board and any irregularities that a given square might have. The *fov* variable is then displayed.
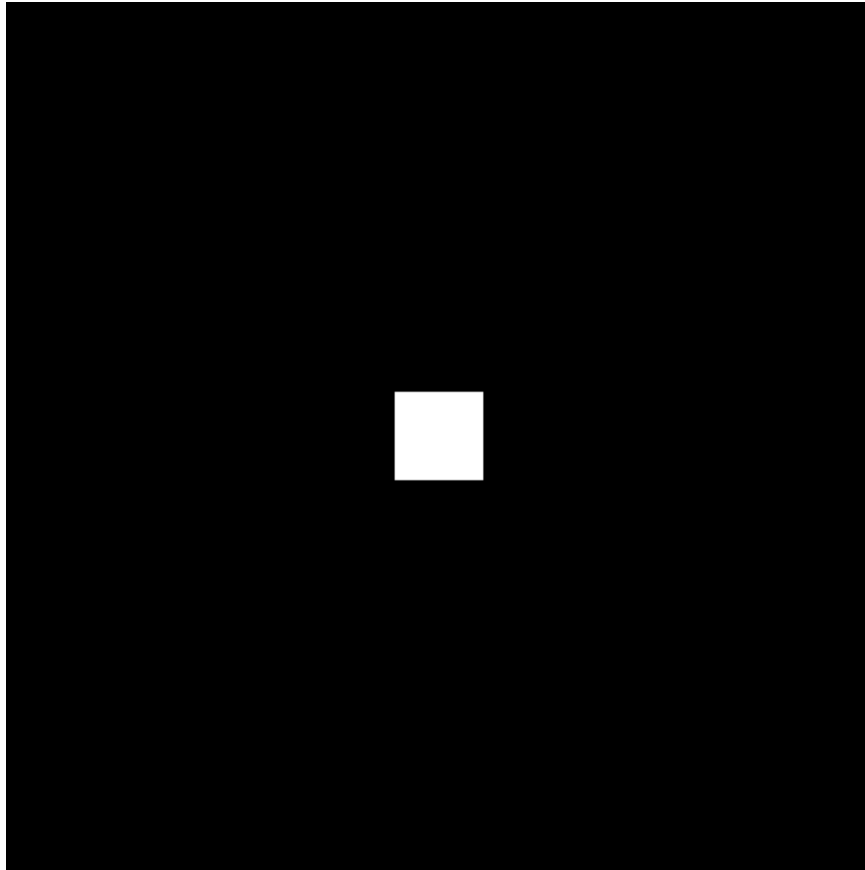
Figure 36: Field of View

The point spread function (*PSF*) is then declared by taking the two dimensional fast Fourier transform of leap *fov*. The PSF is then shifted so that the frequencies are distributed correctly with the origin corresponding to zero frequency at the origin instead of at the bottom left corner as Matlab is programmed to do automatically. The absolute value is then taken so that the absolute values of the complex vectors will be the elements

of the PSF. The absolute value is used because there are a number of negative real and imaginary parts to the complex Fourier transformed numbers and they only represent frequencies when they are represented as absolute values. The largest value of the PSF is then found and the entire matrix is divided by that scalar squared which corresponds to the energy from a point source that will decrease exponentially in three dimensional space. *PSF* is also divided by the number of time steps so that the maximum value of the modulation transfer function will never exceed one. The maximum value is less than one, which represents total coverage of the zero frequency since it is at the center. This factor would be unnecessary in deep space imaging but valuable in shorter range imaging where over-exposure is a possibility. For this simulation the truth image is bright enough to make over exposure a factor. The image is then graphed so that the relative intensities at various frequencies can be seen.

The variable *S* is declared to be the sampling rate of the apertures. Then *w*, which stands for omega, is the variable that corresponds each of the frequencies in the PSF to a certain pixel. This is done so that it can be seen when the modulation transfer function is graphed what frequency each peak corresponds to.

Then a single aperture estimate of the truth image is created called *Estimate*. The image *sat* first has to be two dimensional Fast Fourier transformed and the origin shifted to the middle of the frame. The absolute value is taken from the previous result to transform the complex numbers to the frequency domain. This is then multiplied element wise by the PSF. This multiplication creates an estimate of the truth image that depends on the intensities of the PSF. That means that at a given frequency the point spread function is able to capture a certain amount of the frequency that the truth image emits.

This result is inverse Fourier transformed and the absolute value taken so that all the frequencies are transformed into an image that is recognizable. In our simulation this image is so faint that it can't be seen because such a low percentage of the emitted frequencies are collected. The image is displayed so that it can be seen how one aperture captures the image. If this image is multiplied by a scalar indicating a long exposure. A brighter image will be seen, but it will be very blurry.

The first major loop is the *i* loop. This loop demonstrates the change of the estimation image dependant on the number of complete cycles of interferometry among the satellites. In other words, the estimation of the truth image at every stop and stare configuration is compiled though time. The *i* loop continues to the final time in increments of time between each configuration. A pause is inserted after one iteration of the *i* loop so that the windows can be rearranged to best view the changing of the modulation transfer function and estimated image.

The second major loop is the *j* loop. This loop designates the position of any one satellite from the origin. This satellite is held constant through the next loop.

The third major loop is the *k* loop. First the *k* loop computes the horizontal and vertical distance in meters that a given *j* loop satellite is apart from every other satellite. This loop shifts and compiles the point spread functions based on the locations of the satellites by using the same equations discussed in the section concerning the one dimensional multiple aperture Matlab code.

The angle of each satellite from the initial position at a given instant during the rotation is described by the variable *theta*. The value is expressed in radians so pi is multiplied by the current time step, *i*, and the number of rotations, *rotations*, and the time

step, *dt*, divided by the final time, *tf*. The shifted location of each point spread function before it is integrated into the modulation transfer function is described by *tempa* and *tempb*. The variable *tempb* is just the opposite of *tempa* with respect to the origin. The amount that is shifted through every loop varies depending on a number of factors. First, to ensure that the motion is circular the sine and cosine of the *theta* variable are used to describe the transition from polar to Cartesian coordinates. The shift factor is then multiplied by *k*, the satellite that is corresponds to that loop, so that each PSF will be shifted away from the origin.

The motion in this simulation is circular, it demonstrates satellites on a boom rotating in free space about a fixed point on the boom or rotation of multiple satellites along identical trajectories around a planet. During the planet rotation the satellites would make one rotation with respect to each other for every rotation about the planet and in that way act the same as multiple apertures on a boom. The final shifting term is *.65*LD/d*. This term is the approximate width of the PSF in pixels. We experimentally derived this based on variations of the *fov* variable. A smaller number than .65 covered the lower frequencies very well but did not address the higher frequencies and numbers above .65 left gaps in the lower frequencies which are inevitably more important.

These matrices *PSF*, *tempa* and *tempb* are then combined into the modulation transfer function, known in this code as *MM*. Then an estimate of the image, *MultiEstimate*, is calculated using the exact same procedure for the single aperture estimation except the modulation transfer function is used instead of a single point spread function to estimate the frequencies. This compilation gives an intermediate estimation of the truth image.

Finally the images are graphed each step through the *i* loop. The modulation transfer function, MM, is graphed against *w*, the frequency. Below we show the modulation transfer function graphed at different instances of the *i* loop:
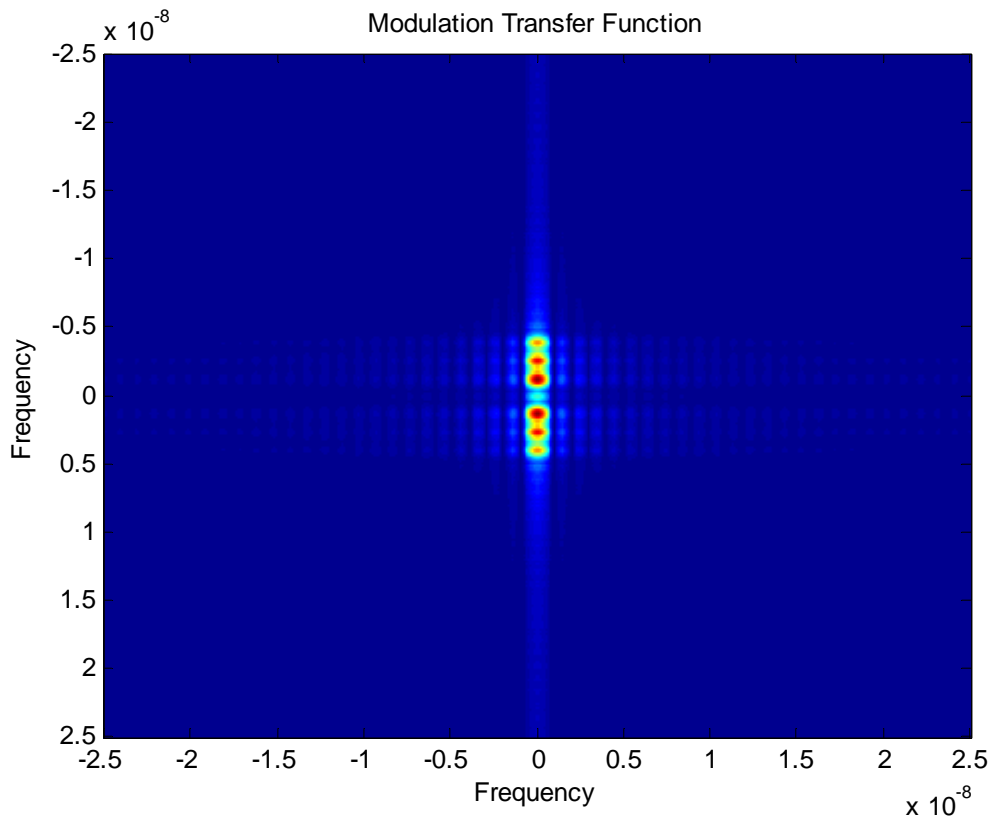
Figure 37: Modulation Transfer Function for *i=4*
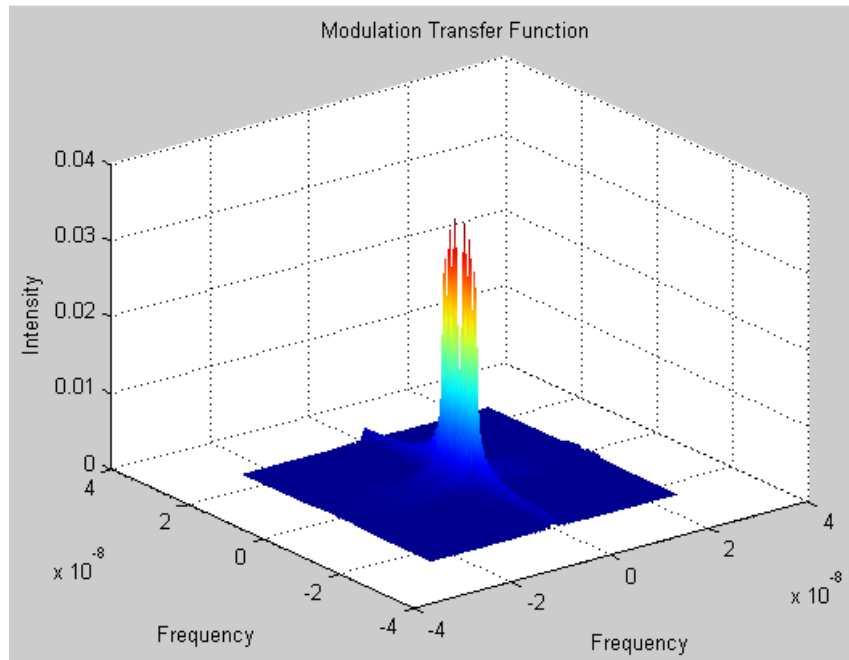
Figure 38: Three Dimensional Representation of MTF at *i=4*
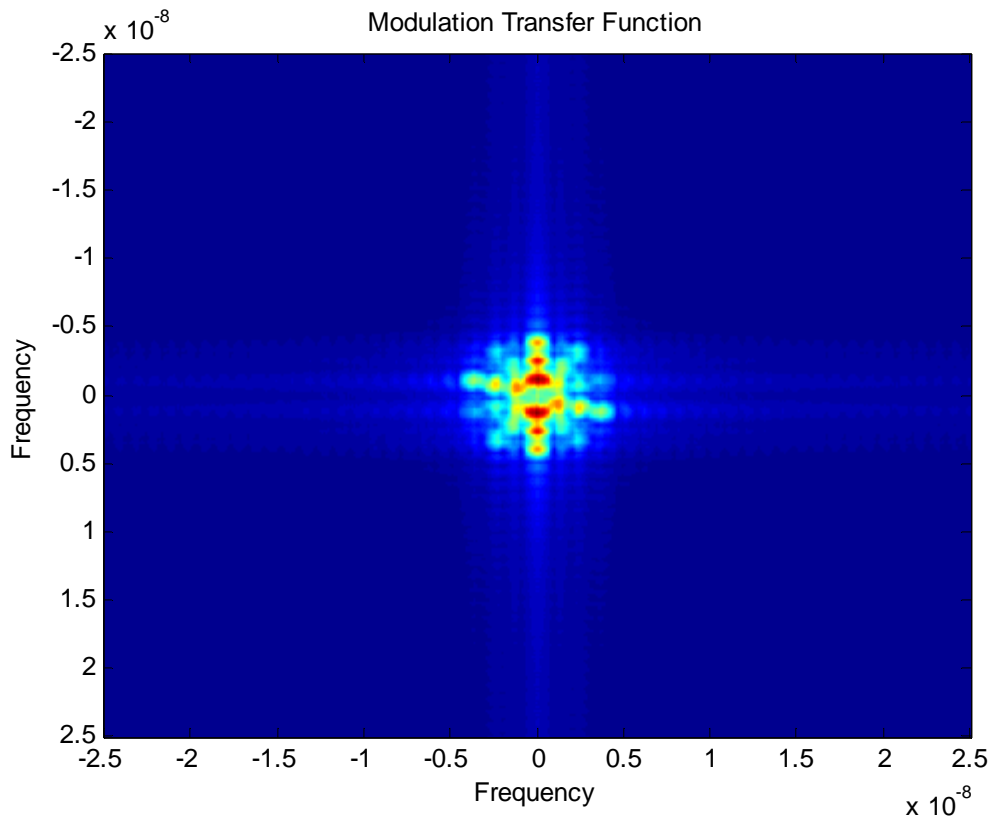
Figure 39: Modulation Transfer Function at *i=20*
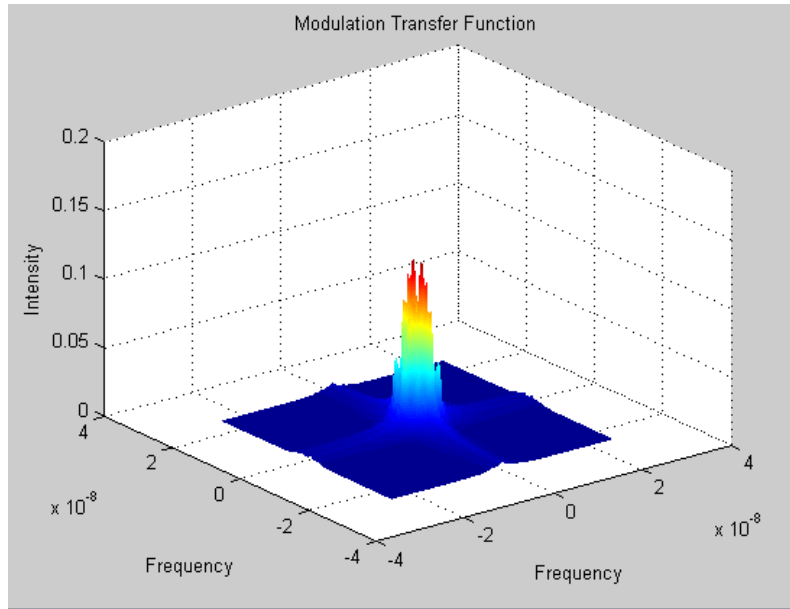
Figure 40: Three Dimensional MTF at *i=20*
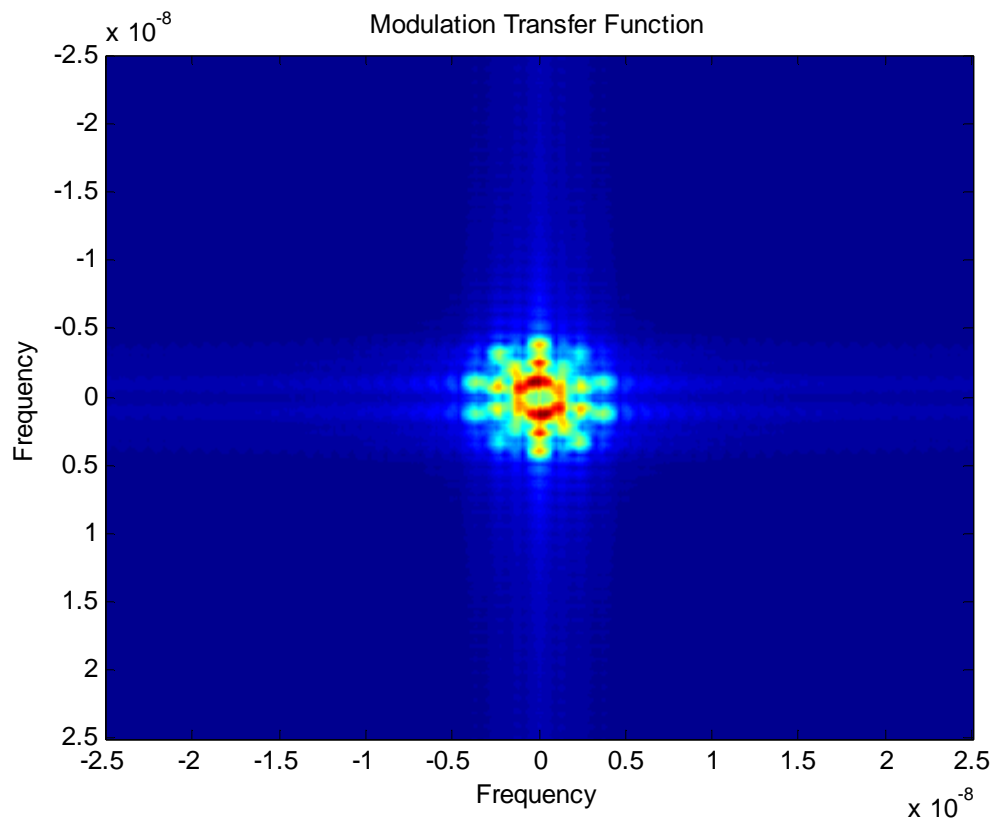
Figure 41: Modulation Transfer Function at *i=40*
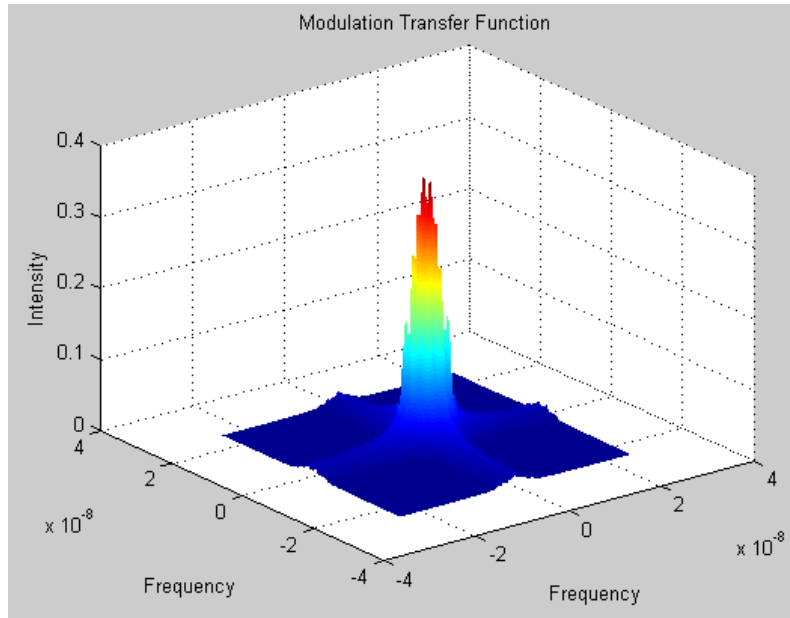
Figure 42: Three Dimensional MTF at *i=40*

Figure 43: Truth Estimate at *i=40*
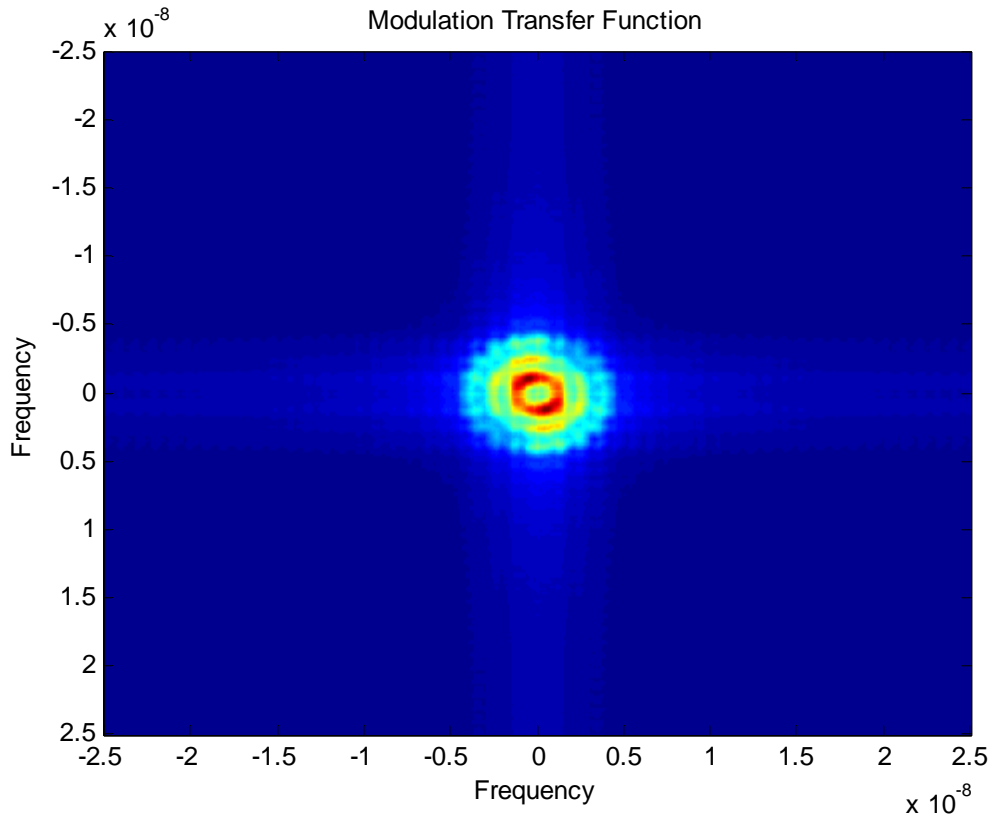
Figure 44: Modulation Transfer Function at *i=80*
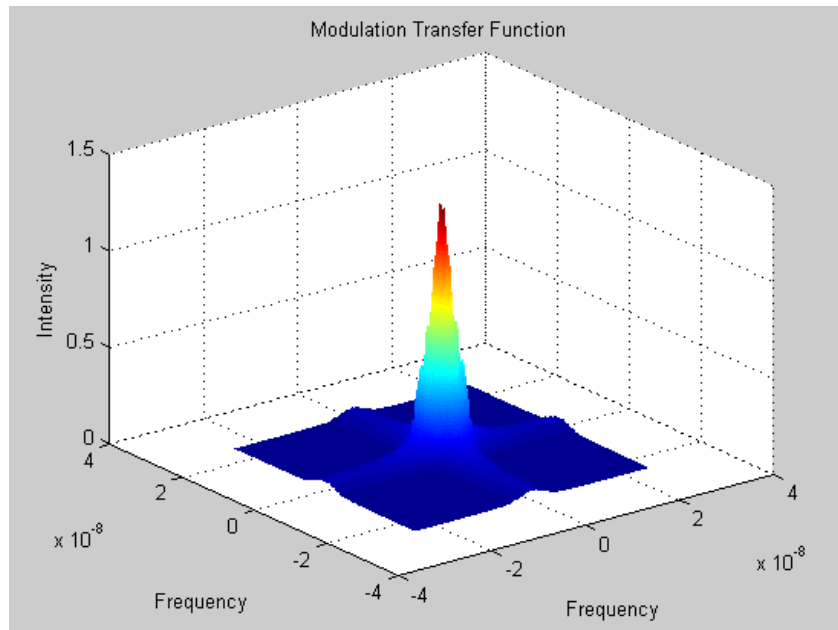
Figure 45: Three Dimensional MTF at *i=80*

Figure 46: Truth Estimate at *i=80*
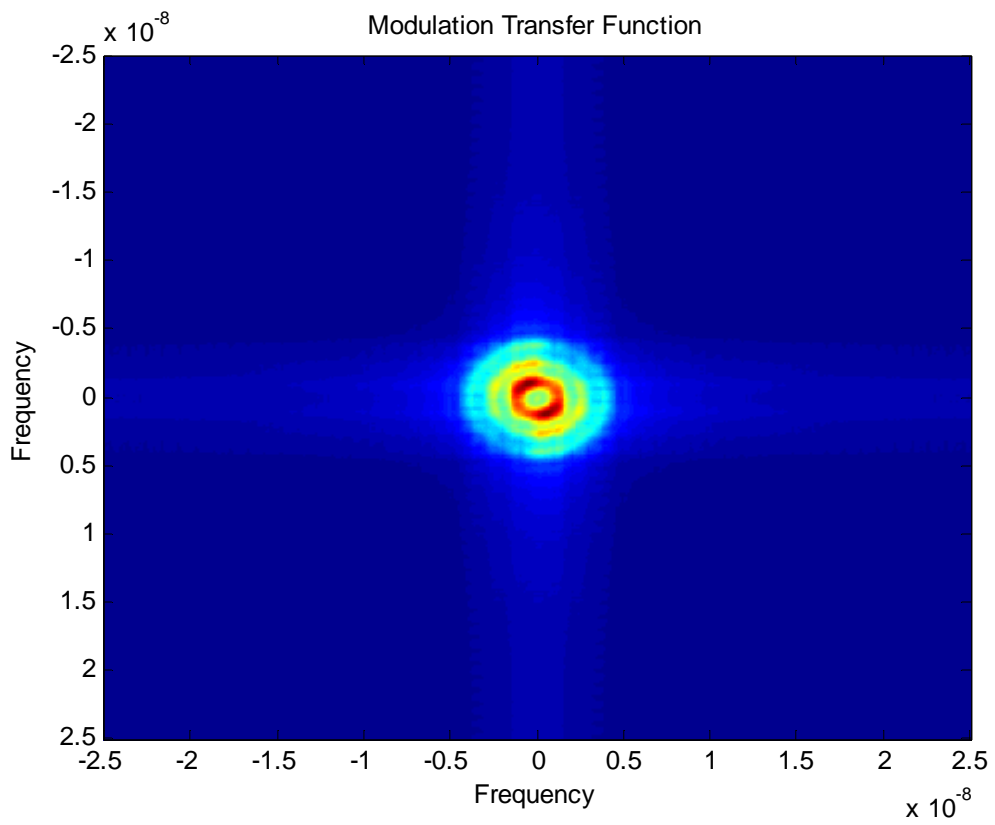
Figure 47: Modulation Transfer Function at *i=100*
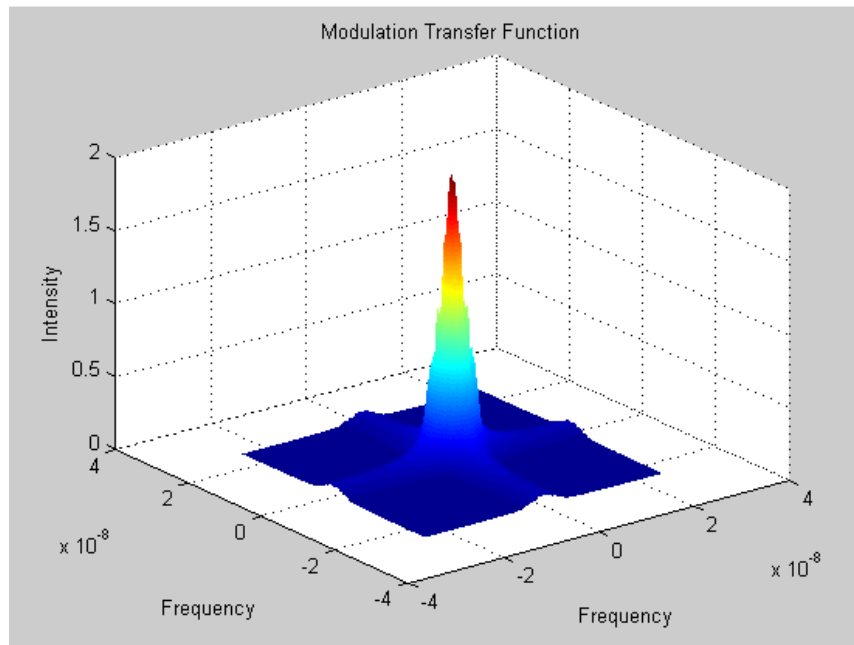
Figure 48: Three Dimensional MTF at *i=100*

Figure 49: Truth Estimate at *i=100*

Movies are then created that show the compilation over time of the modulation transfer function and the estimate of the truth image. The movies are indexed by p, the number of i loops the code goes through. The loops end and the movies are compiled into avi files so that they can be moved and viewed easily in a much shorter amount of time than it takes to run the code. It can be shown on computers without Matlab.

Using these loops the simulation describes the appropriate combination of the individual estimations. This allows easy demonstration that more satellites result in a clearer image as well as more time steps creates a clear image. One of the issues and assumptions that we make is that the combination of images is low. With a large number of combinations in the i loop, perhaps 100, an over exposure would occur and the estimation would appear nearly all white. This is also an accurate simulation that can be likened to taking a picture of a lit light bulb with an exposure of several minutes. After enough time the definition of the filament and eventually the glass would not be visible and only bright light would be seen in the photograph.

Now, we must examine the effects of the individual parameters upon the two dimensional code. The first parameter of interest is the number of satellites. We will hold all parameters constant except the number of satellites, N, which is varied by changing the input matrix X. The modulation transfer functions and resulting estimates for $tf=100$ and $dt=4$ are show below. The resulting estimate is for $N=1$ because is shown above.
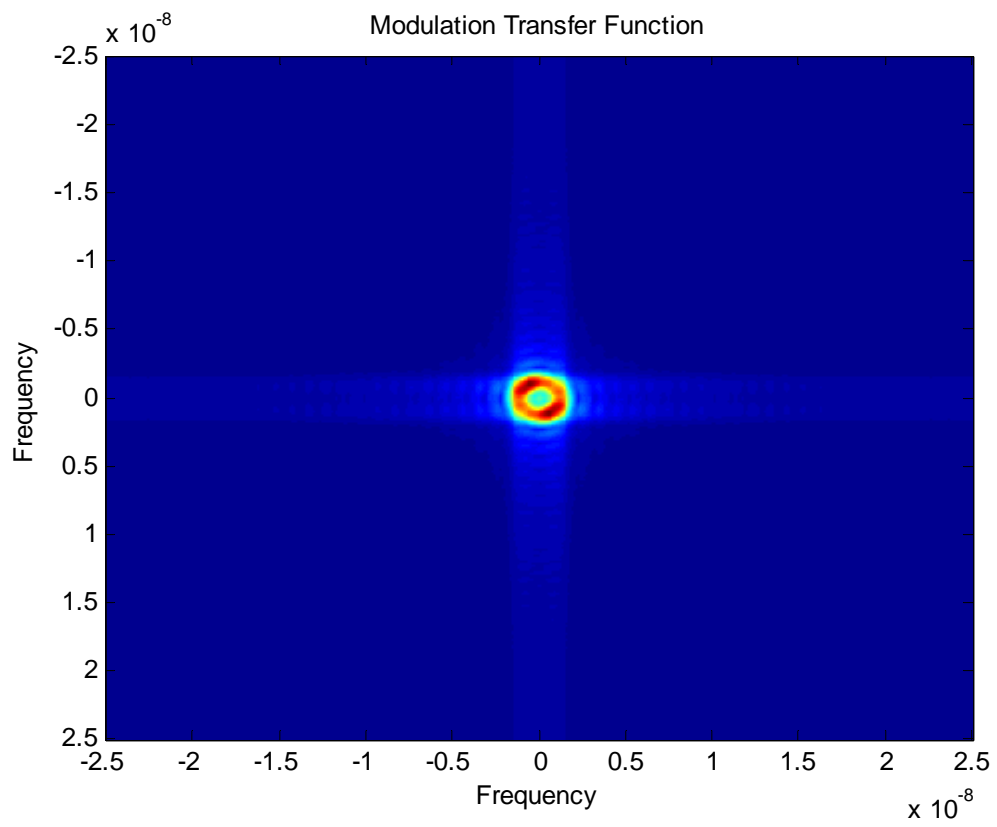
Figure 50: Modulation Transfer Function for *N=1*
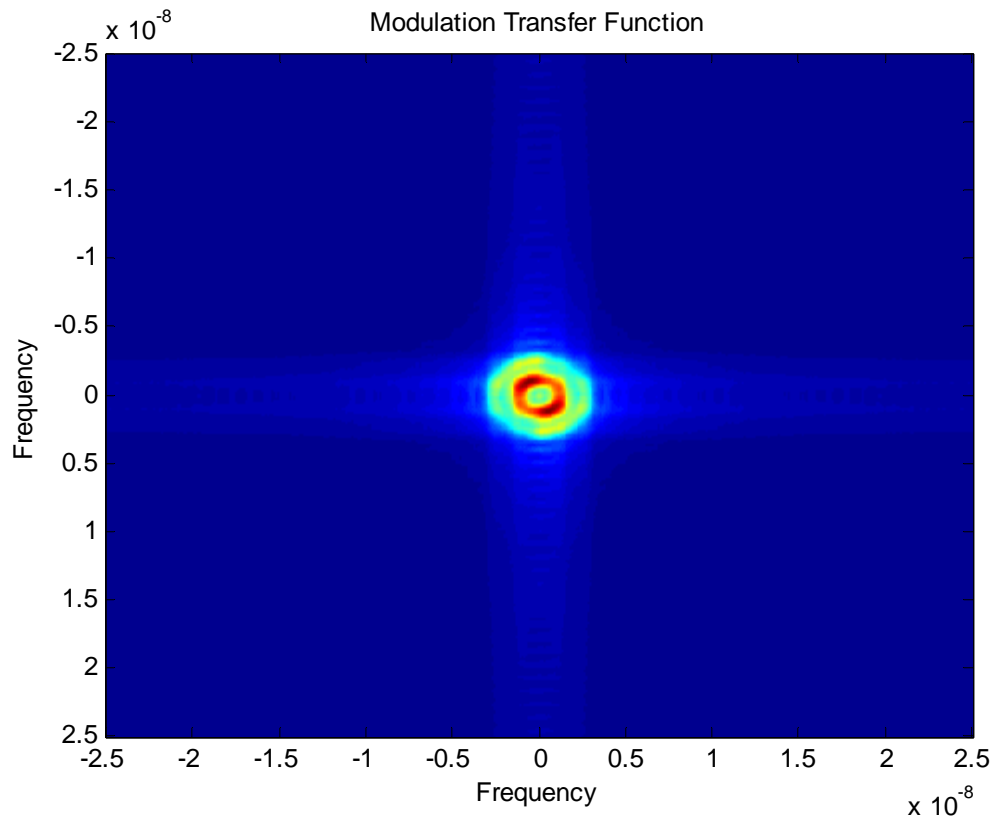
Figure 51: Modulation Transfer Function for *N=2*

Figure 52: Truth Estimate for *N=2*
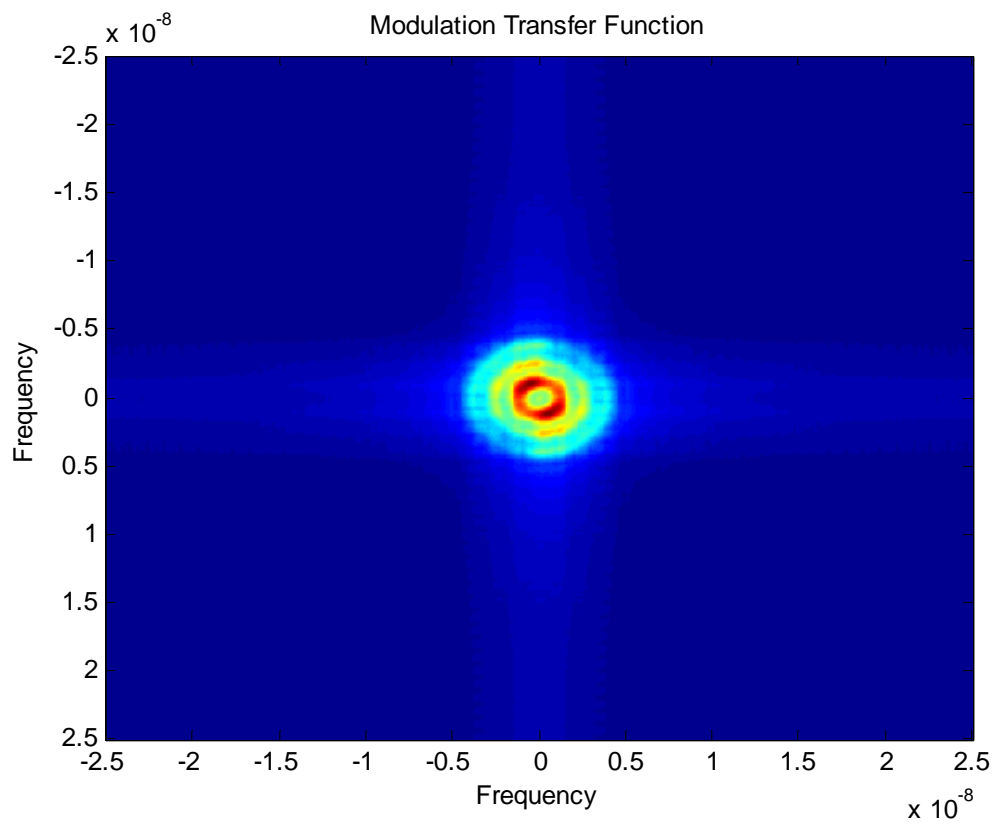
Figure 53: Modulation Transfer Function for *N=3*

Figure 54: Truth Estimate for *N=3*

In looking at the truth estimates for *N=1,2,*3 we recognize a gradual improvement in the clarity of the truth image as *N* is increased. For *N=1*, just as with the one dimensional code, we recognize virtually no signal received by the aperture and for *N=3*, we can begin to discern Saturn appearing in the estimate.

Now we will hold all parameters constant but examine the effects of changing *range*. For the same time parameters as described in the previous analysis, the modulation transfer function is plotted for varying value of *range*.
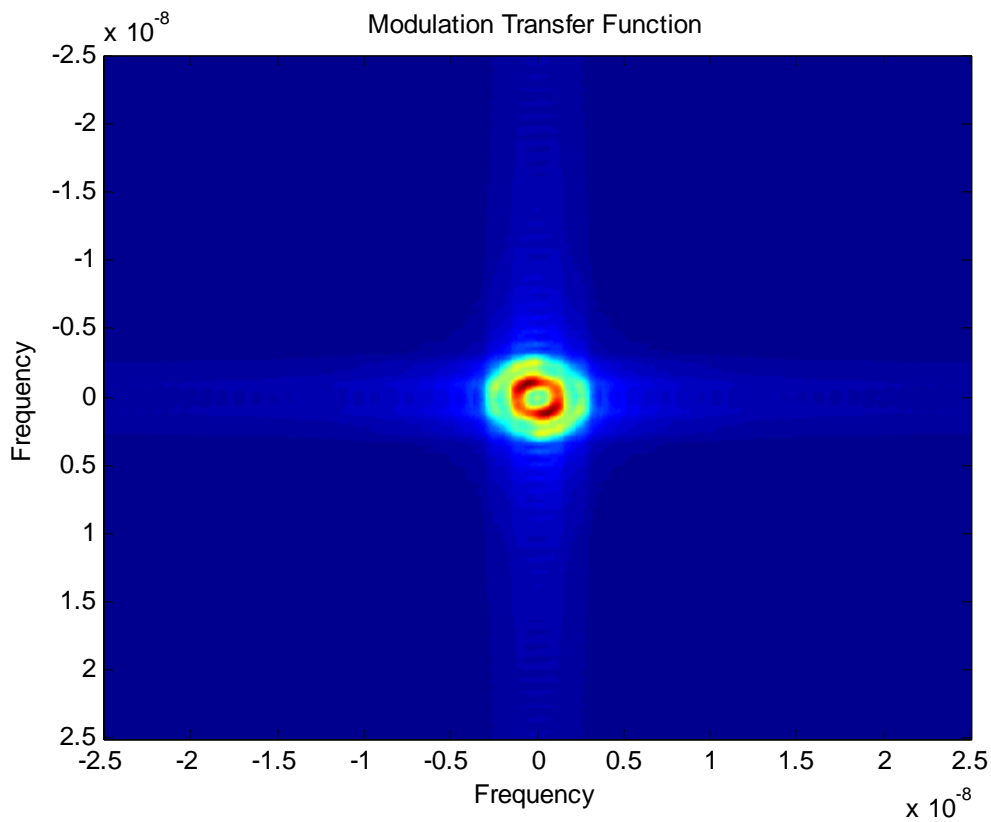
Figure 55: Modulation Transfer Function for *range=10^{16} meters*
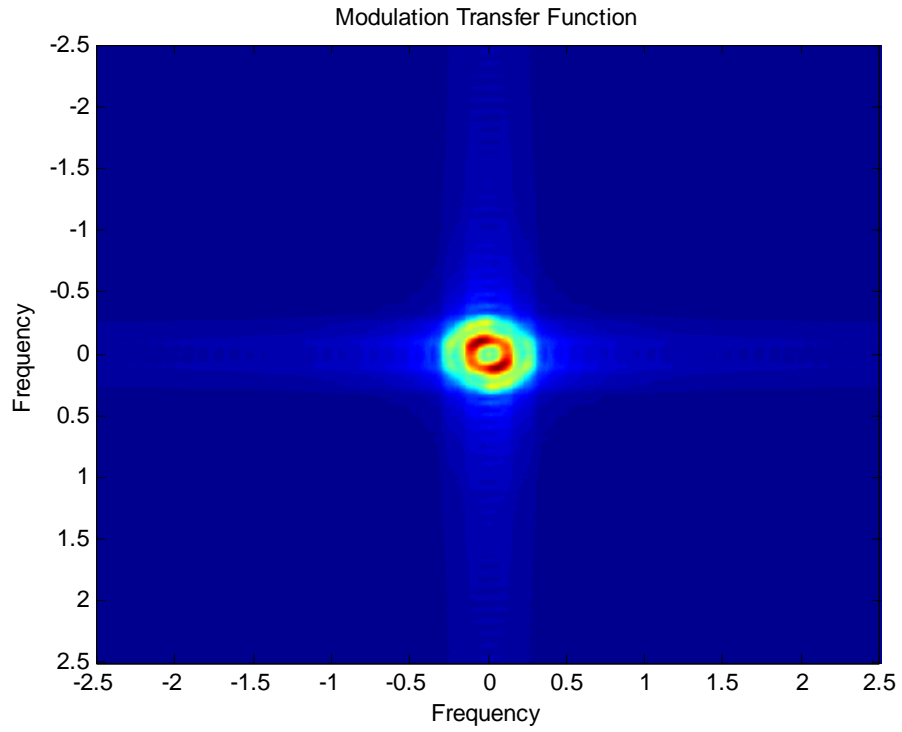
Figure 56: Modulation Transfer Function for *range=10^8 meters*
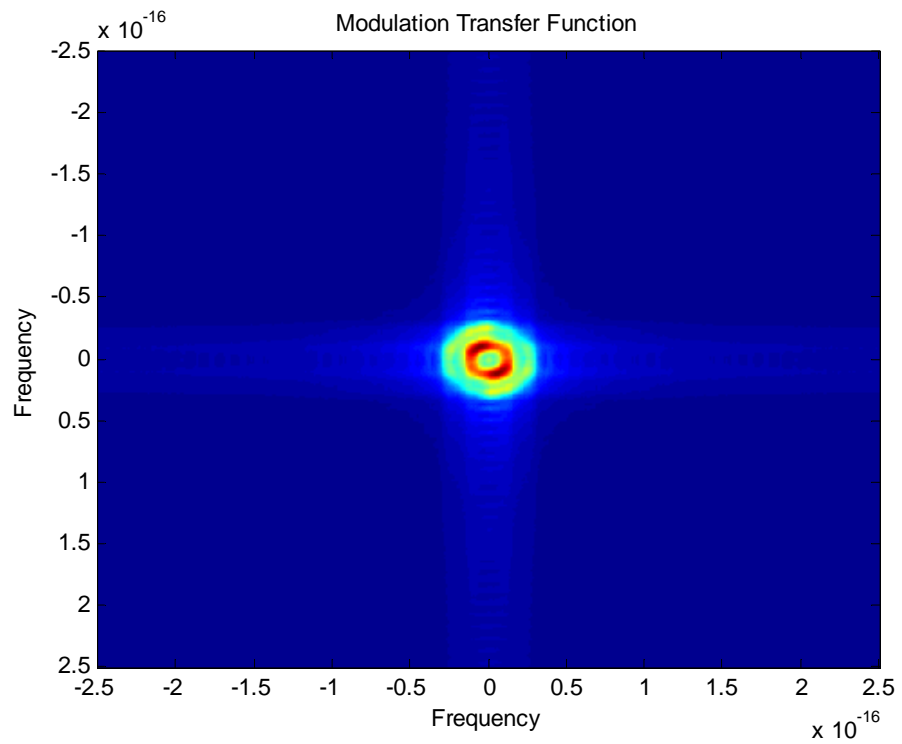
Figure 57: Modulation Transfer Function for *range=10^{24} meters*

Here, the effects of changing *range* are the same as with the one dimensional multiple aperture toolbox. At first inspection, the modulation transfer functions appear the same; however, there is a change in the applicable frequency domain as we change the range. When the range is increased, the efficiency of seeing higher wavelengths is decreased and conversely when the range is decreased, the efficiency of seeing higher wavelengths is increased. Again, this is confirmed when you move closer to an object, you are able to discern finer details with you eye than when further away.

5.0   Experimental Setup

Through a Matlab simulation, we were able to create a toolbox which could simulate the resultant image of an object formulated by a number of satellites at a range equivalent to that required for deep space imaging. In order to further prove that multiple satellite imaging systems were feasible and could improve the resolution over comparable systems, we attempted to create a table top experiment which could replicate the variables of deep space imaging. We began by conducting a feasibility study by investigating the scaling needed for such an experiment, as well as the types of waves we would be detecting in addition to site selection for the experiment. Once we had concluded that the experiment was feasible, we began researching and purchasing necessary equipment to conduct the experiment.

5.1 Feasibility Study

To emulate a deep space imaging experiment we had to scale the experiment range to the aperture size and positioning. We assumed that the distance between the source and the receiver for deep space imaging was twenty parsecs, or 61.7×10^{16} meters. Considering that the aperture of a camera on a deep space imaging satellite is around two meters, the scaling factor (aperture/range) is 3.24×10^{-18}. This scaling factor indicates that to replicate a deep space imager we would need an incredibly small receiver for a reasonably large distance. At a range of 1×10^{3} meters, the maximum distance that we could run an experiment requiring line of sight or to limit interference, the aperture of the receiver would need to be 3.24×10^{-15} meters across, much smaller than any current near infrared systems commercially available. With an aperture size of 1×10^{-3} m across, the

required range would be 308 x 10^{12} m, for positioning, we had to be able to position the receivers within a fraction of a wavelength of the signal. We selected three wave types which we could detect a fraction of a wavelength with simple equipment: infrared, radio, and acoustic. To determine the magnitude of precision for each wave type, we roughly divided each wavelength by ten. The following table summarizes our findings:

Wave Type	Wavelength	Magnitude of Precision
Infrared	750 nm to 2,500 nm	75 nm to 250 nm
Radio	5 cm to 10 m	5 mm to 1 m
Acoustic	3.43 cm to 6 m	3.43 mm to 0.6 m

Table 4: Experiment Scaling for Selected Wave Types

After analyzing our scaling results, we determined that it would not be feasible to scale our experiment directly from a deep space imaging system. As our intent is to simply prove that the addition of receivers at specified distances can improve the resolution of an image that was previously undetectable by a single receiver, we decided that the experiment could still be conducted without strict adherence to the exact scaling.

In order to conduct the experiment on a smaller scale we decided to use sources which produced weak signals. These weak signals would therefore emulate a greater range between the source and the receivers. While not exactly mirroring the scaling of deep space imaging improvements made in the resolution of the signals would prove our concept.

5.2 Site Selection

After determining that a scaled experiment would not be feasible but that a smaller scale experiment would suffice we investigated potential sites to conduct the experiment. The sites needed to be relatively flat to allow line of sight between the source and the receivers. We also narrowed our test sites to the general area surrounding Worcester, Massachusetts. We began our site search looking for testing facilities that fit these requirements. Our initial research yielded several sites of which the main three were Alumni Field, the Wachusett Reservoir, and Harrington Auditorium.

Our first site, Alumni Field, is surrounded by a standard size track which has an approximate length of 100 meters. We could extend our testing area further by using part of the curved track, as well as opening a gate to an adjacent field, increasing our range to around 260 meters.
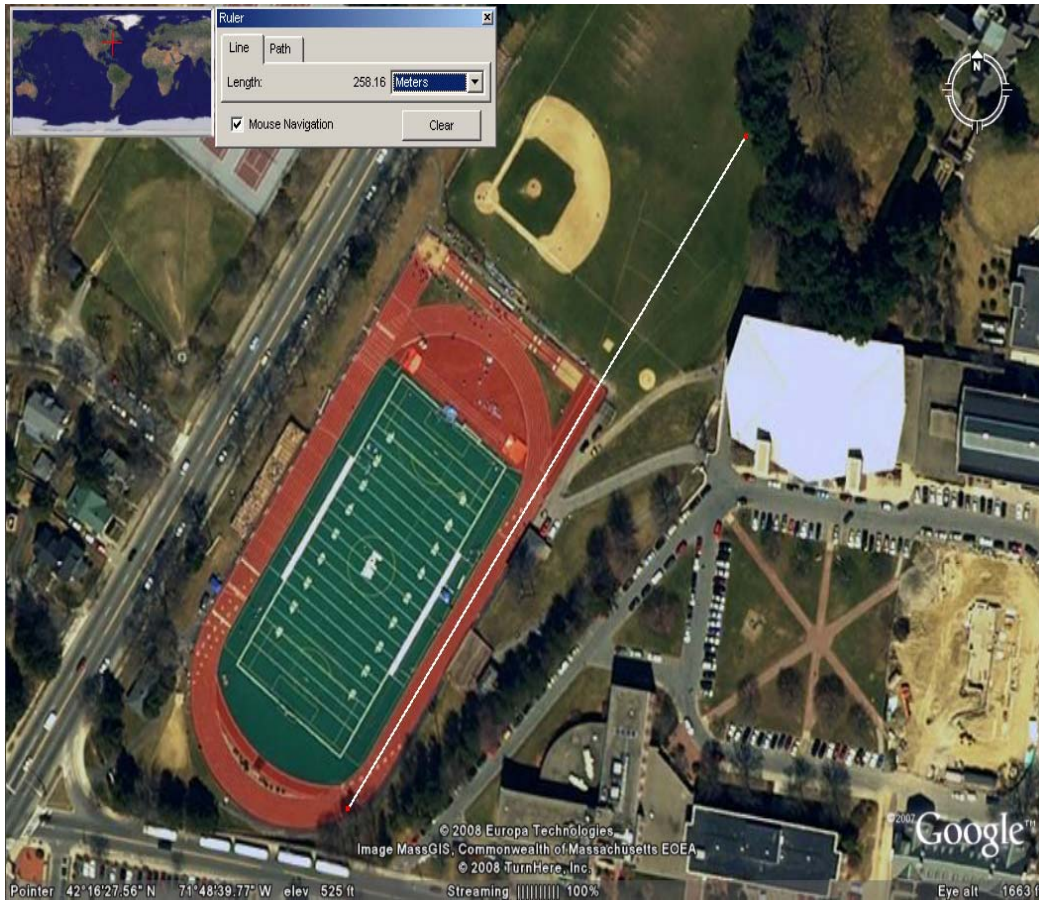
Figure 58: Alumni Field

Since the track is an outdoors facility it causes several interference problems. The track is used frequently during the day potentially interrupting testing. A solution would be to run tests at night, but we still have problems with weather conditions, radio interference, and noise and heat pollution from a nearby street. An ideal testing facility would be in an isolated area away from all types of interference.

The Wachusett Reservoir has similar characteristics to Alumni Field. Depending on how our experiment is tested at this site, we could set it up to use a maximum range of around 7,620 meters.
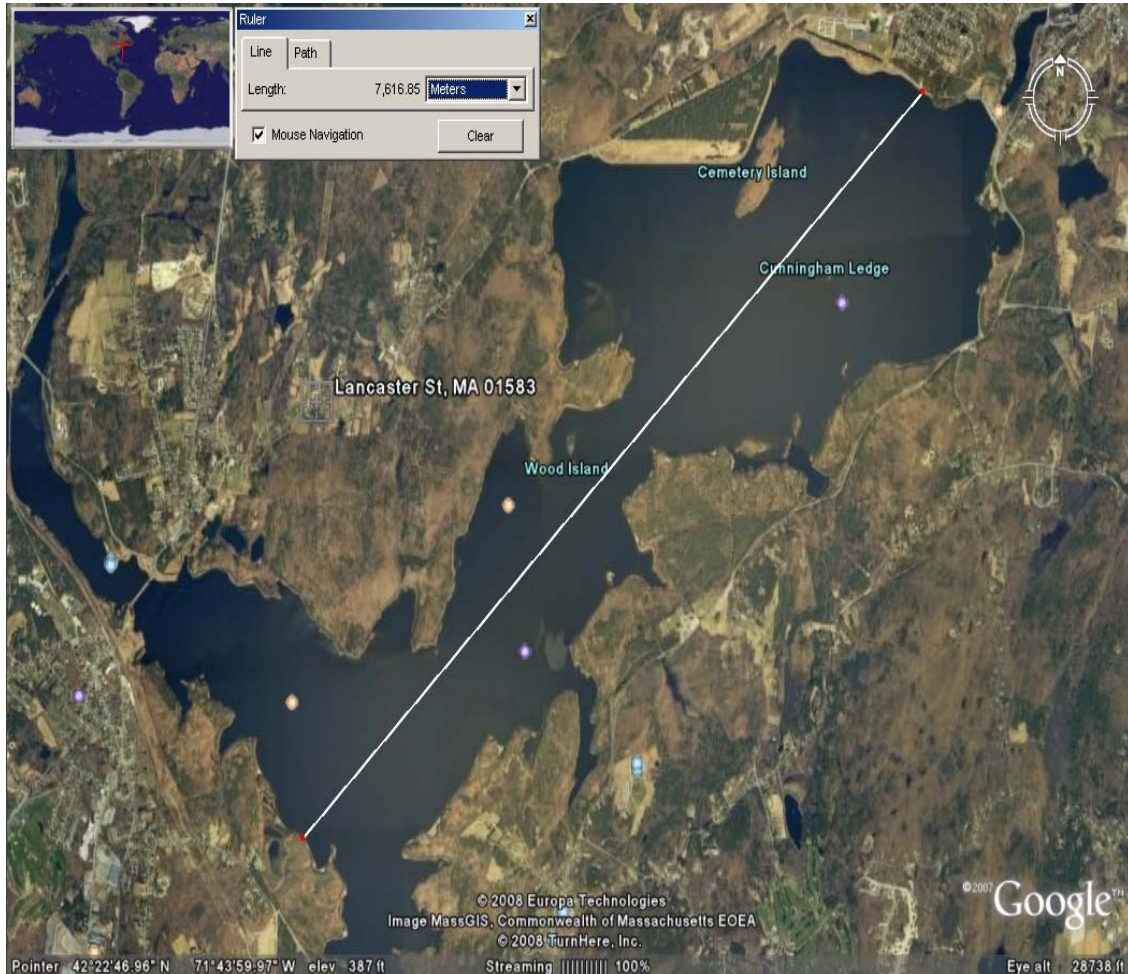
Figure 59: Wachusett Reservoir

As with our Alumni Field the reservoir is outdoors and does not have the ability to prevent outside interference. However, interference would be greater due to humidity near the water.

Harrington Auditorium solves several of the interference issues that both previous sites have since it is an indoor facility. However, there are two problems with this site.

The first problem is that the maximum range would be achieved by testing diagonally across the building which would only be a distance of 50 meters.
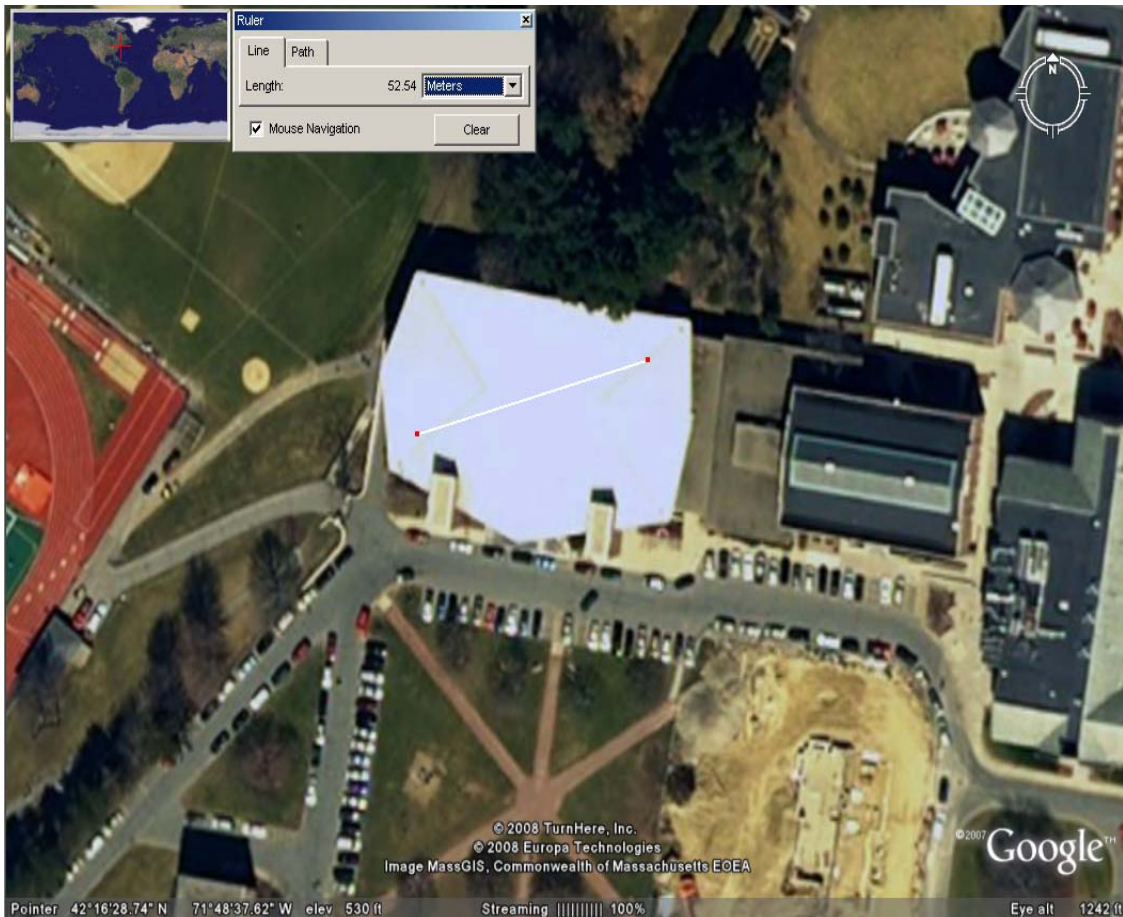
Figure 60: Harringtion Auditorium

The second issue with this testing facility is the design of Harrington does not allow for much room in the corners for all of the computer equipment needed to run the experiment. We would also have a problem on the ground floor making sure that the bleachers are moved to give us more room.

5.3 Experiment Design

For a given source the experiment starts with one source and one receiver. First, we will determine the range of the source, which can be found by starting with one receiver close to the source and increasing the distance between them until the signal from the source is no longer detectable. This distance is the range of the source. Although most sources come with a manufacturer's tested average range, the actual range of our sources may be different due to varying interference levels at different sites.

After the source's range has been determined a second receiver is added at that distance and the signals from the receivers are combined using the technology discussed in this paper. If our concept is true, the combination of the signals should produce a better signal than that of only one receiver. All processing of the signals must be done in the Fourier domain so the recorded incoming signals will be transmitted into Matlab through an Analog-to-Digital Converter, Fourier transformed, averaged, and then inverse Fourier transformed to result in an enhanced truth estimate.

5.4 Experiment Execution

We concluded from our feasibility study that a real world experiment could potentially replicate the results we obtained from our Matlab toolbox. We decided to focus on three similar experiments focusing on three types of waves: near infrared, radio, and acoustic. In all three experiments a source would be detected by two receivers. These receivers would feed into an analog-to-digital converter and the resulting digital data would be manipulated in Matlab. This allowed us to use code similar to our toolbox in a real world application.

For the infrared experiment, we needed near infrared cameras which have small apertures, to gain a closer approximation to the distance between satellites and the objects they are imaging in deep space. After searching the internet we chose the XNite IR Board Camera from LDP LLC (see Appendix B for specifications). This camera had a 3.6 mm lens and had a resolution of 380 vertical lines.

Figure 61: XNite IR Board Camera

For the source we purchased several small near infrared LEDs from the Electrical and Computer Engineering Shop at WPI.

Construction of the infrared setup was not as easy as we had previously thought. The board camera did not come with standard connections, so we purchased a proto board from the ECE Shop, as well as a power adapter and a VGA output adapter that we could

connect to the proto board. We ran power to the board through an XCamPS1100
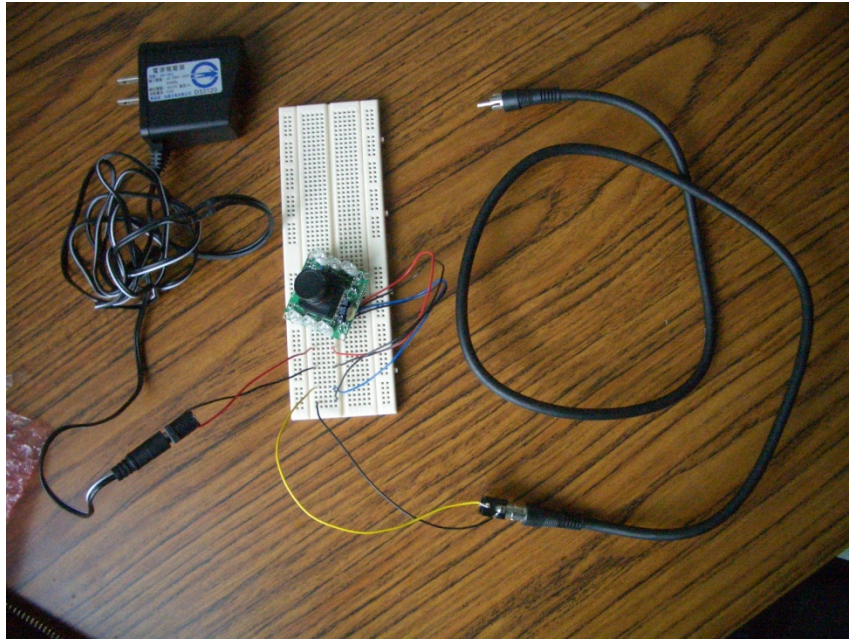
Figure 62: IR Board Camera Assembly

transformer from LDP LLC. into a connector to the protoboard. We then connected the

board camera's power wires to the board in series with the power connector. We then

plugged the video out and ground wires into the protoboard in series with the VGA

connector. We were then able to output the VGA signal to the Analog-to-Digital

Converter.

For the radio experiment, we needed a weak transmitter and two simple radio

receivers. We purchased the Mini FM Transmitter Kit CK105 from Hobbytron and two

FR1C - FM Broadcast Receiver Kits from Ramsey Electronics (see Appendix B for

specifications). Since both kits required assembly we learned how to solder and built the

kits. To capture the output of the receivers, we purchased a 3/32" to 1/8" adapter to

connect to a 1/8" to VGA cable. This VGA cable then connected to our Analog-to-

Digital Converter.
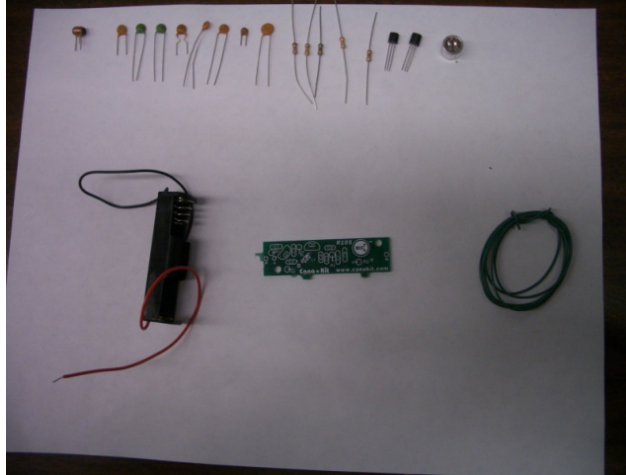
Figure 63: Unassembled Radio Transmitter
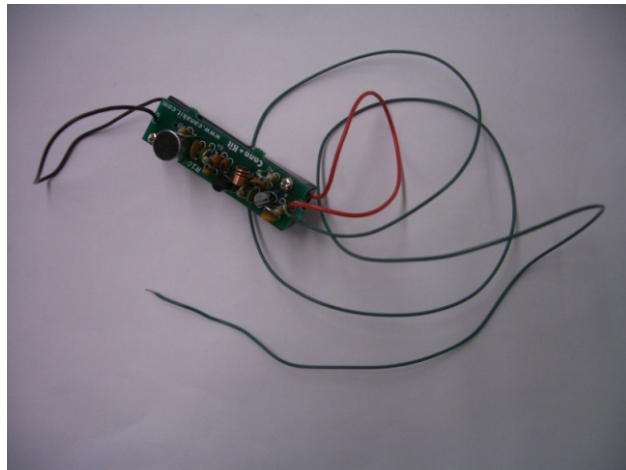
Figure 64: Assembled Radio Transmitter

Figure 65: Unassembled Radio Receiver
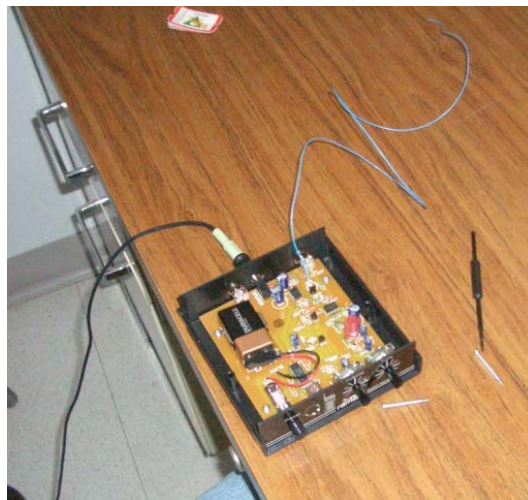
Figure 66: Assembled Radio Receiver

The audio experiment was the simplest to set up. We purchased two microphones from Radioshack to act as the receivers. We used a small speaker for the transmitter. We purchased a female 1/8" to female 1/8" connector so we could connect the 1/8" to VGA cable to the microphones. We were then able to feed the inputs to the Analog-to-Digital Converter.

We used the Quanser Q4 as our Analog-to-Digital Converter. We installed the proprietary Hardware-in-the-Loop (HIL) software to manipulate the data in Matlab R2007b. This converter allowed us to process the analog signals produced by our sensors in Matlab. Unfortunately, we were not able to install the HIL software on our lab computer. Possible problems included a previous version of Matlab being installed (Matlab R2007a) and a 64-bit processor in the computer.

Due to the computer problems we ran into which made it impossible to install the Analog-to-Digital Converter, we were unable to conduct the experiments. We have all of the necessary equipment to run the experiment and potential future research could include the running the experiments to verify our theoretical results. All of the equiptment has tested individually and performed as intended with the exception of the Analog-to-Digital Converter and software.

6.0 Conclusions & Recommendations

6.1 Conclusions

We began the practical work by starting a one dimensional code. This code was written to demonstrate the variation of an estimation of a signal as a function of the number of apertures, size of apertures, time, and aperture motion. The challenge was made greater by the complex functions we had never used before, such as Fourier transforms, that required multiple function commands to satisfy our design requirements. We also had problems making sure the code was in the correct dimensions due to distance imaging; since our code did not replicate the reduction in intensity over distance, and indexing, since the individual matrix values need to correspond to frequencies. These problems were overcome and multiple simulations were created and run to demonstrate the increase in apertures corresponded to an increase in the estimation image, as did moving apertures. In both cases the increase in resolution was due to the gathering of more frequencies.

We created a two dimensional multiple aperture simulation that uses any JPEG as a truth signal to make an estimation based on the number of satellites and their motion The motion of the apertures can be changed to no motion at all, linear motion (although unrealistic), or even spiral motion although the equation for successful spiral motion was not completed due to the need for growth that slows overtime. We were also able to relate the size of the PSF in the frequency domain to the size of the field of view. We learned that a smaller field of view, higher focus, gives more coverage in the frequency domain. This simple optical detail demonstrates that for a satellite system doing deep space imaging it is important to have a narrow, highly focused field of view so that the

maximum amount of electromagnetic signal can be captured. Our simulation often uses a wide field of view to better demonstrate the gradual build up from zero of our image so that the effects of multiple satellites are witnessed over a longer range of time.

To truly reflect the scale of the proposed space imaging system cameras, smaller than one micrometer were required. This proves that an experiment true to scale on earth is not feasible. In theory, we can weaken the signal and still perform the experiment with a larger camera. However, significant problems were encountered with Matlab and the analog to digital converter. These problems were very difficult and we were not able to solve them in order of performing the experiment within the time frame of this project.

6.2 Recommendations

The hardest part of this MQP was the accumulation of new skills. The current aerospace curriculum at WPI does not provide much instruction in the use of intensive programming tools such as Matlab or other finite element software. This deficiency resulted in many hours of our time taken by elementary programming that we did not immediately understand. If we had started the project with more experience in Matlab, we would have been able to create more detailed simulations and devoted more time to executing the experiment.

The experiment part of this MQP was electronics intensive. This technology was also somewhat foreign to us as aerospace majors. Fortunately, we had more experience in this area then in Matlab and the details were relatively easily solved compared to the difficulties with the computer. This is another case where an interdisciplinary group would have the advantage of more experience with electronics and the actual operation of analog to digital converters. It is probable that students with more electronics experience would have a better knowledge of the appropriate equipment required so that less time could be spent researching electromagnetic emitters and receivers.

Now that all of the necessary equipment is purchased and tested all that remains to be done is connect the receivers through the analog to digital converter into the computer using Matlab and combine the images using the technology discussed throughout this paper. This work is a possibility for an independent study group, summer research student, or part of an MQP; although finishing the experiments that we designed would not take the full amount of time of an MQP so additional material would be necessary.

7.0 Appendices

7.1 Matlab Code

7.1.1 One Dimensional Single Aperture

```
close all
clear all
clc

%Define the signal
t=[-10:0.01:10];
x=square(t);

%plot the signal
figure(1)
plot(t,x)
grid
axis([t(1) t(length(t)) -1.5 1.5])

d=.01;
%The aperture with ones from [-d:d]
aperture2=[zeros(length([-10:0.01:-d]),1)' ones(length([-d:0.01:d]),1)'
zeros(length([d:0.01:10])-2,1)'];
%The aperture with ones entirely from [-10:10]
aperture1=[ones(length([-10:0.01:10]),1)'];

%Plot the aperture
figure(2)
plot(t,aperture1)
grid
axis([t(1) t(length(t)) -1.5 1.5])

%Define the PSF
%We define the PSF as the fft of the aperture
PSF=fftshift(fft(aperture2));

%Plot the PSF
figure(3)
plot(t,abs(PSF))
grid

%The result of the multiplication of the PSF and the FFT of the signal
is then plotted.  The output of the "camera" is the plotted using the
ifft of the above expression
figure(4)
plot(t,real(ifftshift(ifft((abs(PSF)).*(fft(x))))))
```

7.1.2 One Dimensional Multiple Aperture

```
close all
clear all
clc

range=10^16;                          %Define the range of interest
Lambda=10^-6;                         %Define the wavelength of interest

t=-10:0.005:10;                       %Define the independent variable
x=square(t);                          %Define the input signal

%Plot the signal
figure(1)
plot(t,x)
grid
axis([t(1) t(length(t)) -1.5 1.5])

%Define the Field of View Function
d=.1;                                 %d is one half the width of the
                                       field of view function
deltt=0.005;                          %deltt is the step that the matrix
                                       fov is defined with

fov=[zeros(length(-10:deltt:-d),1)' ones(length(-d:deltt:d),1)'
zeros(length(d:deltt:10)-2,1)'];

%Plot the Field of View Function
figure(2)
plot(t,fov)
grid
axis([t(1) t(length(t)) -1.5 1.5])


PSF=fftshift(fft(fov));           %Define the point spread function as the
                                   fft of the field of view function
PSF=PSF/(PSF(1,2001));            %Factor the PSF so that the max
                                   intensity is 1

S=1/(range*Lambda);                   %Define the sampling rate for the
                                       imaging process
w=(S*(-(10/deltt):(10/deltt)))/64;  %Define the range of frequencies
                                       for the PSF

%Plot the PSF
figure(3)
plot(w,abs(PSF))
grid

%The output of the "camera" is the plotted using the ifft of the above
%expression
figure(4)
plot(t,real(ifftshift(ifft((abs(PSF)).*(fft(x))))))
grid
```

```matlab
%Define the multiple aperture PSF
MM=zeros(2,length(1001:1:3001));

    for i=1:201;
    PS1=PSF(1001:1:3001);
    temp1=circshift(PSF,[0 (-10*i)]);
    PS3=temp1(1001:1:3001);
    temp2=circshift(PSF,[0 (10*i)]);
    PS4=temp2(1001:1:3001);

    MM(i+1,:)=(MM(i,:)+deltt*(2*abs(PS1)+abs(PS3)+abs(PS4)));
    MM(i+1,:)=MM(i+1,:)/MM(i+1,1001);

    figure(5)
    plot((S*(-(5/deltt):(5/deltt))/64),MM(i+1,:))

end

y=square(-10:.01:10);

%Plot the Final Estimate
figure(6)
plot(-10:.01:10,real(ifftshift(ifft((abs(MM(i+1,:))).*(fft(y))))))
grid
```

7.1.3 One Dimensional Multiple Aperture with Motion

```matlab
close all
clear all
clc

range=10^16;                        %Define the range of interest
Lambda=10^-6;                       %Define the wavelength of interest

t=-10:0.005:10;                     %Define the independent variable
x=square(t);                        %Define the input signal

%Plot the signal
figure(1)
plot(t,x)
grid
axis([t(1) t(length(t)) -1.5 1.5])

%Define the Field of View Function
d=.1;                               %d is one half the width of the
                                      field of view function
deltt=0.01;                         %deltt is the step that the matrix
                                      fov is defined with

fov=[zeros(length(-10:deltt:-d),1)' ones(length(-d:deltt:d),1)'
zeros(length(d:deltt:10)-2,1)'];

%Plot the Field of View Function
figure(2)
plot(t,fov)
grid
axis([t(1) t(length(t)) -1.5 1.5])


PSF=fftshift(fft(fov));         %Define the point spread function as the
                                  fft of the field of view function
PSF=PSF/(PSF(1,2001));          %Factor the PSF so that the max
                                  intensity is 1

S=1/(range*Lambda);                 %Define the sampling rate for the
                                      imaging process
w=(S*(-(10/deltt):(10/deltt)))/64;  %Define the range of frequencies
                                      for the PSF

%Plot the PSF
figure(3)
plot(w,abs(PSF))
grid

%The output of the "camera" is the plotted using the ifft of the above
%expression
figure(4)
plot(t,real(ifftshift(ifft((abs(PSF)).*(fft(x))))))
```

```
grid

%Define the multiple aperture PSF
MM=zeros(2,length(1001:1:3001));

    for i=1:201;
    PS1=PSF(1001:1:3001);
    temp1=circshift(PSF,[0 (-10*i)]);
    PS3=temp1(1001:1:3001);
    temp2=circshift(PSF,[0 (10*i)]);
    PS4=temp2(1001:1:3001);

    MM(i+1,:)=(MM(i,:)+deltt*(2*abs(PS1)+abs(PS3)+abs(PS4)));
    MM(i+1,:)=MM(i+1,:)/MM(i+1,1001);

    figure(5)
    plot((S*(-(10/deltt):(10/deltt))/64),MM(i+1,:))

end

y=square(-10:.01:10);

%Plot the Final Estimate
figure(6)
plot(-10:.01:10,real(ifftshift(ifft((abs(MM(i+1,:))).*(fft(y))))))
grid
```

7.1.4 One Dimensional Multiple Satellite Imaging Toolbox

```
close all
clear all
clc

range=10^16;        %Define the range of interest
Lambda=10^-6;       %Define the wavelength of interest

D=5;                %Define the minimum distance between 2 satellites
X=[1 2 3];          %Define the orientation of the satellites
N=size(X,2);        %Determine the number of satellites

deltt=0.005;        %Define the step of the independent variable
t=-10:deltt:10;     %Define the independent variable for the truth signal

x=square(t);        %Define the truth signal


%plot the signal
figure(1);
plot(t,x);
grid;
axis([t(1) t(length(t)) -1.5 1.5]);

%Field of View
d=.1;               %d= one half the width of the field of view function

fov=[zeros(length(-10:deltt:-d),1)' ones(length(-d:deltt:d),1)'
zeros(length(d:deltt:10)-2,1)'];

%Plot the Field of View Function
figure(2);
plot(t,fov);
grid;
axis([t(1) t(length(t)) -1.5 1.5]);


PSF=fftshift(fft(fov)); %Define the PSF as the fft of the field of view
                        function
PSF=PSF/(PSF(1,2001));          %Factor the PSF so that the max
                                 intensity is 1


S=1/(range*Lambda);                     %Define the sampling rate for the
                                         imaging process
w=(S*(-(10/deltt):(10/deltt)))/64;  %Define the range of frequencies
                                     for the PSF
```

```
%Plot the PSF
figure(3);
plot(w,abs(PSF));
grid;


%%
%The General Case for N Apertures


MM=zeros(1,length((5/deltt)+1:1:(15/deltt)+1));
JJ=zeros(1,length((5/deltt)+1:1:(15/deltt)+1));


y=square(-10:(2*deltt):10);


figure(4);
subplot(2,1,1)
plot((S*(-(5/deltt):(5/deltt))/64),abs(MM(1,:)));
grid;
drawnow


subplot(2,1,2)
plot((-10:(2*deltt):10),real(ifftshift(ifft((abs(MM(1,:))).*(fft(y))))))
grid
drawnow


pause
 dt=1
    for i=1:dt:20;
        %Plot the MTF
        figure(4)
        subplot(2,1,1)
        plot((S*(-(5/deltt):(5/deltt))/64),abs(MM(i,:)));
        grid
        drawnow

        subplot(2,1,2)
        plot((-10:(2*deltt):10),
            real(ifftshift(ifft((abs(MM(i,:))).*(fft(y))))))
        grid
        drawnow

        KK=zeros(1,length((5/deltt)+1:1:(15/deltt)+1));
        for j=1:N;

            %Q is the distance of the satellite being held stationary
             from the origin
            Q=(j/2)*(j-1)*D;
            dist1=inf;

            for k=1:N
                %q is the distance of the changing satellite from the
                %origin
                q=(k/2)*(k-1)*D;
                %cuemn is the distance between the two satellites
                cuemn=Q-q;
                for l=1:((20/deltt)+1);
```

```matlab
                    dista=abs((cuemn/(Lambda*range))-w(l));
                    if dista<dist1
                        dist1=dista;
                    end
                    if dist1==dista
                        indexvalueA=l;
                    end
                end

                tempa=circshift(PSF,[0 (indexvalueA-(10/deltt)-1)]);
                PSa=tempa((5/deltt)+1:1:(15/deltt)+1);
                KK=KK+PSa;
            end
        end

    MM(i+1,:)=(MM(i,:)+dt*(KK));
    MM(i+1,:)=(MM(i+1,:))/(MM(i+1,round(length(MM)/2)));
end
```

7.1.5 Two Dimensional Code for a Single Aperture

```matlab
range=10^16;           %range=the distance between the camera and the
                        object being imaged
Lambda=10^-6;          %Lambda=the wavelength of interest
N=size(X,2);           %N= the number of satellites

%Image input
load sat215

s=size(sat);
m=s(:,1);
n=s(:,2);
pp=size(s);
ppp=(pp(:,2));
if (ppp)>2.5;
p=s(:,3);
end

%Image converted to a 0 to 1 format
if p>2
sat=single(sat(:,:,3))/255;
else if p<1
    sat=single(sat)/255;
    end
end

%Find longest dimension of the truth image
if n>m;
    longd=n;
else if m>n;
        longd=m;
    end
end

%Image changed to a standard size
LD=(n+1);                         %LD is the width of the truth object
if m<LD;
   mm=(LD-m)/2;
   sat=[zeros(round(mm+.1),n); sat; zeros(round(mm-.1),n)];
end
if n<LD;
    nn=(LD-n)/2;
    sat=[zeros(LD,round(nn+.1)) sat zeros(LD,round(nn-.1))];
end

figure(1)
imagesc(sat)

grid off

%%
%Define the field of view function
```

```matlab
d=round(LD/20);                %d is the size of the field of view function
(dxd)
B=round(.5*LD+.1);

%Define the Field of View Function
fov=[zeros(LD,length(-B:-d)-2)';
zeros(length(-B:-d)-2,length(-d:d))' ones(length(-d:d),length(-d:d))'
zeros(length(d:B)-2,length(-d:d))';
zeros(LD,length(d:B)-2)'];

%Plot the Field of View Function
figure(2);
imshow(fov);

S=1/(range*Lambda);                   %S is the sampling rate for the
                                        imaging process
w=single((S*((-B+1):(B-1))));         %w is the range of frequencies of
                                        interest for plotting the
                                        PSF/MTF


psf=(abs(fftshift(fft2(fov))));       %Define the PSF as the fft of the
                                        aperture
scale=psf(B,B);
PSF=psf/(scale*scale);

pack variables

figure(3)
imagesc(w,w,(PSF));

Estimate=abs(ifft2((PSF).*fftshift(fft2(sat))));

figure(5)
imshow(Estimate)
drawnow
```

7.1.6 Two Dimensional Code for Multiple Apertures

```matlab
close all
clear all
clc

%%For this simulation, the assumption is made that the satellites are
%%orbiting earth in a fixed orientation described by the matrix X
%%with Earth acting as the origin.


X=[1 2 3];                  %Defines the locations of the satellites in
                             the xdirection w.r.t. each other

range=10^16;                %range=the distance between the camera and
                             the object being imaged
Lambda=10^-6;               %Lambda=the wavelength of interest
N=size(X,2);                %N= the number of satellites

%Image input
load sat215

s=size(sat);
m=s(:,1);
n=s(:,2);
pp=size(s);
ppp=(pp(:,2));
if (ppp)>2.5;
p=s(:,3);
end
%Image converted to a 0 to 1 format
if p>2
sat=single(sat(:,:,3))/255;
else if p<1
    sat=single(sat)/255;
    end
end

%Find longest dimension of the truth image
if n>m;
    longd=n;
else if m>n;
        longd=m;
    end
end

%Image changed to a standard size
LD=(n+1);                              %LD is the width of the truth object
if m<LD;
   mm=(LD-m)/2;
   sat=[zeros(round(mm+.1),n); sat; zeros(round(mm-.1),n)];
end
if n<LD;
    nn=(LD-n)/2;
```

```matlab
    sat=[zeros(LD,round(nn+.1)) sat zeros(LD,round(nn-.1))];
end

figure(1)
imagesc(sat)

grid off

%%
%Define the field of view function
d=round(LD/20);             %d is the size of the field of view function
(dxd)
B=round(.5*LD+.1);

%Define the Field of View Function
fov=[zeros(LD,length(-B:-d)-2)';
zeros(length(-B:-d)-2,length(-d:d))' ones(length(-d:d),length(-d:d))'
zeros(length(d:B)-2,length(-d:d))';
zeros(LD,length(d:B)-2)'];

%Plot the Field of View Function
figure(2);
imshow(fov);

S=1/(range*Lambda);               %S is the sampling rate for the
                                   imaging process
w=single((S*((-B+1):(B-1))));     %w is the range of frequencies of
                                   interest for plotting the PSF/MTF

psf=(abs(fftshift(fft2(fov))));   %Define the PSF as the fft of the
                                   aperture
scale=psf(B,B);
PSF=psf/(scale*scale);

pack variables

figure(3)
surf(w,w,(PSF));
grid on
colormap jet
shading interp

Estimate=abs(ifft2((PSF).*fftshift(fft2(sat))));

figure(5)
imshow(Estimate)
drawnow

dt=4;                      %Defines the time step for integration
                            purposes
tf=100;                    %Defines the time required for one complete
time=[0:dt:tf];            %Defines the range of time evaluated
rotations=1;               %Defines the number of rotations that the
                            apertures complete
```

```matlab
%variables for loop that shows motion of PSF
MM=zeros(LD, LD);
KK=zeros(LD, LD);
p=0;


% the i loop describes the time that the satellites go through
for i=0:dt:tf
    if i==dt;
        pause
    end
    % the j loop describes the position of each individual satellite
        for j=1:N;
            for k=1:N
                % theta is the angle of the PSF shifted from the j loop
                % compared to the k loop
                theta=(2*pi*i*rotations/tf);
                % .65*LD/d is the approximate width of each PSF. k is
                   the satellite in question and thus scaling factor in
                   the Fourier domain that that PSF is from the origin.
                tempa=circshift(PSF,[round((.65*LD/d)*(k)*cos(theta))
                        round((.65*LD/d)*(k)*sin(theta))]);
                tempb=circshift(PSF,[round(-((.65*LD/d)*(k)*cos(theta)))
                        round(-((.65*LD/d)*(k)*sin(theta)))]);
                PSa=tempa;
                PSb=tempb;
                KK=KK+PSa+PSb;

                MM=(MM+(KK));
                MultiEstimate=abs((ifft2((MM).*fftshift(fft2(sat)))));

            end
        end
        p=p+1;
        %plot the MTF
        figure(9);
        grid off
        imagesc(w,w,abs(MM));
        MOV2(p)=getframe;
        drawnow
        %Plot the estimate
        figure((1000))
        imshow(MultiEstimate)
        MOV(p)=getframe;
        drawnow

end

movie2avi(MOV,'Saturn3Sat')
movie2avi(MOV2,'3Sat')
```

7.2 Experiment Equipment

Company:	LDP LLC	
Website:	http://www.maxmax.com/	
Fax Number:	201-882-0344	
Products:		
Quantity	Product Name	Price
2x	XNiteIRBoardCam	$135 ea
2x	XCamPS1100	$15 ea

XNite IR Board Cam
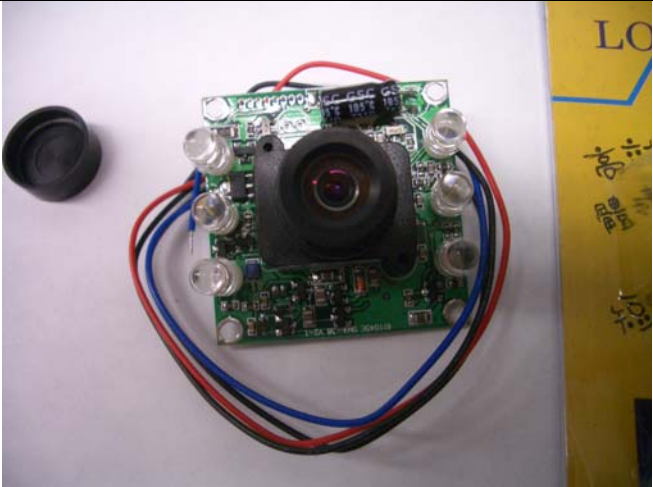
Specifications	
Image Sensor	Interline 1/3" B/W CCD
Effective Pixel	512H x 492V pixels / NTSC
Scanning system	2:1 Interlaced
Sync System	Internal Sync
Sync Pulse	15.734 Khz H, 59.94 Hz V
Resolution	380 TVL
S/N Ratio	More than 46dB
Gamma	0.45
Min Illumination	1.0 Lux/ F2.0 with no LED's
Video Output	Composite video: 1.0 Vp
Electronic Shutter Time	1/60- 1/50,000 Sec NTSC
Power Supply	DC 12V +/- 10%
Power Consumption	130mA Typ
Lens	3.6mm 92Deg F2.0
Operational Temp	-5 Deg C to +40 Deg C
Storage Temp	-10 Deg C to +50 Dec C
Dimensions	1.125 in (w) x 1.125 in (H)
Weight	Appx 20grs

XCamPS1100

Specifications	
Input Voltage	100 to 240 Volts AC
Input Frequency	50 to 60 Hertz
Output Voltage	12 VDC
Output Power	200 mA
Website	http://www.maxmax.com/aXRayPowerSupply.htm

Company:	Hobbytron	
Website:	http://www.hobbytron.com/	
Fax Number:	801-437-1714	
Products:		
Quantity	Product Name	Price
1x	Mini FM transmitter - Wireless Microphone Kit CK105	$12.95

Mini FM transmitter - Wireless Microphone Kit CK105
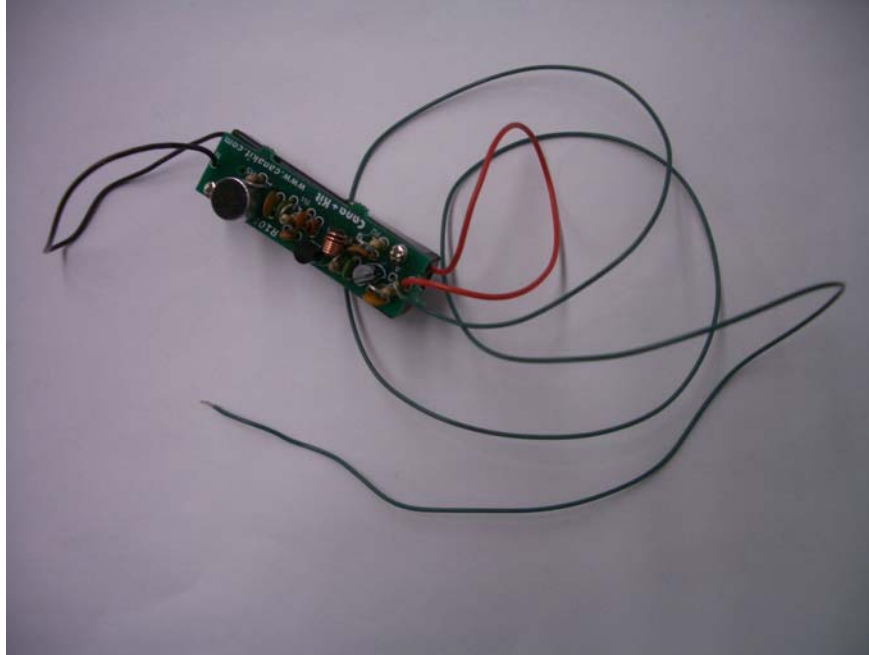
Description
A sensitive microphone makes this kit ideal as an intrusion alarm or wireless babysitter. Transmit your voice through any FM radio up to 100 feet. Frequency range is fixed somewhere in the 88 to 98 MHz range. Comes with instructions and a drilled and etched circuit board with battery holder as shown.

Website	http://www.hobbytron.com/Mini-FM-transmitter-Wireless-Microphone-Kit.html

Company:	Ramsey Electronics	
Website:	http://www.ramseyelectronics.com/	
Fax Number:	585-924-4886	
Products:		
Quantity	Product Name	Price
2x	FR1C - FM Broadcast Receiver Kit	$34.95 ea

FR1C - FM Broadcast Receiver Kit
Description
- Standard FM receiver with a wider tuning range of 70-110 MHz   - Ideal for tuning-in FM wireless mics, phone bugs, SCA programming, or just normal FM broadcasts   - Excellent reception with 1uV sensitivity   - Demodulated audio output for driving our SCA-1 Decoder   Ideal for standard FM broadcast band as well as large portions on each side, making it great for bug monitoring or detection and receiving SCA broadcasts. Features one microvolt sensitivity, 10.7 MHz IF, 250 mW audio output, varactor diode tuning, IC FM detector chip, demod output to drive our SCA-1 decoder and operates on 9 VDC battery (not included). Drives any 4 - 45 ohm external speaker. Includes our matching custom case set, measuring 5"w x 5 1/4"d x 11/2"h.

Website	http://www.ramseyelectronics.com/cgi-bin/commerce.exe?preadd=action&key=FR1C

8.0 References

1. Blair, Bill and Humberto Calvani. "Far Ultraviolet Spectroscopic Analyzer". 14
    Jan 2008. Johns Hopkins University. 23 Jan 2008. <http://fuse.pha.jhu.edu/>.

2. Chakrovorty, Suman. *Multi-Spacecraft Interferometric Imaging Systems: The
    Search for New Worlds*. Doctoral Dissertation. University of Michigan. 2003.

3. Chambers, Lin H.. "Electromagnetic Spectrum." <u>My NASA Data</u>. 06 Nov 2007.
    National Aeronautics and Space Administration. 21 Nov 2008
    <http://mynasadata.larc.nasa.gov/ElectroMag.html>.

4. Duffieux, P.M. <u>The Fourier Transform and its Applications to Optics</u>. 2nd edition.
    New York: John Wiley and Sons, Inc., 1983.

5. Evergreen Optics. "Beginners Guide to Telescopes". UK Telescopes. 12 Feb
    2008.
    <http://www.uk-telescopes.co.uk/beginners_guide%20to%20telescopes.htm>.

6. Gano, S.E. and et. al. "A Baseline Study of Low-Cost, High-Resolution, Imaging
    System using Wavefront Reconstruction." A Collection of Technical Papers:
    AIAA Space 2001 Conference and Exposition, 28 – 30 August 2001,
    Albuquerque: Aug 2001.

7. Gatelli, Fabio, et al. "The Wavenumber Shift in SAR Interferometry." <u>IEEE
    Transactions on Geoscience and Remote Sensing</u> 32.4 (1994): 855,856-865.

8. Hussein, Islam I., D. J. Scheeres and D.C. hyland. *Interferometric Observatories
    in Earth Orbit*. Published by American Institute of Aeronautics and Astronautics.
    Danvers: 3 Oct 2003.

9. Hussein, Islam I. *Motion Planning for Multi-Spacecraft Interferometric Imaging Systems*. Doctoral Dissertation. University of Michigan. 2005.

10. Hussein, Islam I., Scheeres, Daniel J. , Bloch, Anthony M., Hyland, David C., McClamroch, N. Harris. *Optimal Motion Planning for Dual-Spacecraft Interferometry*. IEEE Transactions on Aerospace and Electronic Systems Vol. 43, No. 2. Published: Apr 2007.

11. Jackson, Randal. "Getting the Big Picture: Multiple telescopes, one target". Planet Quest. National Aeronautics and Space Administration. 23 Oct 2007. <http://planetquest.jpl.nasa.gov/technology/formation_flying.cfm>.

12. Jackson, Randal. "How to take snapshots of distant worlds." Planet Quest. National Aeronautics and Space Administration. 23 Oct 2007. <http://planetquest.jpl.nasa.gov/technology/planet_imaging.cfm>.

13. Jackson, Randal. "An instrument for ground-based planet searches". Planet Quest. National Aeronautics and Space Administration. Sep 2007. <http://planetquest.jpl.nasa.gov/lbti/lbti_index.cfm>.

14. Jackson, Randal. "Keck Interferometer". Planet Quest. National Aeronautics and Space Administration. Space.com. Sep 2007. <http://planetquest.jpl.nasa.gov/Keck/keck_index.cfm>.

15. John M. Brayer, Ph. D. "Introduction to Fourier Transforms for Image Processing". University of New Mexico, Albuquerque. Aug 2007 <http://www.cs.unm.edu/~brayer/vision/fourier.html>.

16. Joseph W. Goodman. Introduction to Fourier Optics. 3rd Edition. Greenwood Village: Ben Roberts, 2005.

17. Knight, Andrew. <u>Basics of Matlab and Beyond</u>. Boca Raton: Chapman & Hall, 2000.

18. Lori Tyahla. "Introduction – Overview". <u>The Hubble Space Telescope</u>. 01 Nov 2006. National Aeronautics and Space Administration. 01 Nov 2007. <http://hubble.nasa.gov/overview/faq.php>.

19. Lavoie, Sue. "Spacecraft and Telescopes." <u>Photo Journal</u>. National Aeronautics and Space Administration. Sep 2007. <http://photojournal.jpl.nasa.gov/index.html>.

20. Overcast, Marshall C. and Paul W. Nugent. <u>Computing the 2-D Discrete Fourier Transform or Sweet-talking MATLAB into Making Cool Pictures</u>.

21. Owens, Robyn. "Fourier Transform Theory." 29 Oct 1997. 12 Oct 2007. <http://homepages.inf.ed.ac.uk/rbf/CVonline/LOCAL_COPIES/OWENS/LECT4/node2.html>.

22. "Point spread function." 28 Aug 2007. Wikipedia. 07 July 2007. <http://en.wikipedia.org/wiki/Point_spread_function>.

23. Rarogiewicz, Lu. "Interferometry 101: How light is combined from multiple telescopes." 05 July 2001. 12 Sep 2007. <http://www.space.com/scienceastronomy/astronomy/interferometry_101.html>.

24. Reynolds, George O. et. al. <u>The New Physical Optics Notebook: Tutorials in Fourier Optics</u>. New York: American Institute of Physics, 1989.

25. Rodenburg, John M. "The Fourier Transform of a one-dimensional aperture (a harbour entrance)". 21 Oct 2004. <http://images.google.com/imgres?imgurl=http://www.rodenburg.org/theory/Figs/f6200.gif&imgrefurl=http://www.rodenburg.org/theory/y1400.html&h=267&w=505&sz=4&hl=en&start=16&tbnid=4ORouMEy05qZ9M:&tbnh=69&tbnw=130&prev=/images%3Fq%3Dhat%2Bfunction%26gbv%3D2%26svnum%3D10%26hl%3Den>.

26. "Spitzer Space Telescope" Spitzer Science Center. California Institute of Technology. Sep 2007 <http://www.spitzer.caltech.edu/>.

27. Steel, William Howard. Interferometry. New York: Cambridge University Press, 1983.

28. Steve Unwin. "Origins." Origins Project. National Aeronautics and Space Administration. Sep 2007. <http://origins.jpl.nasa.gov/index1.html>.

29. Steward, E.G. Fourier Optics: An Introduction. 2nd Edition. Chichester: Ellis Horwood Limited Publishers, 1987.

30. Tracy Vogel. "Hubble Essentials." Hubble Site. National Aeronautics and Space Administration. Sep 2007. <http://hubblesite.org/the_telescope/hubble_essentials/>.

31. Watanabe, Susan. "Jet Propulsion Laboratory: California Institute of Technology". National Aeronautics and Space Administration. Sep 2007 <http://www.jpl.nasa.gov/index.cfm>.

32. Weaver, H. Joseph. Theory of Discrete and Continuous Fourier Analysis. New York: John Wiley and Sons, Inc., 1989.

33. Williams, Charles Sumner and Orville A. Becklund. <u>Introduction to the Optical Transfer Function</u>. New York: Wiley, 1989.

34. Yang, Xiangyang, and Yu, Francis, T. S. <u>Introduction to Optical Engineering</u>. New York: Cambridge University Press, 1997.